NSK Technical Journal

Motion & Control

No. 30 June 2019

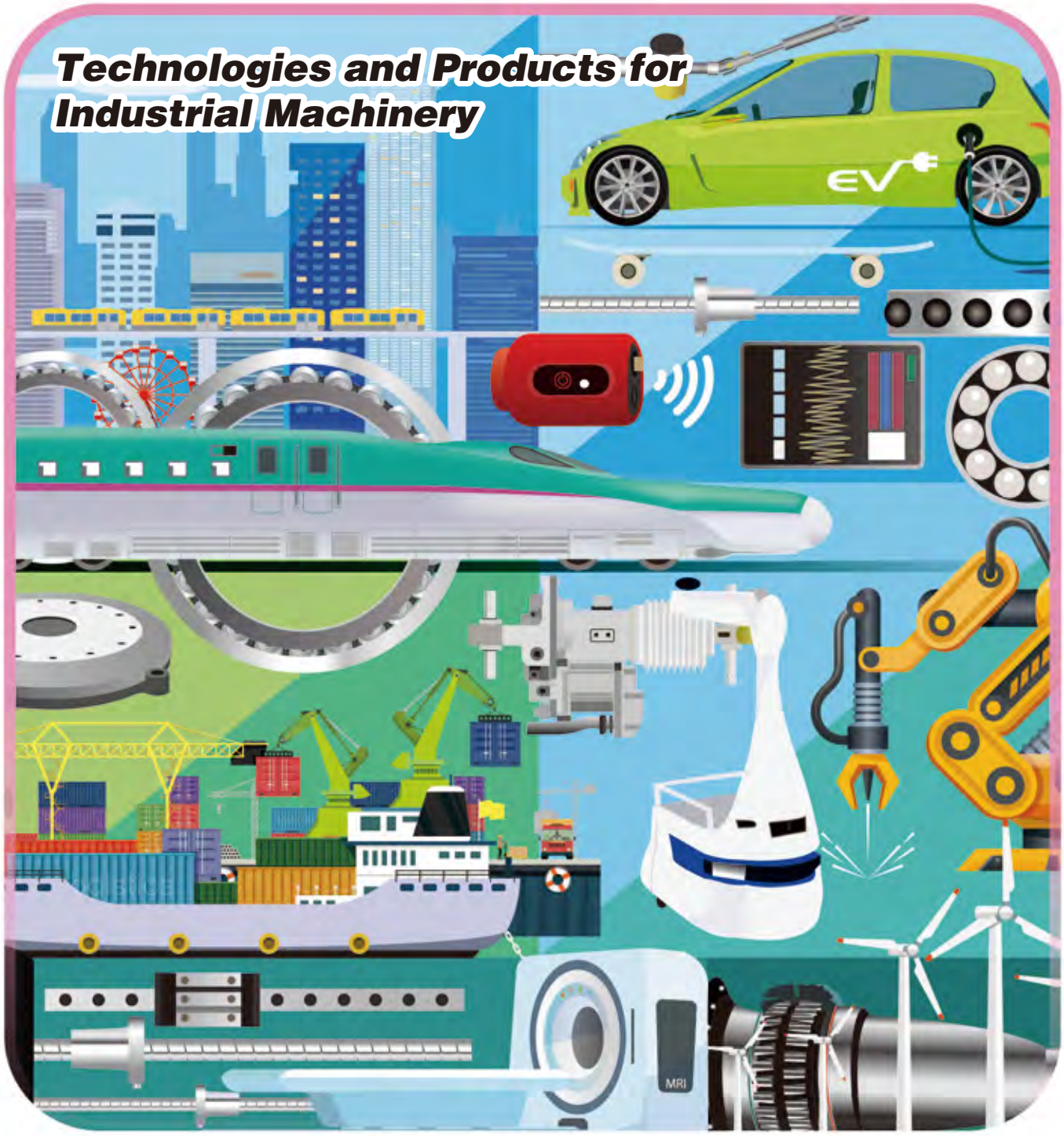

ISSN1342-3630

NSK

MOTION & CONTROL No. 30
NSK Technical Journal
Printed and Published: June 2019
ISSN1342-3630
Publisher: NSK Ltd., Ohsaki, Shinagawa, Tokyo, JAPAN
Public Relations Department
TEL +81-3-3779-7050
FAX +81-3-3779-7431
Editor: Nobuo GOTO
Managing Editor: Hitoshi EBISAWA
Design, Typesetting & Printing: Kuge Printing Co., Ltd.

NSK Technical Journal
Motion & Control
No. 30
June 2019

NSK

Contents

NSK's Latest Technologies and Products for Industrial Machinery

Seiji Ijuin
Executive Officer,
Head of Industrial Machinery Technology Center

The United Nations adopted the Sustainable Development Goals (SDGs) in 2015, a set of targets that demand the pursuit of economic development and affluence as well as protection of the global environment, elimination of poverty and disparity, and assurance of a safe life for people. In response to such social requirements, and in addition to the rapid development of ICT, IoT, and AI, the industrial world is evolving dramatically. Involved in industrial machinery on a large scale, NSK will contribute to the Earth, society, and industry through the development of new products and technology. Here in this Special Issue of Products and Technology for Industrial Machinery we introduce these technologies.

In this era of transition from tangible goods to intangible goods ("*Mono Kara Koto*" in Japanese), NSK will start a business of **condition monitoring** for bearings. We have developed unique technology for diagnosing bearing abnormalities through our long-standing service for customers. These articles present our work of commercializing this technology, the product of simple diagnosis equipment **BD-2**, and new diagnosis technology.

This issue introduces the technological trends in the areas of bearings and direct-acting products used in **robots**, for which there is ever-growing demand; **wind power generators** coming to receive much attention in Japan, spurred by rapid changes in the global business world to achieve a decarbonized society; **machine tools** with ever-increasing performance involving the recent trends of IoT and robots; and **railroad vehicles**, which are being expanded particularly in developing countries. In addition, we will introduce NSK technology and products that are being used in a variety of industries, such as the **motor industry, mining,** and **steel industries**. Furthermore, we will introduce **guidance robots, omni-direction mobile wheel units**, and **vibration control actuators for train cars**, creating new product regimes.

With four core technologies (material, tribology, analysis, and mechatronics) as our foundation, our company will add new core technologies (organic functional material and sensing technology) while continuing to contribute to the development of society and industry as well as protection of the global environment.

Seiji Ijuin

Approach of Condition Monitoring in Industrial Machinery

Akihide Sakano, Keiichiro Taguchi, and Hiroki Mizokuchi
Industrial Machinery Technology Center, CMS Development Department

Abstract

In industrial machinery fields, IoT (Internet of Things) based solutions are expected to improve O&M (Operation and Maintenance) efficiency. Condition Monitoring, one of applications leading the realization of IoT concept, enables a predictive maintenance to optimize O&M. In this article, we will introduce NSK's latest approaches for condition monitoring by taking an example in wind turbine application.

1. Introduction

Keywords such as IoT (Internet of Things) have become widespread among the general public, indicating a rapid shift to a society where everything is connected to the Internet. Proposals made in many countries (e.g., Industry 4.0, Industrial Internet, Made in China 2025, and Connected Industries) place great importance on the application of IoT. Condition monitoring is regarded as the field that will play a leading role in the realization of IoT, and it is in progress from various aspects.

In the fields of IT and ICT, the predecessors of IoT, NSK has provided technical services of health diagnosis for rotating machines including bearings through providing a diagnostic device NSK Bearing Monitor and the unique analysis system NSK ACOUS NAVI™[1)], which connects global worksites and NSK technical representatives via the Internet.

Bearing Monitor has been replaced with Bearing Doctor BD-2 (to be described later in an article on new products). NSK is making progress in the condition monitoring field through upgrading various products on the basis of analysis and diagnosis technology of ACOUS NAVI™. The present article describes technical research content developed through a research and development project of the National Research and Development Agency, New Energy and Industrial Technology Development Organization (NEDO), as part of the approach to condition monitoring for wind turbines.

2. Condition Monitoring of Industrial Machinery

In the field of industrial machinery, various types of data are gathered from sensor devices installed on equipment (sent via the Internet to be stored on databases and in the cloud) and then analyzed with large-scale data analysis. This leads to benefits in various fields, including design support, production optimization, operation optimization, and preventive maintenance.

In the field of condition monitoring, optimization of Operation & Maintenance (O&M) is expected by promoting preventive maintenance through real-time monitoring of the operating conditions and malfunctions of the facilities and system, including infrastructure such as power generators, railway vehicles, and machine tools.

Before the advent of condition monitoring, O&M was carried out with Time Based Maintenance (TBM), assuring proper machine performance by periodic inspection. It consists of the inspection and replacement of parts after each prescribed period with the objective of preventing malfunctions of facilities. Although its planning is easy, excessive maintenance cannot be avoided. Besides, responding to sudden machine failure is difficult. Moreover, measurement devices for periodic inspection are designed with a priority on portability and easy installation, limiting the capability. Furthermore, the judgment of a machine fault highly relies on knowhow and the experience of maintenance staff.

In contrast, facility maintenance based on condition monitoring uses condition monitoring devices while taking full advantage of IoT. It continuously evaluates the condition of the facility and predicts the machine fault before it happens. It is Condition Based Maintenance (CBM) that maintains the facilities more reasonably. The monitoring devices installed on the facilities continuously transmit the measurement data to the server through the network. The server analyzes various evaluation values, detects the changes in time sequence, and reports the result to the maintenance staff. That enables the maintenance staff to make a timely and appropriate maintenance plan based on the result. Extension of the period between maintenances along with adequate arrangement of spare parts reduce cost.

3. Condition Monitoring of Wind Turbines

Due to a recent increase of the momentum of renewable energy, more wind turbines are expected to be installed over the medium and long term. Further reduction of power generation cost requires an improvement of the capacity factor (facility availability). Figure 1 shows the failure frequency for subcomponent part of a wind turbine and the associated repair downtime (period of non-operation ≒ maintenance period). The downtime of the rotation parts near the drive train of the item on the bottom row exceeds 20 days on average. Some repairs can be done inside the nacelle, but in case the failed part should be moved out of the nacelle, heavy machinery such as a large crane must be arranged. In Japan, where more than 70% of the land area is mountainous, the land available for installation is limited. Consequently, it is expected that offshore wind turbines will increase but become more difficult to access. In such a circumstance, operation optimization with condition monitoring would provide a great advantage.

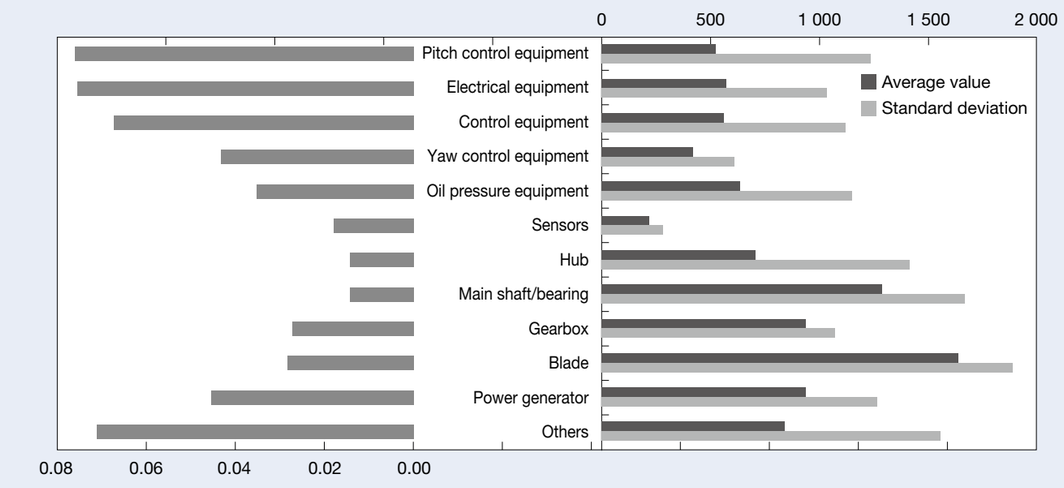

Fig. 1 Failure frequency and repair downtime[2)]

3.1 Objective of condition monitoring

When a large component such as a gearbox needs to be replaced, in addition to the parts for replacement, heavy machinery such as a crane has to be arranged for the purpose of lifting the component to the nacelle and taking down the old part. With a weak wind duration, summer in Japan is suitable for maintenance work. The lack of power generation during maintenance work in a weak wind duration makes for a small disadvantage for power generation. Requirements for condition monitoring are the early detection of a machine fault and estimation of the life time before the wind turbine plunges into a major failure. In general, wind turbines power generators are operated in a wind farm where there are multiple wind turbines. Early detection of a machine fault and life time estimation would enable an efficient maintenance plan, such as a crane, which can be arranged for maintenance work for multiple wind turbines.

3.2 Issues of condition monitoring

Figure 2 shows the structure of a standard wind turbine. The main object of condition monitoring is the drive train, which comprises a generator, and the main shaft bearing, which supports the main shaft connected to the gearbox and the blade. The main shaft of an MW class wind turbines rotates at 10–30 rpm by the wind. The gearbox amplifies the rotation speed by 80–100 times, driving the generator. Detecting a fault of the main shaft bearing is quite difficult because the SN ratio is extremely low. The signal level from the damage source is low due to a small vibration energy lead by slowly rotation. Moreover, there is a variety of noise sources, such as the gearbox, the generator connected to it, the yaw control system rotating the nacelle, and the pitch control system adjusting the blade angle.

The fault detection of the main shaft bearing was addressed in the NEDO project. Measuring real wind turbines clarified the issue and proposed its solution. The next chapter describes its content.

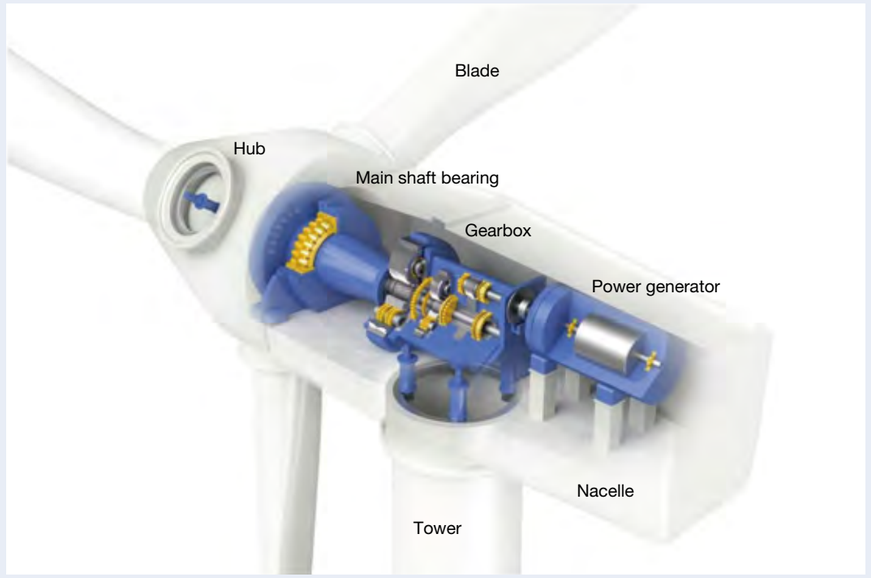

Fig. 2 Schematic image of a wind turbine

4. Damage Detection of the Main Shaft Bearing for Wind Turbines

As the first task in the fault detection of the main shaft bearing, a damage simulation test was carried out with the aim of investigating the relationship between the extent of the bearing damage and vibration. Then, vibration of a real wind turbine was measured, and vibration data up to the point of damage and replacement was obtained. On the basis of comparison of these sets of data, some issues are described. Some solutions are proposed for them.

4.1 Damage simulation test

A damage simulation test was carried out with main shaft bearings for a 2 MW class wind turbine. As shown in Figure 3, bearings with four levels of artificial defects were prepared, ranging from extremely minor damage to serious damage prohibiting continued operation. The numbers in parentheses are the ratios of the damage area, the fraction of the damaged area to the bearing raceway surface as indication of the extent of the damage. The testing conditions set were the load equivalent to a real machine and three conditions of rotating speed.

Figure 4 shows the test result, with $d_m \cdot n$ (roller pitch radius of the bearing d_m × rotation speed n) as the horizontal axis and the ratio of effective values of vibration acceleration (absolute value) to normal values (relative value) as the vertical axis. In tests with no vibration source in the environment, the vibration levels increased with higher rotation speeds and are further enhanced uniformly with higher damage levels.

4.2 Measurement in the real wind turbine

A measurement of vibration has been carried out on 4 wind turbines at a standard power output of 1 MW

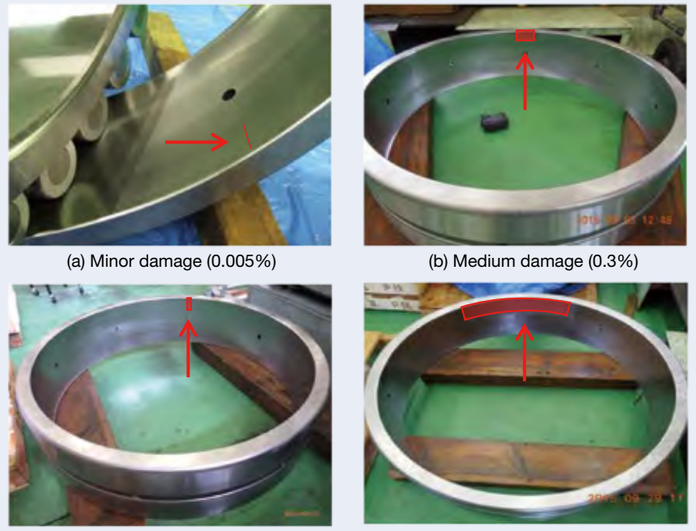

(a) Minor damage (0.005%)
(b) Medium damage (0.3%)
(c) Major damage (1.3%)
(d) Serious damage (13.2%)

Fig. 3 Artificial defect on rolling bearings

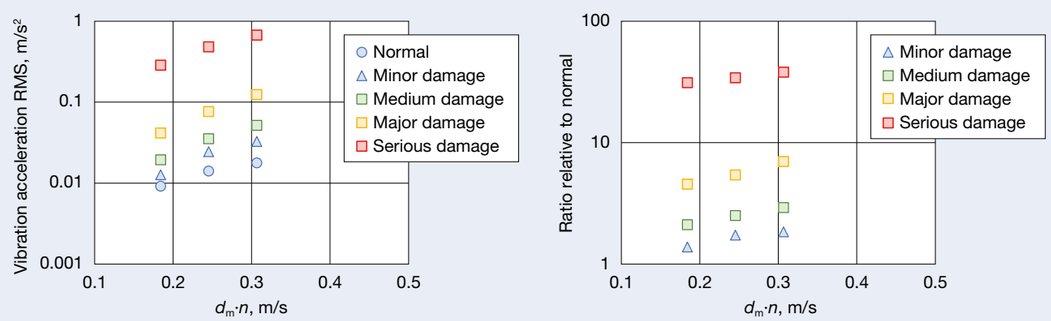

(a) Absolute value evaluation
(b) Relative value evaluation

Fig. 4 Experimental results using artificial defected rolling bearings

in the same wind farm. Figure 5 shows the outline of the measurement. The measurement data was sampled simultaneously at 25 kHz with a monitoring system installed in the nacelle.

Measurements were carried out continuously from November 2015 to October 2017, during which period a failure was found in the main shaft bearing in one of the wind turbines, which was replaced in May 2017. As shown in Figure 6, a flaking which had a damage area ratio of about 3% occurred in one place on the outer ring raceway surface and the vibration acceleration measured on the main shaft bearing on which the flaking occurred is shown in Figure 7. It shows the average and the standard deviation of RMS value in the selected three months (December 2016: six months before replacement, April 2017: immediately before replacement and September 2017: immediately after exchange). As demonstrated in the damage simulation test, the vibration depends on the rotation speed. Therefore, only the data with a rotation speed of 21.4–21.6 rpm near the nominal rotation speed of this wind turbine was taken. The average value itself moves up and down before and after the damage replacement. However, the variation represented by the standard deviation is too large. The comparison with the test results are shown in Figure 4 (real wind turbine $d_m \cdot n$ = 0.24 m/s). The absolute value of April 2017 reaches serious damage level; however, relative value (ratio of values before the replacement to those after) are within the range of minor damage.

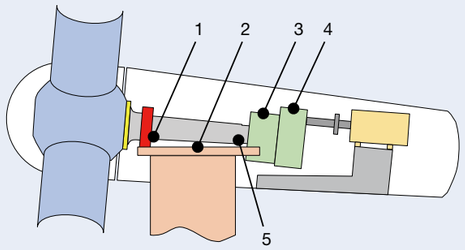

Number	Location	Measurement
1	Main shaft bearing	Vibration acceleration
2	Nacelle floor	Vibration acceleration
3	Gearbox: planetary part	Vibration acceleration
4	Gearbox: high speed part	Vibration acceleration
5	Main shaft	Rotation speed

Fig. 5 Measurement points on a wind turbine drive train

Fig. 6 Flaking damage on the outer-ring of a main shaft bearing

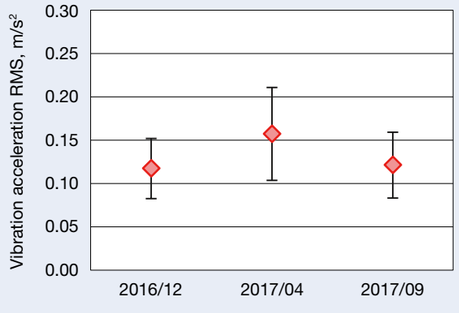

Fig. 7 Measurement results of a main shaft bearing

Figure 8 shows the time waveform of the main shaft bearing vibration during the damage simulation test (medium damage) and the real machine measurement (immediately after the damage replacement). In the test result, an interval of impact vibration 0.24 seconds matches a specific bearing defect frequency from artificial defect. In contrast, the real wind turbine measurement result of a normal condition immediately after replacement is equivalent to the impact vibration of the test. Impact vibration of a much larger amplitude also occurred.

Figure 9 is a schematic of the vibration transfer path around the main shaft bearing of a wind turbine. Blade/hub vibration driven by the wind is transmitted to the main shaft bearing through the main shaft. Similarly, gearbox vibration is transmitted to the main shaft bearing too. The structural vibration of the tower supporting the nacelle including the drive train is also transmitted. Therefore, the issue is to assure an appropriate SN ratio for damage detection of the main shaft bearing by reducing the influence of these disturbance vibration.

4.3 Damage detection at the real wind turbine

In this section, to obtain an appropriate SN ratio for damage detection of the main shaft bearing, the environmental vibration should be adequately processed as external disturbance. Accordingly, each vibration from the surrounding structure shown in Figure 9 was analyzed. Here all analyses used data from the wind turbine without any damage detected on the main shaft bearing and from operation at the nominal rotation speed.

(1) Gearbox

Figure 10 shows a frequency analysis result of the vibration at the gearbox planetary part and the main shaft bearing, measured synchronously. The gearbox of this wind turbine has one planetary stage and two parallel stages. Table 1 shows the vibration characteristic such as a gear mesh frequency resonated by gearbox components.

In the spectrum of (b) the gearbox planetary part, gear mesh frequency of second parallel stage can be seen up to 4th harmonic frequency (3.2 kHz). On the other hand, at the main shaft bearing, up to the third harmonic (2.4 kHz) of it can be confirmed, indicating that the influence range of the gearbox vibration is lower than 3 kHz. However, the vibration level of second harmonic or higher frequency are largely decrease.

(2) Blade / Hub

The high level impact vibration shown in Figure 8 (b) can be detected inside and outside the nacelle by human ears. The source can be identified inside the hub, and the occurrence, frequency, and amplitude depend on each wind turbine. the time wave form and frequency analysis results of the main shaft bearing vibration for a case in which impact vibration occurred significantly. The impact vibration occurred at an interval of about 3 seconds, and the main shaft rotation period is confirmed to have an influence on the spectrum range from 1 kHz to 6 kHz.

(3) Tower / Nacelle

Figure 12 shows a frequency analysis result of the vibration at the nacelle floor and the main shaft bearing measured synchronously. Both show approximately similar results in the frequency range up to 10 Hz, where the structural vibration arises. The peak at 0.5 Hz is the

Table 1 Gearbox spectrum frequency

Item	Fundamental frequency (Hz)
Low speed axis rotation	2.39
Medium speed axis rotation	11.94
High speed axis rotation	25.00
Planetary part meshing	36.55
Low-medium speed meshing	215.00
Medium-high speed meshing	800.28

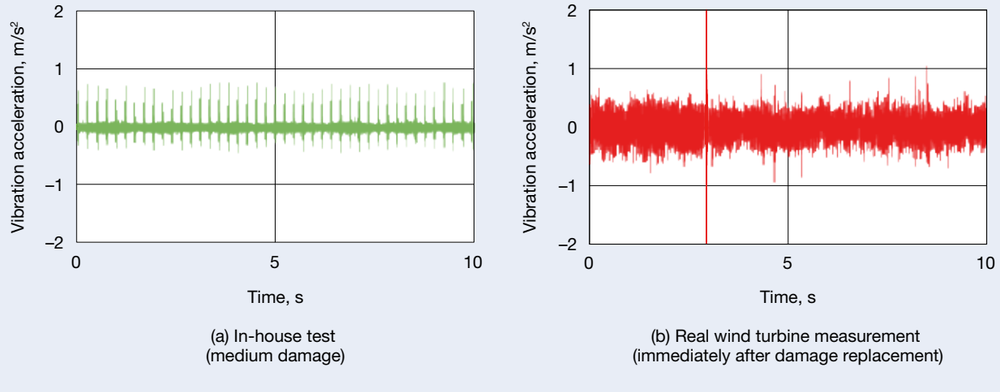

Fig. 8 Time domain waveform of main bearing vibration

fundamental frequency of the characteristic vibration of the tower. This spectrum range covers the main shaft rotation frequency of about 0.33 Hz and the blade pass frequency of about 1 Hz = 3 × 0.33 Hz. However, these levels are low compared to the characteristic vibration of the tower including higher harmonics.

The vibration signal measured at the main shaft bearing is superimposed of these external disturbances and the main shaft bearing internal vibration. Based on these result, the data before and after the damage replacement is analyzed, and an appropriate damage detection method is proposed. Figure 13 shows the time wave form of the main shaft bearing vibration before and after the damage replacement. The impact vibration occurring before the replacement has an interval of about 0.2 s, which is different from the impact vibration of the blade / hub described above. In contrast, this impact vibration disappeared after the damage replacement.

The frequency analysis result of the time wave form in Figure 13 is shown in Figure 14. Before the replacement, vibration level in the frequency range from 2 kHz to 6 kHz is strongly excited, and the level of near 100 Hz is also high. The result of envelope analysis applying to the each excited frequency range is shown in figure 15. Although it is more obvious for 2 kHz to 6 kHz before replacement, shown in figure 15 (b), the spectrum peak 4.9 Hz is visible

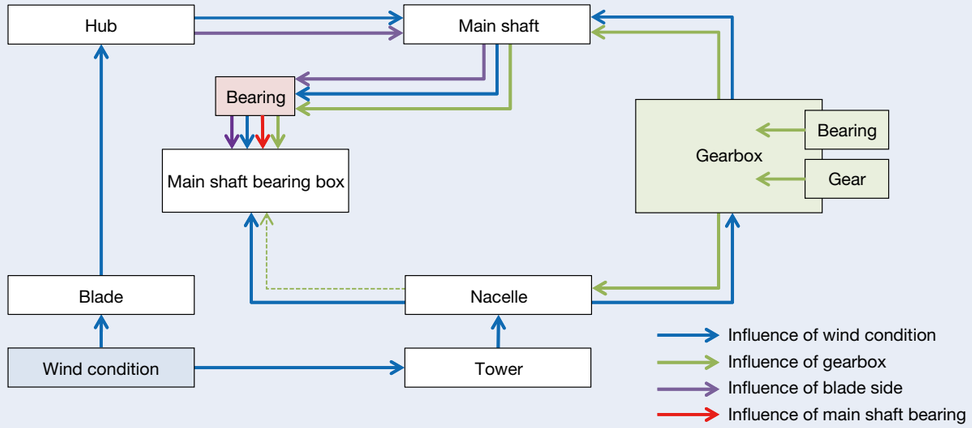

Fig. 9 Vibration transfer path around a wind turbine main shaft bearing

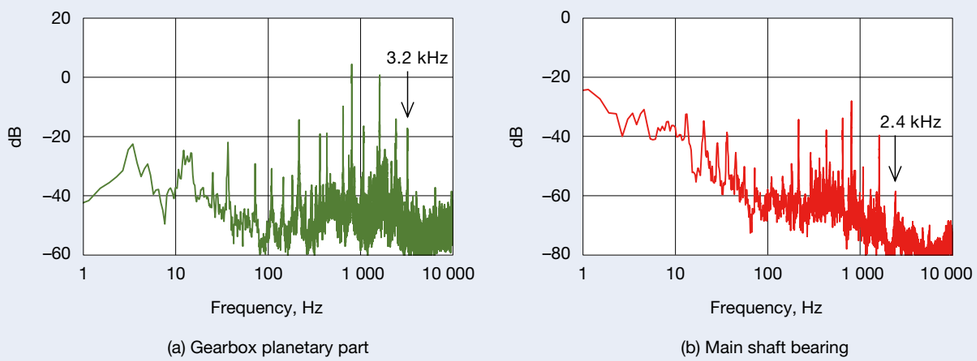

Fig. 10 Effect of gear mesh vibration from a gearbox

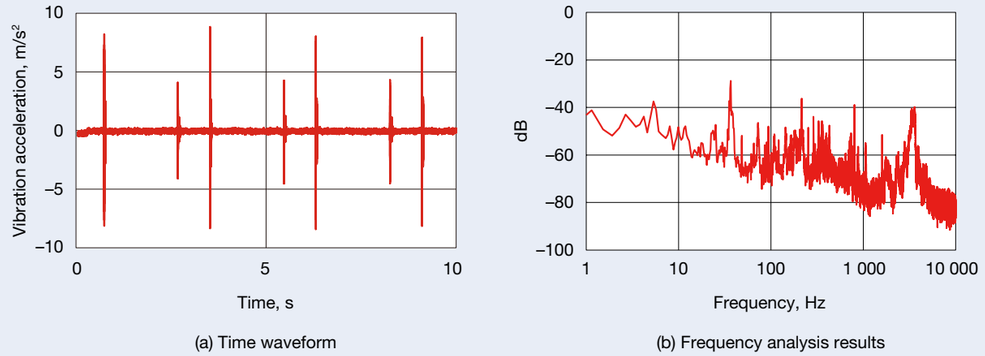

Fig. 11 Effect of impulse vibration from a blade and hub system

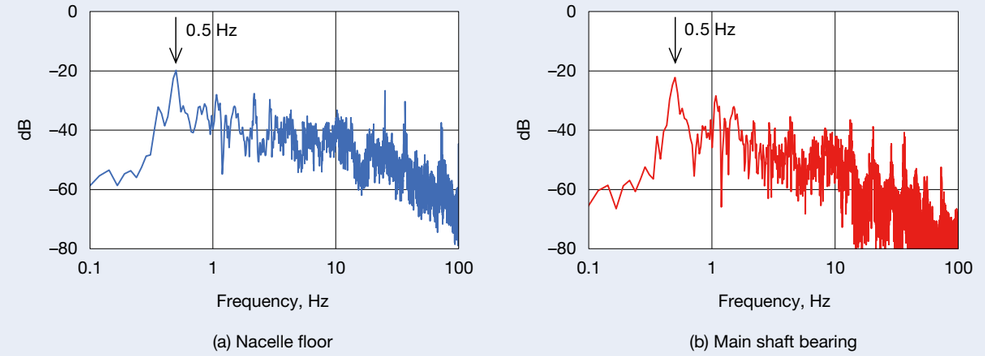

Fig. 12 Effect of structural vibration from a nacelle (tower)

up to the higher harmonics. These results indicate that the outer ring of the main shaft bearing is damaged. This peak frequency of 4.9 Hz is consistent with the interval of 0.2 s of the impact vibration confirmed by the time wave form mentioned above. Here, 50 Hz to 200 Hz is the frequency range of the influenced gearbox vibration, and 2 kHz to 6 kHz is that of the impact vibration from the blade/hub, hence the SN ratio at each frequency range is reduced. However, the influence of the gear vibration component of the second harmonic or higher is small. From these results, the frequency range of 50 Hz to 150 Hz is the most adequate for the bearing detection of this wind turbine main shaft bearing.

Figure 16 shows the result after having applied a band path filter of the frequency range of 50 Hz to 150 Hz to the same data shown in Figure 7. For bearing damage detection, the sensitivity indicated by the difference in the vibration level can be improved and the variation can also be significantly reduced. A comparison with the result of the similar filtering on the damage simulation test data is shown in Figure 17. (a) In the absolute value evaluation, the damage level is not evaluated correctly. This means that because the vibration transfer path between the vibration source and the sensor position is different between the real wind turbine and the test rig, it is difficult to perform an evaluation with the absolute

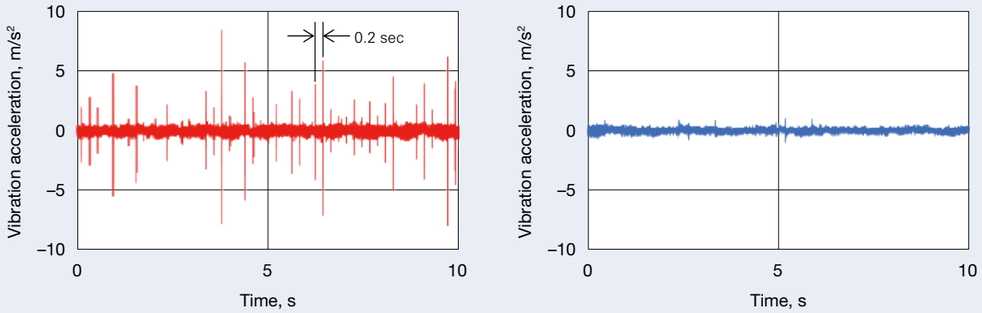

(a) Before damage replacement

(b) After damage replacement

Fig. 13 Time waveform of the main shaft bearing vibration before and after replacement

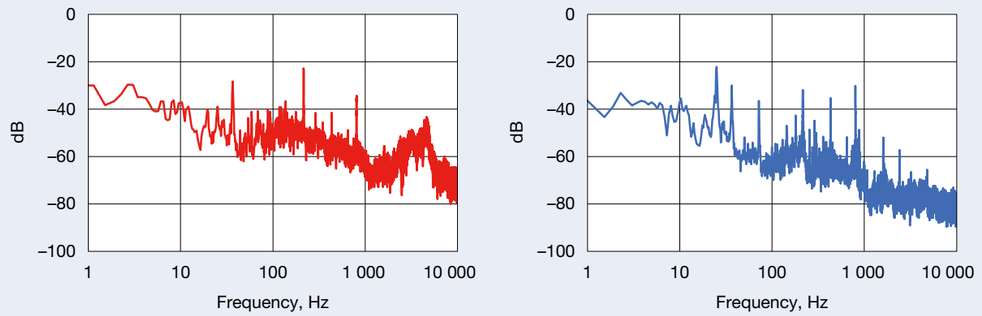

(a) Before damage replacement

(b) After damage replacement

Fig. 14 Frequency analysis results of the main shaft bearing vibration before and after replacement

value. In contrast, (b) in the relative value evaluation, damage level is similar to the serious damage level (damage area ratio = 1.3%). The vibration transfer path involves nonlinearity such as the bearing gap and temperature change, etc. However, it regards that the taking of a ratio largely cancels out the difference in the vibration transfer paths and leads to this result. This evaluation methods mentioned above require the setting of filtering on each type of wind turbine, which presupposes the understanding of the wind turbine mechanism. In contrast, the trends in IoT, such as machine learning and big data analysis, are expected to contribute to the evaluation.

5. Postscript

This report introduces the technical research content regarding NSK projects on condition monitoring of industrial machinery, taking the wind power field as a subject.

NSK continues to grapple with the development of condition monitoring, not only with wind power generators but also in a variety of fields covering NSK products. NSK proposes new technologies and develops new products on the basis of the market needs obtained through measurement data as well as through condition monitoring.

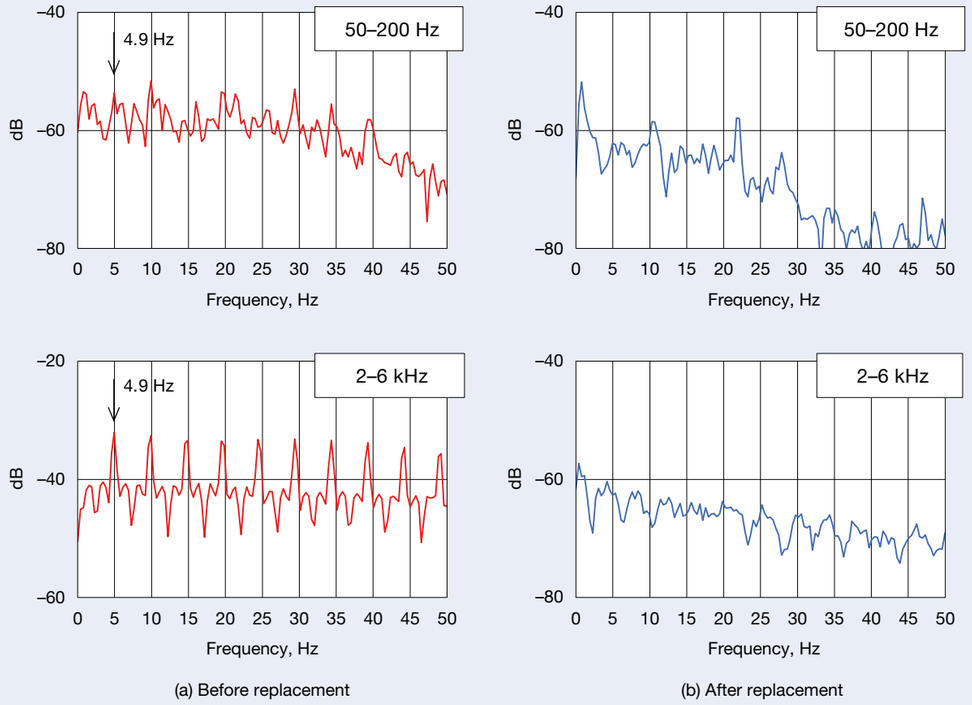

(a) Before replacement

(b) After replacement

Fig. 15 Envelope analysis results of the main shaft bearing vibration before and after replacement

6. Acknowledgments

This article describes technical research content on condition monitoring of wind turbines developed through a research and development contract of the National Research and Development Agency, New Energy and Industrial Technology Development Organization (NEDO). We would like to express our sincere gratitude to NEDO, other research collaborators, and wind power companies for their cooperation in the measurement on real machines.

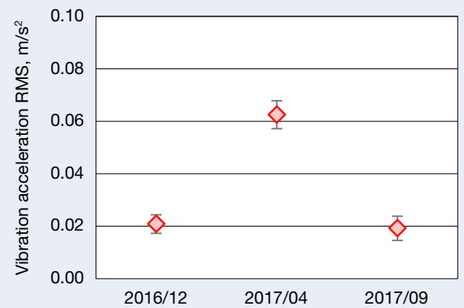

Fig. 16 Measurement results of the main shaft bearing applying a noise reduction filter

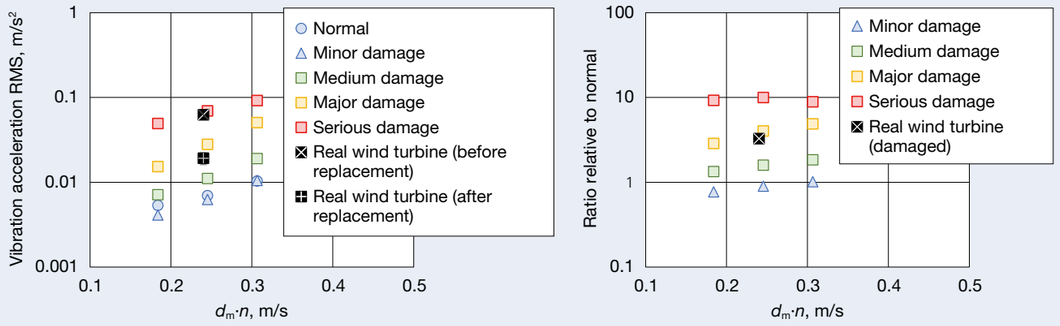

Fig. 17 Comparison between experimental and measured main shaft bearing vibration applying a noise reduction filter

References

1) Y. Muto and T. Miyasaka, "Bearing Noise Digital Analysis System ACOUS NAVI," NSK Technical Journal, Vol. 674, 2002, pp. 27–30.
2) Y. Kikuchi, R. Saito and T. Ishihara, "Assessment of operation and maintenance cost considering uncertainty in repair coasts and down times," Wind Energy Symposium, Vol. 38, 2016, pp. 55–58.

Akihide Sakano

Keiichiro Taguchi

Hiroki Mizokuchi

Technical Trend of Industrial Machinery Bearings

Hiroshi Ishiguro
Industrial Machinery Bearing Technology Center,
Robot & Motor Bearing Technology Department

Abstract

In recent years, industrial machineries demand remained steady and it will continues to good result in the future. In the globally, efforts to solve universal problems are expanding such as sustainable consumption, production, and climate change countermeasures for all countries. The industrial machinery industry has greatly contributed to a sustainable society by daily technological innovation. This paper introduces the latest technology of bearings used in these industrial machines such as Robot reducer, Servomotor, Mining machinery and Shale gas related machines.

1. Introduction

Over the past few years, the decrease in the working-age population and increase in labor costs have spurred a rapid increase in demand for industrial robots. In addition, increases in the global population and the economic growth of developing countries are promoting the mining of iron ore, copper, and other mine resources as well as natural gas.

On the other hand, the United Nations has instituted the Sustainable Development Goals (SDGs), including sustainable measures for consumption, production, and climate change for all countries, adopting a resolution to address these issues with the aim of resolving them.

A variety of industrial machinery fields are deeply involved in the SDGs and are contributing greatly to a sustainable society through daily technology innovation. This article describes the state-of-the-art technology of the bearings used in these industrial machines.

2. Technology of a Reduction Gear for Robots and Servomotor Bearings

The main drive source of the robot uses an electric servomotor with good controllability and easy handling. However, since the motor output is high speed rotation and low torque, a reducer is needed to convert the output to low speed rotation and high torque. This article describes the technology of the bearings used in servomotors and reducers.

2.1 Technology for servomotor bearings

Robot-mounted servomotors are operated in harsh environments where they are subjected to significant switching between forward and backward rotation, and between start-up and shutdown. They are also operated in harsh environments with external forces and vibrations due to high speed movement of the arms and with high temperature in the arms. The required functions are a precise control of rotation, stopping, and positioning, which are undertaken by brakes and encoders attached to the motor shaft. Technological issues include brake slippage and read errors due to oil contamination on the surface of the brake plates and encoder plates.

NSK performs simulation experiments to confirm the relationship between the grease scatter inside the bearing and the contamination of the encoder. Figures 1–4 show the outline and the result of contamination. These results have confirmed the effectiveness of the technologies NSK developed, such as low dust LGU grease and light contact DW seals, and earned a reputation in the market for high reliability.

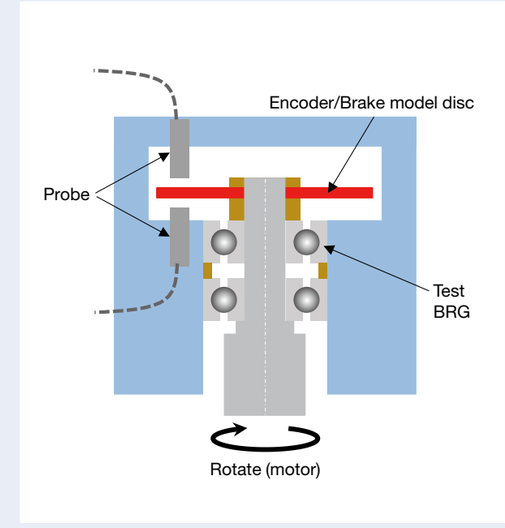

Fig. 1 Simulation test outline of encoder

2.2 Technology of bearing for robot's reduction gear

Since reduction gears for robots are used in arm joints, the requirements include compactness, light weight, low backlash, high rigidity, and long life. Since the output shaft is exposed to heavy external weight and moment loads, NSK takes full advantage of its analysis technology to provide special bearings compatible with both high rigidity in a limited space and long life. Figure 5 shows a specific example. Here, the optimized internal design such as the number of balls, and contact angles and operation preload are set to achieve both high rigidity and long life.

Also, the input shaft and intermediate shaft are exposed to heavy weight loads, leading to the adoption of small needle bearings and tapered roller bearings with low volume and high load capacities.

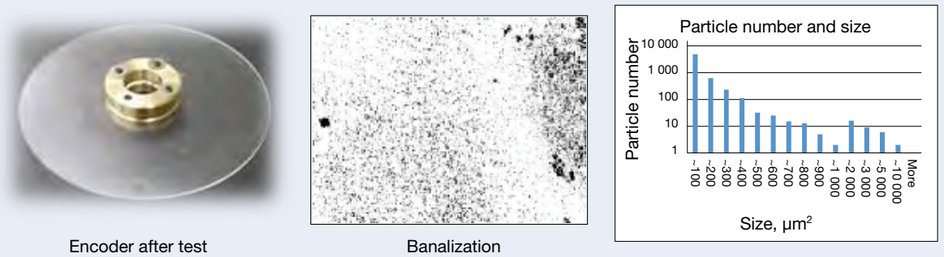

Fig. 2 Out gas adherence on the encoder surface (none contact seal)

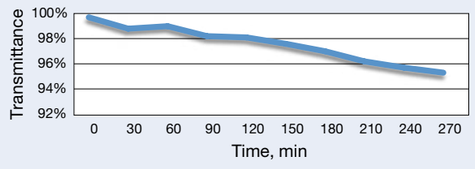

Fig. 3 Change in transmittance of encoder disc by out gas adherence (none contact seal)

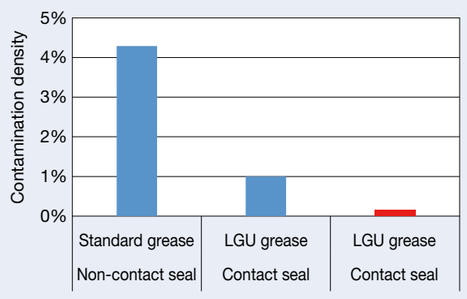

Fig. 4 Encoder simulation test result (grease/seal type)

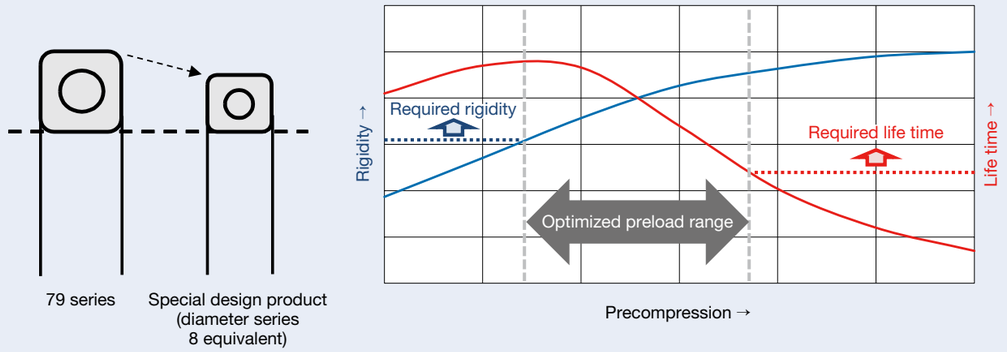

Fig. 5 Design examples of robot reducer bearings

3. Technology of Bearings for Mining Machinery and Shale Gas Industry Machinery

This section describes the long lifespan technology of the bearings for mining machinery and the technology of bearings for thermal power generation by natural gas, with the lowest amount of CO_2 emission among fossil fuel thermal power generation.

3.1 Technology for bearings used in mining machinery

The pulleys for mining conveyors that have a total length of several kilometers or more use self-aligning roller bearings that can absorb shaft deflection with high load capacity. The bearing replacement work requires precise control of internal clearance, leading to the adoption of the seal-less type bearing. NSK developed a "high sealing and self-aligning roller bearing" (Photo 1, Figure 6), which adopts a unique bolting seal, enabling precise control of clearance during bearing installation with high sealing performance. It has a good reputation in the market. The design of this new bearing is optimized so that the width remains the same as the conventional bearing even after high performance seals installed. Furthermore, Hi-TF technology[1)] with long life makes the load capacity of the bearing similar or superior to conventional products. Consequently, this new bearing achieves long life even in a harsh environment with a high weight load and where there is a lot of dust.

Figure 7 shows the test operation result at a mining site of the conventional products and the new product. While the conventional product showed flaking after being operated for about one year, the new bearing showed no abnormalities such as flaking. The amount of contaminants in the grease was about 1/10 of the amount in the conventional product, proving high sealing performance.

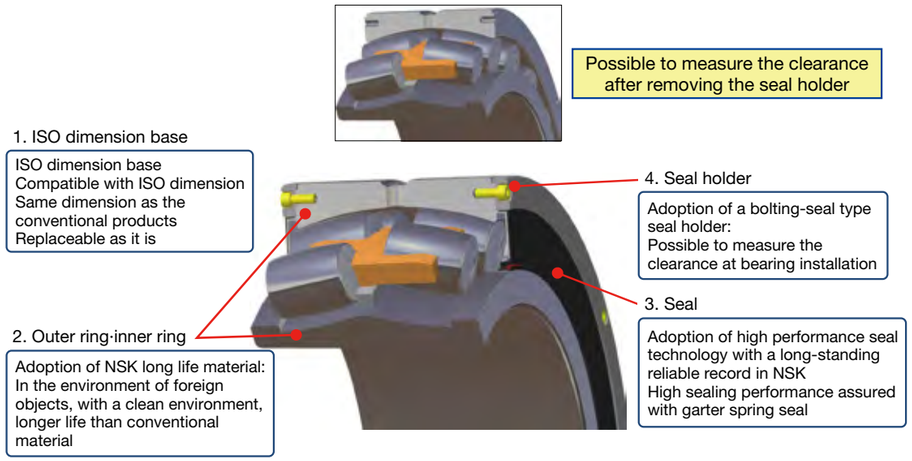

Fig. 6 Specifications of the new bearing

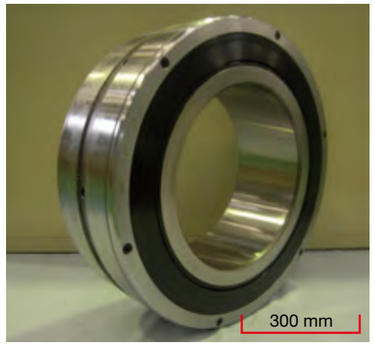

Photo 1 Spherical roller bearings featuring high reliability and excellent sealing performance for conveyors

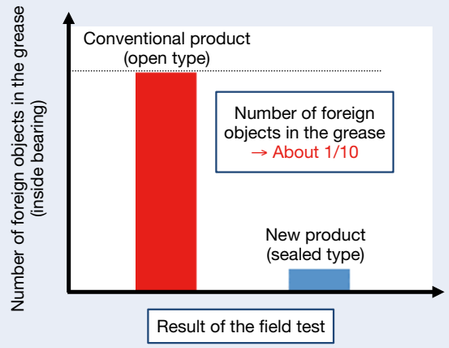

Fig. 7 Comparison of particles in grease

3.2 Technology of bearing for liquefied gas pump

Liquefied gas pumps are specialized pumps (Figure 8) for accepting, transporting, and feeding a variety of liquefied gases on a tanker or in an onshore plant. Representative liquefied gases include liquefied natural gas (LNG, −162ºC), liquefied petroleum gas (LPG, about −40ºC), and liquid nitrogen (LN2, −196ºC). The impeller of this pump are supported by a bearing lubricated by liquefied gas. Rust inhibitors for bearings cannot be used due to the cryogenic environment. Therefore, stainless steel with high corrosion resistance is adopted for the bearing. The cage material is a low-temperature, highly self-lubricating fluorocarbon resin, which is fastened with special rivets (Figure 9).

In recent years, adoption of silicon nitride ceramic ball bearings has been increasing as a measure to prevent electrolytic corrosion due to inverterization of the pump motor. Since these balls have excellent performance against erosion, they are expected to have a longer lifespan and improved reliability. However, since the coefficient of linear expansion of this ceramic ball is extremely small compared to the stainless steel of the inner and outer rings, there is a problem that the radial internal clearance largely changes in the range from room temperature to extremely low temperature (−196ºC). As a countermeasure, we are promoting the commercialization of the high-performance new ceramic ball bearing spaceaCRYO™ (Photo 2) using a new ceramic material with a linear expansion coefficient close to that of stainless steel in the inner and outer rings.[3]).

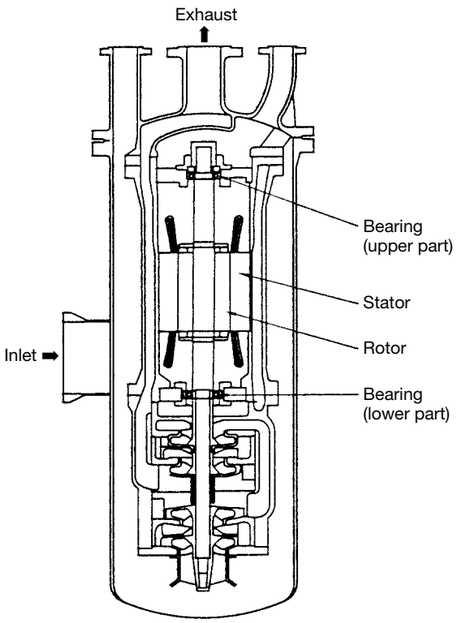

Fig. 8 Outline structure of liquefied gas pump

Photo 2 New high-performance ceramic ball bearing; spaceaCRYO™ and new ceramic balls

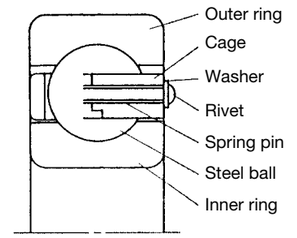

Fig. 9 Outline structure of bearings for liquefied gas pump

3.3 Technology of bearings for a shale gas mining drill head

Recently, the mining of petroleum and natural gas has become possible from the shale layer at around 2 000 m below the surface of the ground, resulting in a rapid increase in the mining output, mainly in North America. The drill motors for drilling a hole reaching the shale layer have a large load, with a structure where the internal bearing is lubricated by muddy water (the structure of a drill motor is shown in Figure 13). The main requirements for the bearing are the least amount of raceway wear possible even with muddy water lubrication and no fracture of raceway rings and rolling elements during operation. The specifications of the bearing satisfying the requirements above are 4 point contact ball bearings (multistage all balls), inner and outer rings made of carburized steel, and balls made of S2 tool steel (ASTM A681).

NSK has completed a field evaluation of the new bearings, adopting unique materials for the inner and outer rings. As a result, it was confirmed that there was no fracture in the bearing, and the wear characteristics were also equal to or less than the current carburized material (Photo 3). NSK continues to collaborate with drill manufacturers with the goal of establishing the specifications of optimized bearings.

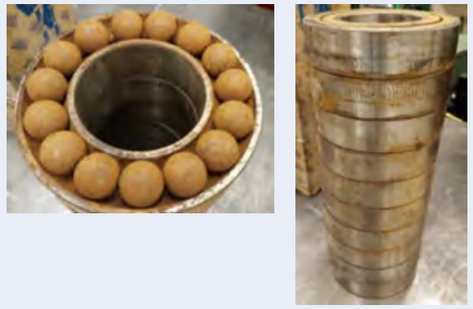

Photo 3 Internal bearing condition after field test

Fig. 10 Structure of drill motor

4. Postscript

This article describes the technology of the bearings used in industrial machinery. In recent years, “smart”, which shows optimization, multi-functionalization, energy saving, etc., using AI technology and IoT, which are increasing in all fields. Similarly for industrial machines, “smart” development has been promoted for the purpose of high efficiency and energy saving production and labor saving in the area of maintenance. It is necessary not only to respond to the conventional small size, light weight, high load capacity, and long life of bearings but also to meet new requirements such as bearing deterioration diagnosis and prediction of bearing life expectancy. NSK will continue the development of bearings to meet these needs.

References

1) NSK Technical Journal No. 652 (1992) 9–16.
2) S. Niizeki, K. Nonaka, S. Matsunaga, “Rolling Life of Ceramic bearings under oil lubrication and water lubrication,” Proceedings of the International Tribology Conference, Yokohama (1995) 1,399–1,404.
3) NSK Technical Journal No. 689 (2017), 78–79.

Hiroshi Ishiguro

Technical Trend of Wind Turbine Bearings

Kim Leong LEE
Industrial Machinery Bearing Technology Center,
Wind Turbine & Heavy Industries Technology Department

Abstract

In recent years, wind turbines are growing in size and shifting their installation location from onshore to offshore to improve power generation efficiency and reduce power generation cost. As higher torque applies to the bearings used in large wind turbines than conventional wind turbine, larger size and higher capacity bearings are required. Technical trend, typical failures and its countermeasure details for bearings used in main rotor shafts, gearboxes and generators are explained. Due to the repair cost for large offshore wind turbines is higher than onshore wind turbines, higher bearing quality control is required to improve reliability of wind turbine.

1. Introduction

Construction of wind turbines evolved rapidly after 2005 in its expanding market. Since 2009, installations of new wind turbines has slowed; however, as global environmental protection is highly valued, the number of wind turbines is steadily increasing as a renewable energy source that does not produce CO_2. This increase in wind turbine installations is likely to continue (Figure 1).

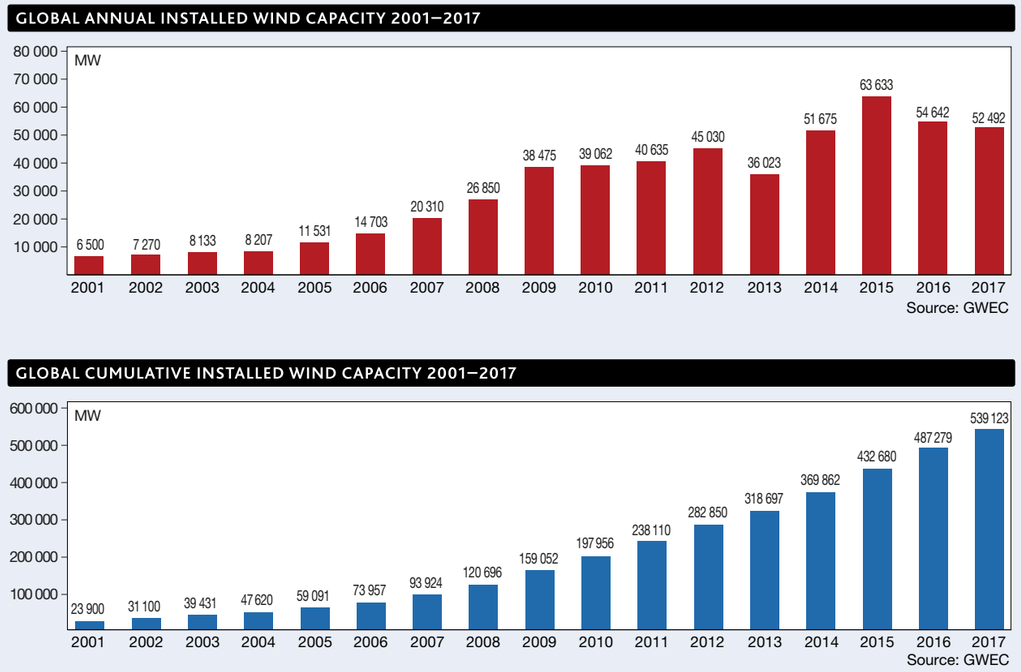

Fig. 1 Global installation of wind turbines

2. Technological Trend of Wind Turbines

Recently, in order to improve power generation efficiency and reduce the cost of power generation, there has been a shift to create bigger wind turbines and install them offshore. At present, the mass-produced offshore wind turbine of the largest power generation capability is produced by MHI Vestas, and it generates 8.0 MW. MHI Vestas has announced that they developed a successor with a capacity of 9.5 MW. Furthermore, GE announced in March 2018 that they will develop a 12 MW offshore wind turbine. The shift to creating bigger wind turbines and installing them offshore is picking up speed.

There are two types of wind turbines, one with a speed-up gear and the other without one (Figure 2). In the current top ten list (Table 1) of large capacity wind turbines, both types exist. Elimination of the speed-up gear would diminish the number of mechanical elements that may fail, thus improving reliability. However, the wind turbine would become larger and more complex, making it more expensive and heavier. The mass-produced MHI Vesta turbine (8.0 MW) and the new 9.5 MW model both have a speed-up gear, and it is thought that future offshore large wind turbines will utilize this gear as well.

3. Bearings for Wind Turbines

Figure 3 shows the equipment constituting the drivetrain of a general wind turbine with a speed-up gear, and the typical bearings used in the drivetrain. In the main shaft, the speed-up gear and generator of the drivetrain of a wind turbine, bearings of different types and sizes are used. One or two bearings with an outer diameter of 1–2 m are used in the main shaft, depending on the support type. Many bearings with an outer diameter of 0.2 m–2 m are used to support several gear shafts in the speed-up gear. The generator uses bearings with an outer diameter of 0.4–0.6 m to support the rotor shaft.

As wind turbines get bigger, market demand for larger bearings and bearings with high load capacity will increase. The next section describes bearings for the wind turbines that NSK developed in response to these demands.

3.1 Main shaft bearings

Since the bearings supporting the main shaft bear the large radial and axial loads transmitted from the wind-facing blades to the main shaft, they require high rigidity.

One of the main shaft structures of typical wind turbines is a three-point-support type supported by a single bearing (Figure 2). This type uses spherical roller bearings for the main shaft bearing.

As wind turbines get bigger, the load on the bearings becomes larger. A big wind turbine supports the main shaft with two bearings (Figure 2). This type uses single-row or double-row tapered roller bearings, single-row cylindrical roller bearings, and spherical roller bearings.

Table 1 Ten of the biggest wind turbine

Order	10 of the biggest wind turbines	Type
1	MHI Vestas V164 / 8.0MW	Gear
2	Adwen AD-180 / 8.0MW	Gear
3	Siemens-Gamesa Renewable Energy SWT-8.0-154	Gearless
4	Enercon E-126 7.5MW	Gearless
5	Siemens 6.0 154 / 7.0 154	Gearless
5	Ming Yang SCD 6.0MW	Gear
6	Senvion 6.2M152	Gear
7	GE Haliade 6MW	Gearless
7	Sinovel SL6 000	Gear
8	Dongfang/Hyundai Heavy Industries 5.5MW	Gear
9	Hitachi HTW 5.2MW-127	Gear
10	Adwen AD5-135	Gear

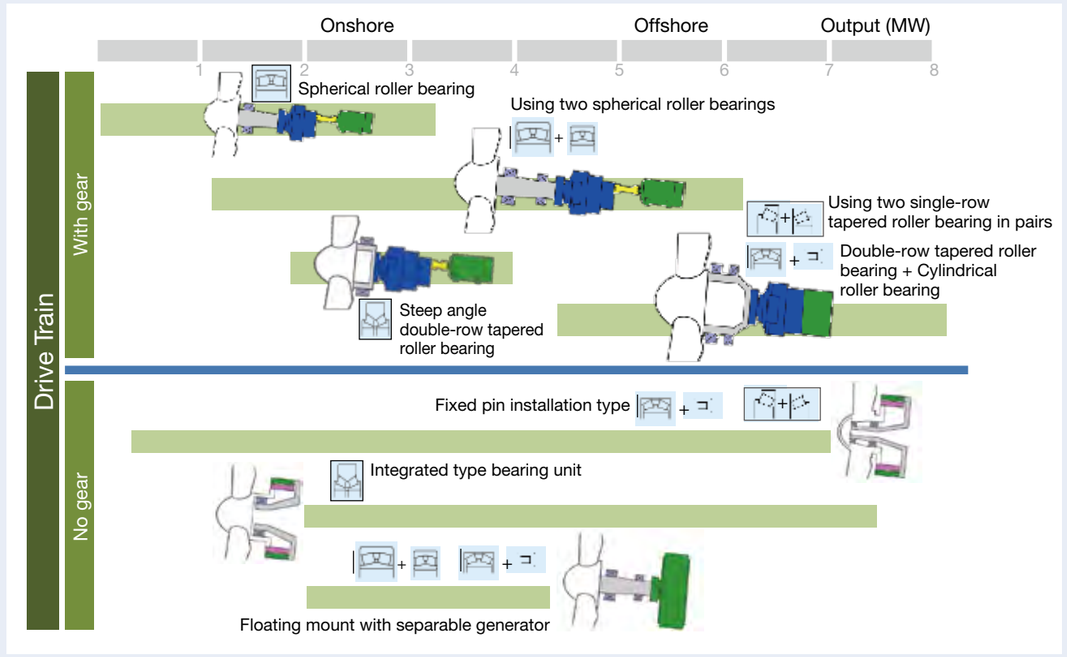

Fig. 2 Types of wind turbines

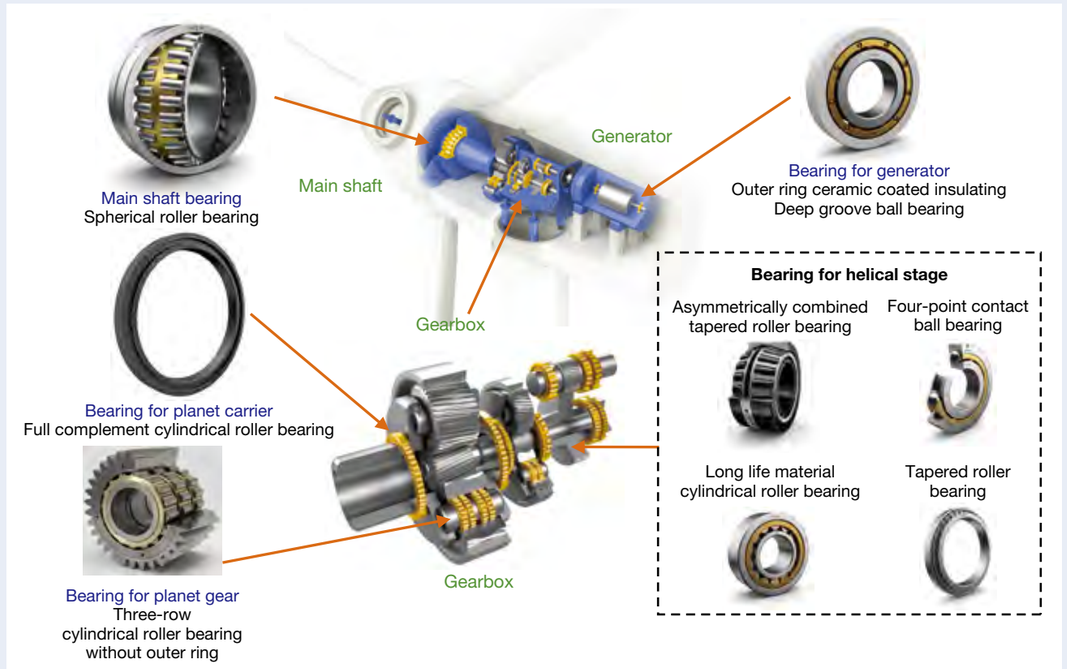

Fig. 3 Wind turbine components

The main shaft rotates at a very slow rotation speed of 8–15 rpm, so the lubrication condition inside the grease-lubricated bearing is poor. Moreover, in a spherical roller bearing, a specific differential slippage occurs, which often wears out and damages the bearing (Figure 4). NSK, considering that the coating of Diamond-Like Carbon (DLC) on the spherical roller bearing is effective against that wear, is carrying out the evaluation.

3.2 Bearings for speed-up gears

A speed-up gear is used to increase the extremely slow rotation speed of the main shaft to the high rotation speed of the generator. Many gears are used for a high speed-up ratio. The gear shafts use 10–20 bearings for support.

The main shaft of the 4 MW class rotates at around 11 rpm, while the 4-pole generator rotates at 1 500–1 800 rpm, requiring a speed-up ratio of over 130. On the other hand, since the blade edge speed is restricted due to the wind noise issue, the main shaft rotation speed must be lowered as the wind turbines become larger (blades become longer). For the case of speed up the low main shaft rotation speed to the rotation speed of a 4-pole generator, a speed-up ratio of over 150 is required. Therefore, a system adopts a generator having more than 4 poles and a speed-up gear of a low speed-up ratio (around 50)[1)] (Medium Speed Type) is also used.

As Figure 5 shows, 1 planetary + 2 helical speed-up gears are used for up to 2.5 MW, but for a higher speed-up ratio, 2 planetary + 1 helical type is used. Some medium speed types with a low main shaft rotation speed adopts 2 or 3 planetary gears[1)].

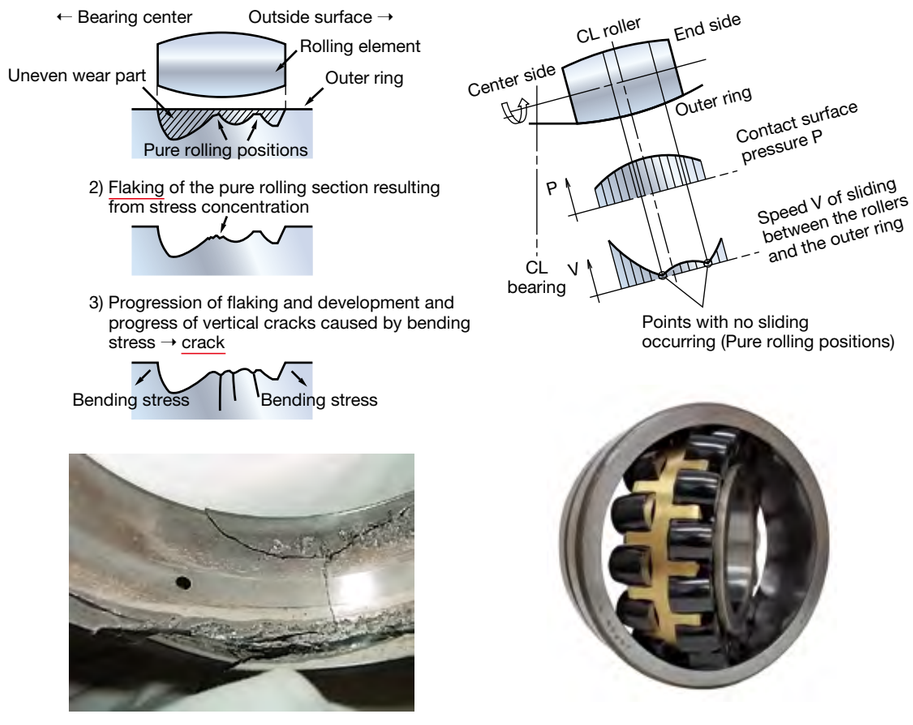

Fig. 4 Differential sliding and wear in a spherical roller bearing and DLC-coated spherical roller bearing

As the size of a wind turbine becomes bigger, the input torque from the wind is increased, intensifying the load on the bearing. A planetary gear uses a bearing supporting the carrier shaft and a bearing supporting the planetary gear shaft. As the torque is increased, the drive shaft thickens, making the carrier bearing bigger and the bearing load capacity larger. However, as the shift to more compact and lighter-weight planetary gears continues, there will be an especially high demand for a planetary gear bearing with a high load capacity. Consequently, in more cases the outer ring is eliminated, the bearing bore of the planetary gear is made of the raceway surface of the outer ring and the bearing load capacity is made

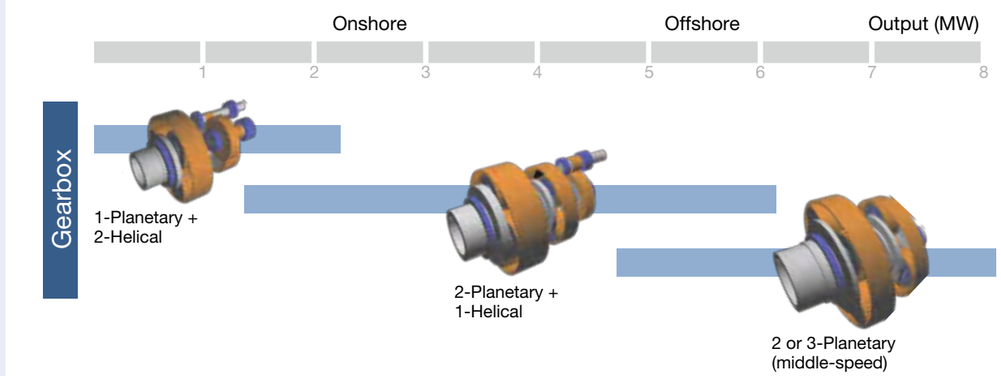

Fig. 5 Types of gearbox

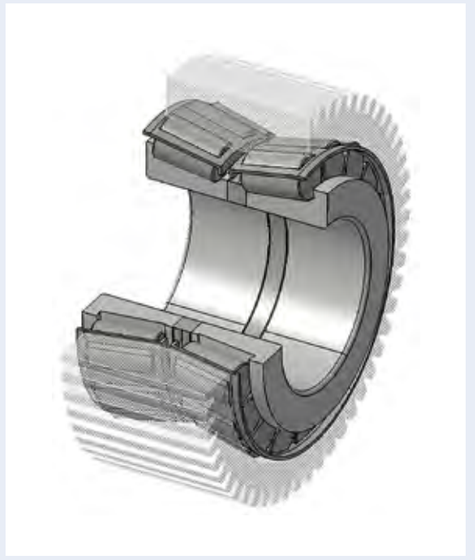

Fig. 6 Integrated tapered roller bearing

larger with a larger roller diameter (Figure 6)[1].

The speed-up gear bearing for a wind turbine often becomes damaged at an early stage due to a peculiar flaking involving a microstructural change. This type of flaking is called white structure flaking or white etching crack[2], since the part of the flaking cross section with microstructural change looks white after etching (Figure 7). The white structure flaking can be reproduced in a rolling contact fatigue test with a hydrogen-charged specimen. Accordingly, the white structure flaking of a speed-up gear bearing of a wind turbine is estimated to be also caused by hydrogen[2]. The white structure flaking is considered to occur through the four steps shown in Figure 8. Step 1: Due to additives in the lubricant and influence of slippage, vibration, and electricity, the lubricant is decomposed, generating hydrogen, and the generated hydrogen penetrates into the steel of the bearing. Step 2: Repeated stress leads to the formation of a white structure in the steel. Step 3: Cracking occurs along the boundary surface of the white structure. Step 4: Cracking propagates, leading to flaking.

There is a measure to apply a black oxide coating on the surface of the bearing. Hydrogen is generated through the decomposition of the lubricant due to a chemical reaction with a fresh metal surface formed by metal contact. Black oxide coating suppresses the formation of a fresh metal surface, stopping the hydrogen generation. However, wear of the black oxide coating leads to shortened bearing lifespan. Therefore, use in an environment with sufficient oil film is desirable.

The research that has been carried out thus far has demonstrated that improvement of the steel alloy components suppresses the white structure flaking, resulting in increased lifespan. Adequate addition of alloy elements is considered to delay the progress of microstructural change. Also, the carbonitriding heat treatment is effective for prolonging the lifespan limited by white structure flaking. The compressed residual stress near the surface can delay crack propagation, and the increase in the residual austenite amount can delay the concentration of hydrogen at the position of high shear stress[2].

Consequently, NSK has developed anti-white-structure-flaking steel (AWS-TF™) through the optimization of an alloy composition and special heat treatment. AWS-TF™ achieved a lifespan, limited by white structure flaking, of over seven times longer than standard steel (SUJ2) (Figure 9). Our unique steel for the measure against surface originating flaking, Super-TF™, is also effective against white structure flaking and has a lifespan that is four times longer than that of standard steel (SUJ2).

3.3 Bearings for generators

Deep groove ball bearings and cylindrical roller bearings are generally used for generators. In a generator bearing, a voltage difference occurs between the inner and outer rings, often causing electrical erosion (micro melting by current passing spark.) (Figure 10).

As a countermeasure against this electrical erosion, although the periphery of the generator can be insulated, the standard bearing can be replaced with an insulated bearing of the same size as a countermeasure. An insulated bearing is either an insulated deep groove ball bearing with ceramic balls or an insulated bearing with its outer ring (or inner ring) processed with ceramic thermal spraying (Figure 11).

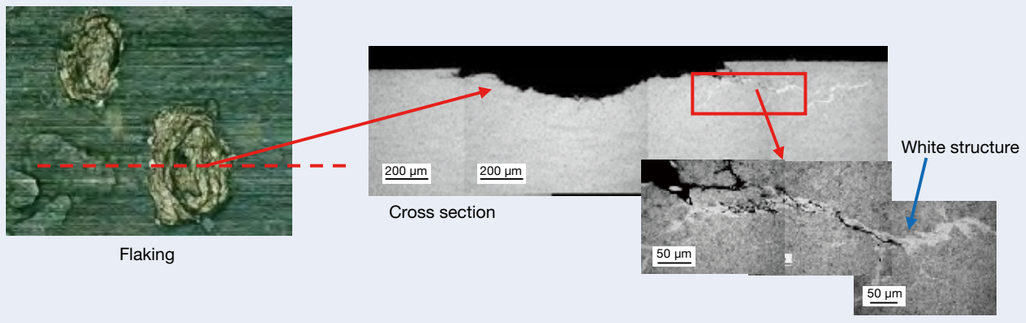

Fig. 7 White structure flaking and observed white structure in material cross section

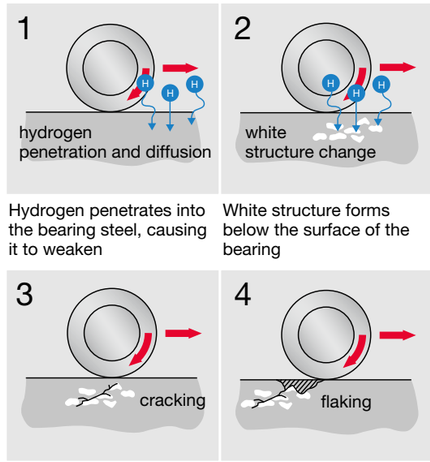

Fig. 8 Occurrence mechanism of white structure flaking

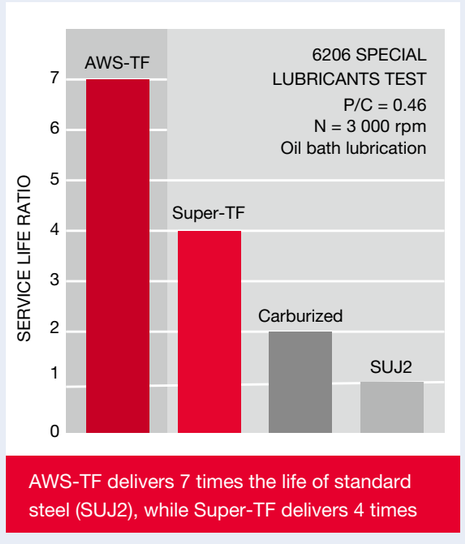

Fig. 9 Comparison of service life between AWS-TF™ and other materials

Fig. 10 Electrical erosion on the outer raceway of a deep groove ball bearing

Fig.11 Ceramic-coated insulated bearings

4. Quality with High Reliability

Wind turbines generate electricity onshore and offshore under harsh conditions where wind conditions are constantly changing. Ample power generation requires high performance in all parts used in the drivetrain and generator.

In particular, regarding the recent increase in size of offshore wind turbines, there is demand for reliability that is higher than that of land-based wind turbines due to the rise in repair costs of the main shaft, speed-up gears, and generator. In order to meet these requirements, NSK manages the quality history of bearings and improves quality stability. It also produces and delivers bearings that have undergone special quality control with a higher degree of assurance.

5. Design Assistance by Analysis

Increasing the size of wind turbines requires bearings with a high load capacity. In addition, since the cost increases, including the construction cost, the weight of the speed-up gear is kept low and the rigidity is also lowered. Therefore, a bearing design that takes into account deformation of the entire speed-up gear is in demand. To increase the bearing's load capacity, FEM analysis is used to optimize the cage shape (Figure 12). FEM analysis is carried out for the entire speed-up gear, including the housing and planetary carrier, as a means of investigating the influence of speed-up gear deformation. In addition, this type of analysis is used to estimate the load of each roller inside the bearing, estimate the lifespan, and examine the bearing specifications (Figure 13).

Looking ahead, analysis technology will play an increasingly important role, and NSK is working on the sophistication and improvements in the efficiency of analysis technology.

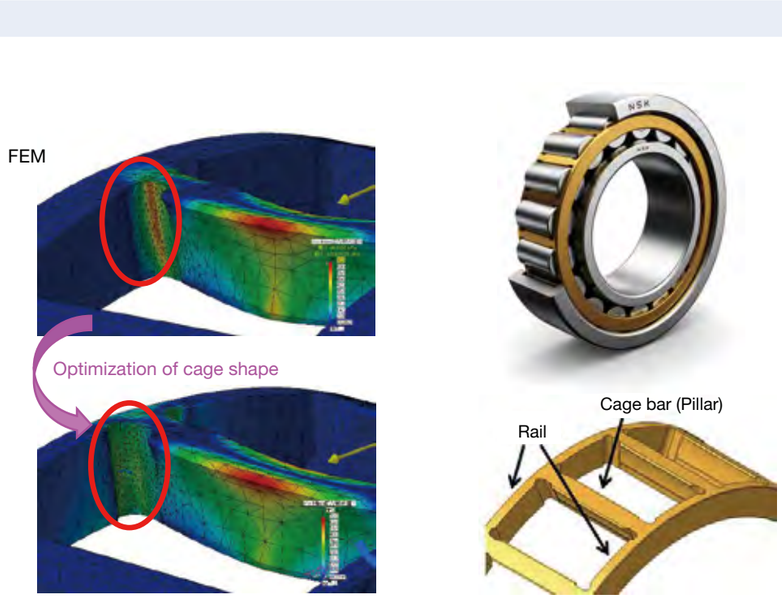

Fig. 12 Development of a cage for high load capacity cylindrical roller bearings utilizing FEM analysis

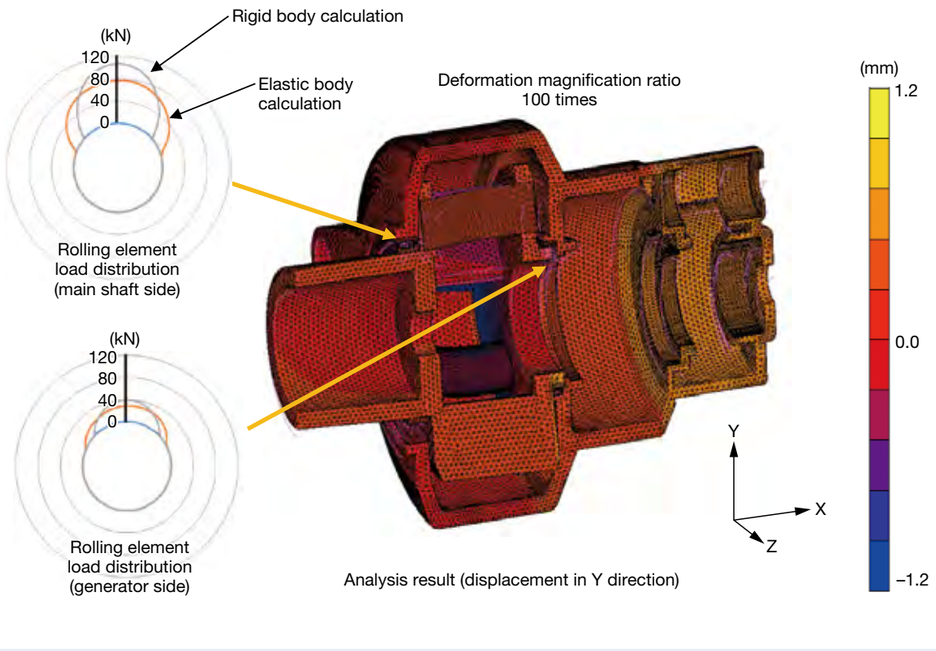

Fig. 13 FEM analysis for the entire gearbox

6. Summary

Wind turbines shift from onshore installations to offshore installations, where wind conditions are better. In addition, onshore wind turbines are increasing in size in areas with medium and low wind conditions. Accordingly, market demand is growing for larger bearings that are capable of bearing high loads and bearing with high load capacity and higher reliability. To address these needs, NSK will continue to develop bearings with high reliability and high load capacity while also contributing to advances in the wind turbine industry and to the protection of the global environment.

References

1) Seiji Ijuin, "Increasing Sizes of Wind Turbines and Bearing Trends," Journal of Wind Energy, JWEA Vol. 37 (Serial No. 108), No. 4 (2013), pp. 462–464.
2) Hiroki Yamada, Hideyuki Uyama, "White Structure Flaking in Rolling Bearings for Wind Turbine Gearboxes," NSK Technical Journal Motion & Control, 28 (June 2017), pp. 6–14.

Kim Leong LEE

The Technical Trend of Machine Tool Components

Mitsuho Aoki
Industrial Machinery Technology Center, Industrial Machinery Bearing Technology Center, Machine Tool Technology Department
Hidenori Saito
Industrial Machinery Technology Center, Linear Technology Center, BS Department

Abstract

In recent years, machine tool has been under the condition of rapid environment change such as increase of electric vehicle, expansion of IoT/Industry 4.0 and rising labor cost due to decrease of engineering workforce. Under the circumstances, machine tool manufacturers promote technological developments to achieve higher productivity and accuracy. Machine elements that contribute to performance increase of machine tool have to be adaptable to the needs and technologies of machine tool for greater sophistication.

In this article, we will explain trends of machine tool technologies in recent years and latest technologies of machine elements such as spindle, ball screw and linear guide based on the trends of IoT/Industry 4.0 for machine tool and machine tool exhibition.

1. Introduction

The conditions surrounding machine tool manufacturing have recently been changing rapidly. These include the electric vehicle conversion of automobiles, expansion of IoT, and rising labor costs due to the global decrease of the working population. To respond to these changes, manufacturers of machine tools across the world are aiming for further improvement of productivity and precision, and they continue to develop machine tool technology to achieve that goal. The machine element parts contributing to performance improvement also need to respond to the needs of sophistication of manufactures of machine tool and end users.

NSK has an extensive lineup of important machine element parts, including spindles, bearings for spindles, ball screws and their support bearings, and linear guides, which determine the performance of machine tools. NSK has been developing products that meet exactly the changing needs of machine tools.

This article describes recent technology trends of machine tools and the state-of-the-art technology of NSK in response to them.

2. Trends of Machine Tool Technologies

2.1 Trend of IoT/Industry 4.0 in machine tools

One recent trend in manufacturing sites is Industry 4.0 with the background of expanding IoT. Industry 4.0 is a manufacturing revolution promoted by the German government under industry-academia-government collaboration, also called the fourth industrial revolution, and it aims for the mass-production of customized products (mass-customization) at a cost that is equivalent to mass-produced products of the same specification. This strategy is for the survival of the German manufacturing industry with high wages compared to those in Asian countries. Under these circumstances, machine tools are required to be more efficient.

Figure 1 shows the finding on the exhibition related to IoT/Industry 4.0 at the 28th Japan International Machine Tools Fair (JIMTOF) in 2016.

Examination of exhibitions from 150 companies shows that 36% of the exhibitions are related to IoT. More than half of the exhibitions aimed to improve operation rates, such as operation monitoring and the visualization of the whole factory. The percentage of exhibitions dealing with condition monitoring systems (CMS), with a focus on failure prediction and diagnosis, was only about 17%.

In the future, it is expected that further development will be made in each company toward practical realization of CMS, which will boost the percentage of exhibitions related to CMS.

2.2 Technology trend of spindles

Figure 2 shows the finding of an independent examination performed by NSK for over 30 years since the 11th JIMTOF held in 1982 on the number of high speed spindles over 10 000 rpm exhibited at JIMTOF. This indicates that since the 20th JIMTOF held in 2000, the number of high speed spindles over 10 000 rpm on exhibition hovers at a high number.

Until then, the practical realization of light and strong ceramic balls capable of suppressing the centrifugal force on the ball in a high speed operation, and the popularization of the Robust Series, with low sensitivity to heating, change enabling stable high speed operation, accelerated the spindle speed, and improved manufacturing efficiency.

In recent years, the technology for improving efficiency by increasing the cut depth guided by a stability limit diagram from rigidity characteristics of the machine tools to avoid reproducible chatter vibration has been applied to practical use.

Also, progress in small-volume production of many various products has raised the issue of improving cast production efficiency. Streamlining the time-consuming final polishing process requires refining the quality of worked surfaces by improving the precision of spindle rotation.

These efficiency-related trends are in accord with the demands from Industry 4.0 mentioned in the previous section.

In addition, in the production sites, not only the improvement of the production efficiency but also care for the environment are in demand. Therefore, the needs regarding the spindle lubrication method are shifting from oil-air lubrication using a huge amount of energy-consuming compressed air to grease lubrication.

In light of these spindle technology trends, NSK has developed an angular ball bearing while adopting the new SURSAVE™ cage and ultra-high speed high frequency spindle with grease lubrication, which will be explained in the next chapter.

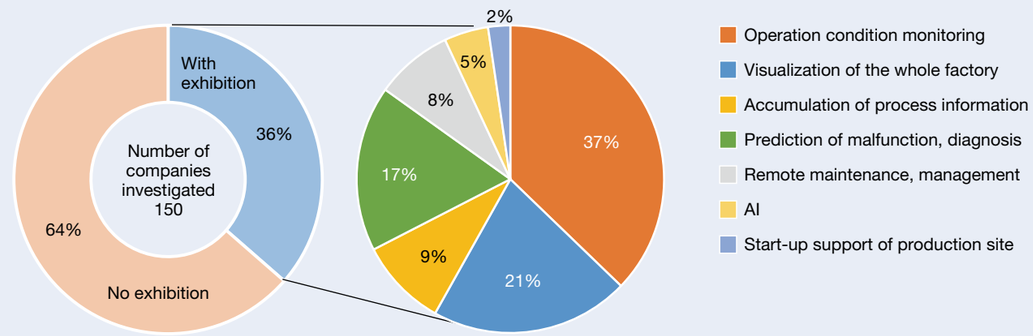

Fig. 1 Findings of an exhibition related to IoT/Industry 4.0 in JIMTOF2016

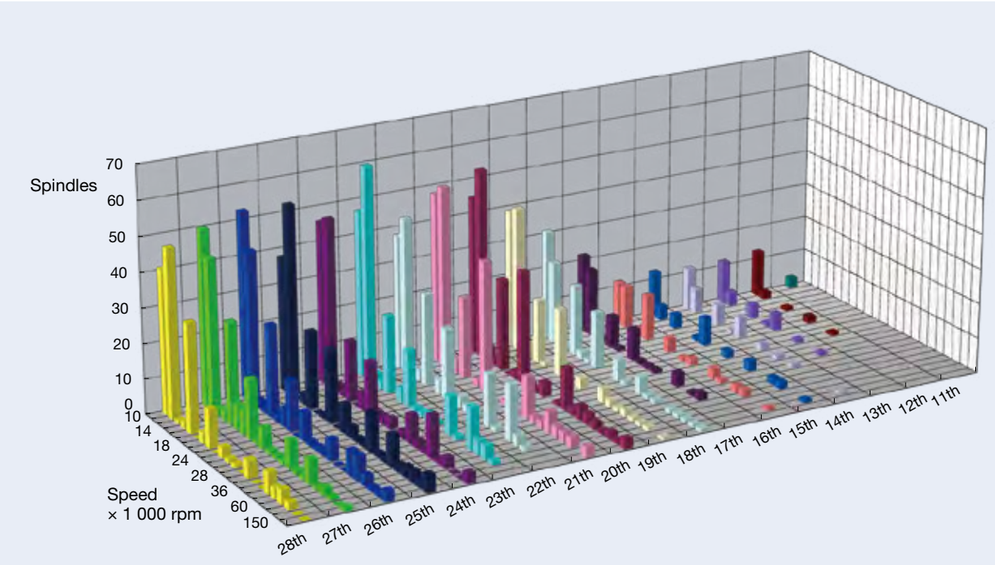

Fig. 2 Findings of the number of machine tools with a spindle speed of 10 000 rpm or more in JIMTOF

2.3 Technology trends of the feed system

2.3.1 Rapid traverse speed of the machining center

Figure 3 shows data from independent research performed by NSK in regard to the trend of JIMTOF exhibitions over 20 years on rapid traverse speed and the amount of ball screw-type machining centers. This result indicates an annual increase at the rate of 50–60 m/min, but leveling off at 60 m/min.

In contrast, Figure 4 shows data from independent research carried out by NSK in regard to the rapid traverse speed of ball screw-type machining centers exhibited in the European Exhibition of Machine Tools (EMO). EMO is one of the world's four largest exhibitions of machine tools together with IMTS (USA), CIMT (China), and JIMTOF (Japan). The research was centered on European manufacturers. The percentage of high velocity machines over 60 m/min exhibited at EMO 2017 was 14%, significantly exceeding the 5% of JIMTOF 2016.

With this in mind, the rapid progress of higher traverse speed, especially in Europe, is one aspect of the promotion of streamlining machine tools required by Industry 4.0, as mentioned in 2.1.

Japanese manufacturers limit the ball screw lead up to 20 mm and set the rotation speed to 3 000 rpm, achieving a traverse speed of 60 m/min with a tendency to aim for both high precision and high efficiency.

In contrast, European manufacturers seem to have achieved a speed exceeding 60 m/min by using high lead ball screws with a lead of 30 mm at a rotation speed of 3 000 rpm. As a measure against degradation of positioning accuracy associated with high ball screw leads, they adopt fully closed loop control, directly detecting the machine position in the linear scale.

NSK has developed a high speed, low noise deflector-type ball screw, compatible with the German industrial standard (DIN) for the European market, where speed enhancement is more advanced, and gave a press release in 2017. The details are explained in the next chapter.

2.3.2 Guide-way type on the machining center

Figure 5 shows the result of independent research carried out by NSK in regard to the guide-way type on machining centers on exhibit at JIMTOF. The rate of roller guide adoption is on the rise, reaching 50% in 2016. Behind this development, for roller guides with a high load capacity and rigidity, the reliability of the machining center is recognized as an appealing aspect. This trend of adopting rollers originated from Europe. Figure 6 shows the research result regarding the guide-way type on machining centers on exhibit at EMO. In Europe, the roller guide is established in the standard specification, with its adoption rate reaching 87% in 2017. Moving forward, we will keep a close eye on the trends of the roller guide adoption rate in Japan to find out whether it will boost to a level similar to that in Europe.

NSK is working on performance improvement of roller guides in response to this shift to the roller-type guide-way, described in the next chapter.

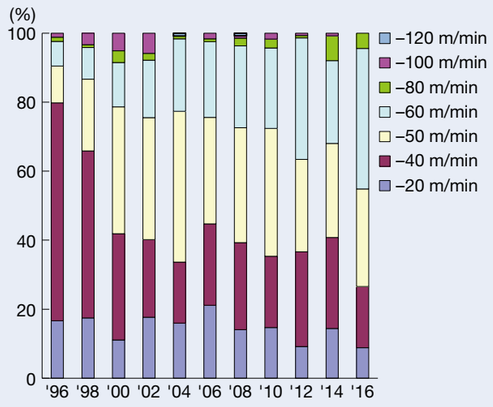

Fig. 3 JIMTOF trend of rapid traverse speed on the machining center

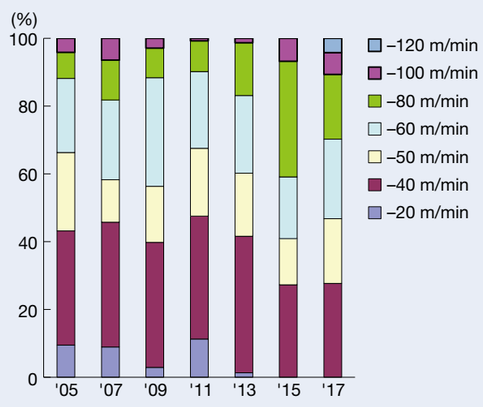

Fig. 4 EMO trend of rapid traverse speed on the machining center

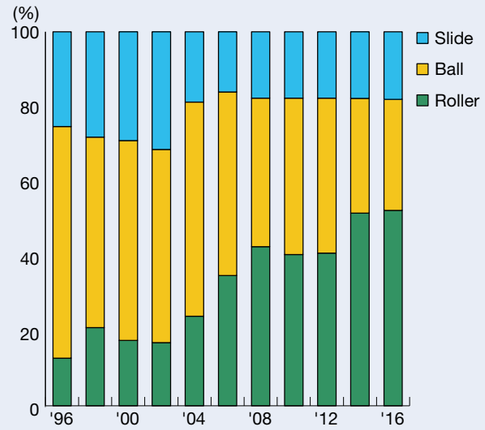

Fig. 5 JIMTOF trend of the guide-way type on the machining center

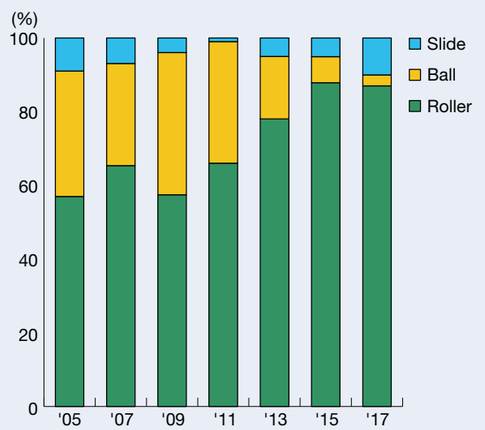

Fig. 6 EMO trend of the guide-way type on the machining center

3. State-of-the-Art Technology of Element Parts of Machine Tools

NSK has been developing new products in response to the changes in the environment surrounding machine tools as already described. In the following, state-of-the-art technology of spindles and guide-ways will be introduced.

3.1 State-of-the-art technology of spindles

3.1.1 Angular ball bearing adopting the new SURSAVE™ cage

High quality appearance is in demand for the mold used in the injection molding of plastic products. Accordingly, the conventional standard was machining the cavity surface of a mold into the designated shape, followed by the final polishing of the surface. In recent years, the progress of control technology of NC machines and speeding up of spindles have enabled machining up to the final finishing process as much as possible, with the aim of improving the efficiency of mold manufacturing.

The issue here concerns the spindle rotation precision, particularly the lowering of non-repetitive run out (NRRO). As Figure 7 shows, the cutting work as typified by end mills, unlike the grinding work with a whetstone, is an intermittent process. With end mills, processing is carried out by transferring a spindle while intermittently cutting the work with multiple blades with each rotation of the axis. At this time, the depth at which the blade cuts again after cutting the workpiece once and rotating must be as similar as the previous cut as possible. In the case of spindle rotation precision, especially NRRO, it is degraded and the blade does not come back to the same position after one axis rotation. Moreover, a slight difference in each cut depth occurs.

Repeated machining of the whole workpiece in this manner would create random roughness on the work surface, deteriorate the appearance quality, and require extra time for polishing.

Spindle rotation precision is roughly divided into repetitive run out (RRO), affected by rotational balance and component accuracy, and non-repetitive run out (NRRO) mentioned previously. While RRO is largely determined by the setting of the spindles, NRRO, which influences the machined surface quality, is mostly dictated by the rotation precision of the bearing.

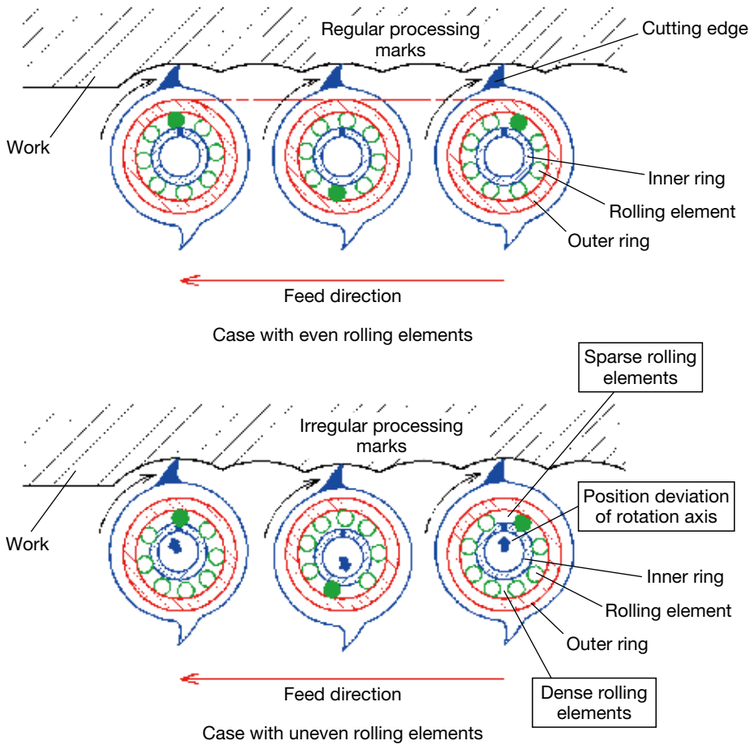

Fig. 7 Mechanism whereby the appearance quality of the processing surface decreases due to NRRO

To tackle these issues, NSK has developed an ultra-high speed angular ball bearing with the new SURSAVE™ cage (Photo 1), mainly for high precision processing machine such as mold finishing machines.

While there are several contributing factors determining the NRRO of bearings, NSK focused on the cage runout amount, a major determining factor.

The function of the cage is to position the rolling element as evenly as possible. Uneven positioning of the rolling element would cause a deviation in radial rigidity. The part of dense rolling elements becomes highly rigid, and the part of sparse rolling elements less rigid. This slight rigidity deviation would position the rotation axis slightly shifted in the direction of sparse rolling elements with low rigidity. Axis rotation makes the rolling element revolve, but since the revolution speed is slower than the axis rotation, each axis rotation makes changes of the dense-sparse phase of rolling elements. This is one of the main causes of NRRO.

For the new SURSAVE™, super engineering plastic developed by NSK was selected for the material. This material has characteristics superior to conventional materials in strength, elasticity, and dimensional stability, boosting the design freedom and enabling the optimization of internal design. This has allowed for a decrease in cage deflection to a minimum and suppressing NRRO by about 50% compared to conventional products (Figure 8).

In addition, by not only enhancing the spindle rotation precision but also by eliminating unnecessary cage motion, the dynamic friction torque during high speed operation has been reduced by about 20% (Figure 9)[1].

Adoption of this bearing would allow for a reduction in the mold polishing process, which is considered to contribute to improvement of production efficiency.

Photo 1 Angular contact ball bearing with SURSAVE™

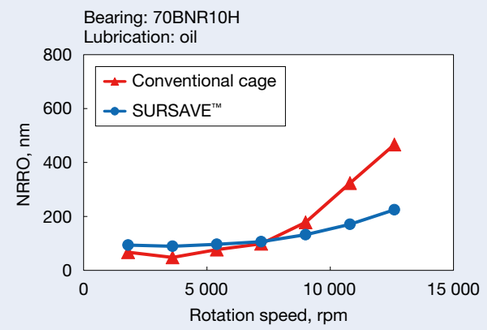

Fig. 8 Test result of NRRO of SURSAVE™

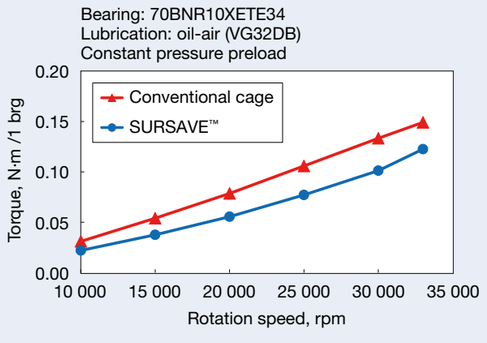

Fig. 9 Test result of torque of SURSAVE™

3.1.2 Ultra-high speed high frequency spindle with grease lubrication

The lubrication methods of bearings for spindles of machine tools are mainly divided into oil-air lubrication and grease lubrication. Table 1 shows the characteristics of both methods.

Spindles for grinding carry lighter weight loads than spindles for cutting, but are required to allow higher rotation speed. Accordingly, they generally adopt small radius bearings rotated at a high speed with oil-air lubrication.

With oil-air lubrication, a nozzle is used to spray compressed air mixed with lubrication oil inside the bearing at high speed. As only a small amount of oil is needed, it is possible to lower the dynamic friction torque. In addition, a large amount of compressed air delivers lubrication oil to the inside of the bearing without fail, making the bearing highly reliable. As a result, oil-air lubrication has been used for a long time in high speed spindles of machine tools and automobile part processing machines requiring reliability.

However, oil-air lubrication consumes 20–30 Nl/min of compressed air for one row of bearings. For a spindle with 4–5 rows of bearings, the amount of compressed air consumption is 100 Nl/min for a spindle.

At production sites with many machines, like automobile part process lines, reduction of this compressed air consumption is an important task.

In addition, maintenance work such as periodical feeding of lubrication oil and filter exchange is needed.

NSK, in response to these tasks, has developed “Ultra-high speed high frequency spindle with grease lubrication” for the grinding process (Photo 2)[2].

Grease lubrication needs to maintain the lubrication condition only with the grease initially included in the bearing. Unlike oil-air lubrication, grease lubrication has a finite lifespan, since physical deterioration by stirring inside the bearing and chemical deterioration

Photo 2 Ultra-high speed, high frequency spindle with grease lubrication

Table 1 Comparison between oil-air lubrication and grease lubrication

		Oil-air lubrication	Grease lubrication
Cost	Spindle design	Complex with lubrication hole and oil outlet, etc.	Simple
	Periphery equipment	Lubrication device is necessary	Unnecessary
	Ease of spindle assembly	Piping performance occurs	Simple
Performance	High speed performance	High speed	Medium to low speed
	Noise	High wind noise	No wind noise
	Consumption of compressed air	Huge consumption	No consumption
	Operation environment	Oil scattering	Clean
	Maintenance	Oil feed and filter exchange etc.	Maintenance-free
Reliability	Lifespan	No lifespan limit due to lubrication malfunction	Finite lifespan
	Waterproof performance	Strong against grinding water ingress	Weak against grinding water ingress

of base oil by heat are unavoidable. In addition, ingress of grinding water for processing into inside the spindle would significantly deteriorate lubrication performance due to mixing of water into grease. In some cases, grease may flow out of the bearing. Improvement of reliability was a priority. Prevention of these problems required installation of an air purge by compressed air on the tool side of the spindle.

The optimized grease selection, improvement of grease inclusion method and optimization of internal design have enabled the ultra-high speed high frequency spindle to achieve a 30% increase in speed compared with conventional grease lubrication spindles. So far grease lubrication has achieved 70 000 rpm (d_m·n 200 × 10^4), which used to be the range of application of oil-air lubrication (d_m·n is a measure of bearing rotation speed, expressed by the product of rolling element pitch diameter d_m and the speed of rotations n).

In addition, to respond to the need of reducing the amount of compressed air used, a large-size flinger has been installed on the tool side of the spindle (Figure 10). This has reduced the risk of grinding water ingression without air purge.

Adoption of this spindle would lower compressed air consumption in grinding processes and contribute to mitigation of environmental loads.

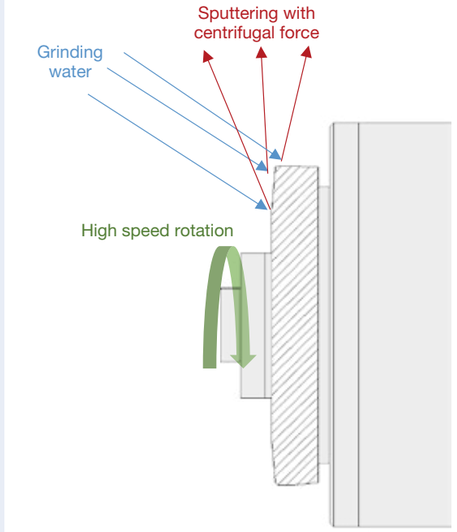

Fig. 10 Large flinger

3.2 State-of-the-art technology of element parts of the feed system

3.2.1 High speed low noise deflector-type ball screw

As mentioned in the previous chapter, feed systems of machine tools have made progress in speeding up with the goal of productivity improvement. To respond to this demand, NSK has been working on increasing the speed of ball screws. Especially, improvement of the parts for ball recirculation has boosted the d·n value, the product of the shaft diameter d, and number of rotations n, which is a parameter corresponding to the revolution speed of the ball. They were released for a variety of applications since the beginning of the 2000s as the High Speed Low Noise Ball Screw Series. Major examples are the BSS Series (2003) and HMD Series (2008) with a new ball recirculation part called an end deflector, and the HMS Series (2010) with an improved conventional ball recirculation tube.

Photo 3 High speed, low-noise deflector-type ball screw

On the other hand, in Europe, where the increase in speed is more advanced than in Japan, partly due to Industry 4.0 aiming at productivity improvement, the German industrial standard (DIN) prevails. As the standard size of DIN is compact, the ball recirculation type of ball screws in the European market is dominated by the deflector type, which recirculates balls by deflectors and enables minimization of the nut outer diameter.

Now, improvement of the deflector has led to the development of the DIN-compatible High Speed Low Noise Deflector-Type Ball Screw with the highest speed in the industry.

Ball screw characteristics, such as high speed, low noise, and good smoothness, are greatly influenced by the ball recirculation. In order to improve those characteristics, it is important to recirculate the ball smoothly by ball recirculating parts. Also for the high speed low noise series already developed, realization of smooth ball recirculation has improved the performance.

Development of the High Speed Low Noise Deflector-Type Ball Screw also focused on this ball recirculation. The technology for performing a three-dimensional analysis of the ball motion inside the deflector passage was established, and an optimized deflector passage was identified so that the ball recirculates most smoothly. In addition, modification of the fixture method of the deflector on the ball screw nut and the material of the deflector has realized the following advantages.

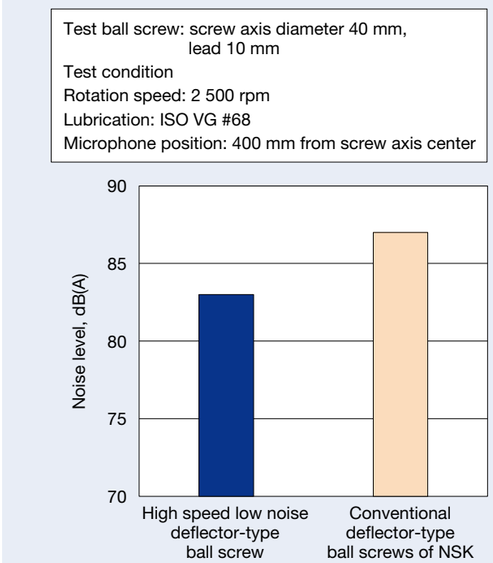

Fig. 11 Noise level of the deflector-type ball screw

(1) High Speed Performance

Achieved a d·n value of 160 000, 1.3 times higher than the conventional deflector-type ball screws of NSK. Achieved a feed rate of 100 m/min with a ball screw of a screw axis diameter of 32 mm and a lead of 20 mm.

(2) Low Noise

Achieved a noise level 4 dB(A) lower than that of the conventional deflector-type ball screws of NSK. (Figure 11)

(3) Smoothness

Established a unique simulation technology for the analysis of ball behavior and thus achieved stable smoothness. (Figure 12)

Fig. 12 Proprietary simulation technology for analyzing ball behavior in a nut

Photo 4 Roller guide with highly dustproof seals

3.2.2 Roller guide with highly dustproof seals

As mentioned in the previous chapter, for roller guides with high load capacity and rigidity, the reliability of machine tools is the appeal, and adoption rates have reached 50% in Japan and 87% in Europe for machining centers. Under these circumstances, especially in recent years, diversification of machining objects and the popularization of high pressure coolant enabling high speed, high efficiency processing of difficult-to-machine materials have boosted the number of cases in which machine element parts are used in environments where the complete prevention of ingress of chips and coolant is impossible. Ingress of foreign objects inside the bearings of roller guides would deteriorate the lubricating agent and cause failure of the roller recirculation, and, as a result, there is a risk of damage occurring within a short time.

With this in mind, NSK has developed a highly dustproof V1 seal and V1 bottom seal and achieved long operation life of roller guides in an environment surrounded by foreign objects, aiming at improvement of dustproof performance of the roller guide.

(1) Highly Dustproof V1 Seal (Side Seal)

Side seals are installed to make the bearing edge dustproof. In prolonged operation in a harsh environment, lip damage due to contact with foreign objects and lubricant removal due to foreign objects causes tears and erosion of the seal lips. The highly dustproof V1 seal, with optimized seal lip shapes and materials with high anti-erosion performance, has reduced the foreign object ingress to about half compared to conventional standard seals. Furthermore, the occurrence of damage such as tears is reduced even in a degraded lubricating condition, enabling sustainment of high dustproof performance for a long time (Figures 13 and 14).

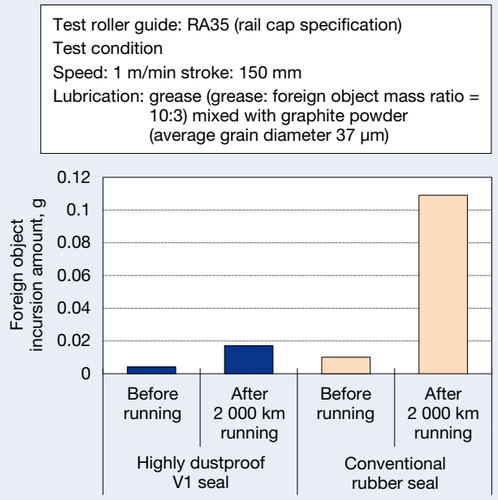

Fig. 13 Test results of the amount of foreign matter incursion for the V1 seal

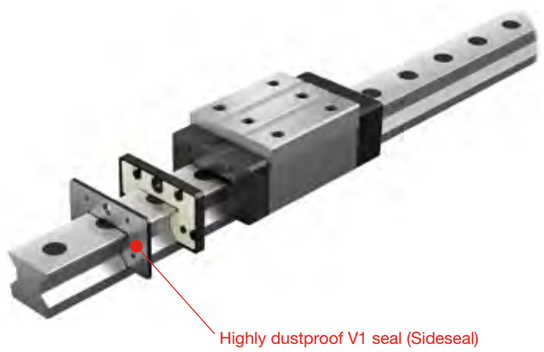

Photo 5 Highly dustproof V1 seal

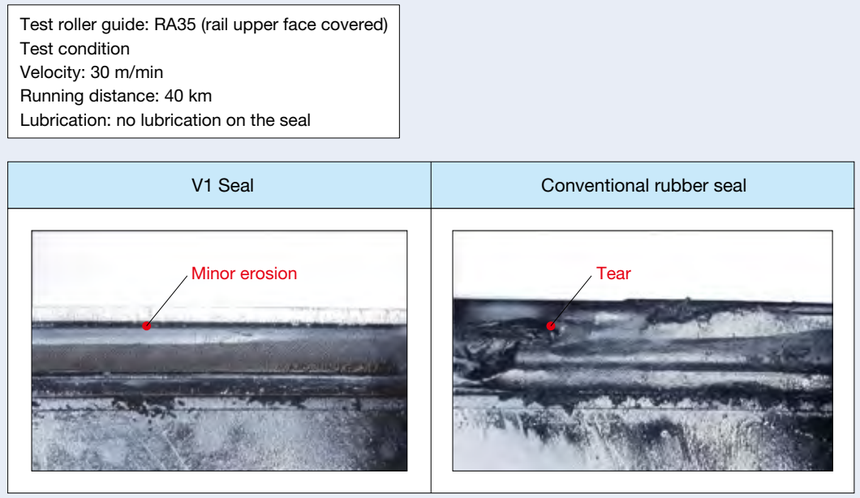

Fig. 14 Test results of wear resistance for the V1 seal

(2) Highly Dustproof V1 Bottom Seal

In the automobile part processing machines, as shown in Figure 15, the structure of a roller guide used in an upside-down arrangement with fixed bearings and rail-guided movement of the main shaft is shown. This structure allows arrangement of x, y, and z axes in the back of the machine, enabling a system adaptable to a variety of production modes. However, as rails in the processing room are exposed, the dustproof performance against the coolant and cutting chip ingress from the bearing bottom is required more than ever. To meet such needs, by adoption of the lip shape and material similar to the highly dustproof V1 seal (side seal), the highly dustproof V1 bottom seal has been developed, with dramatically improved dustproof performance against foreign objects ingressing from the bearing bottom. By making a double seal by installing it on the outer side of the conventional bottom seal, coolant ingress has been suppressed to 1/10 of the conventional standard seal. In the same manner as the highly dustproof V1 seal (side seal), anti-erosion performance of the seal has been improved, and it is capable of maintaining high dustproof performance for a long time.

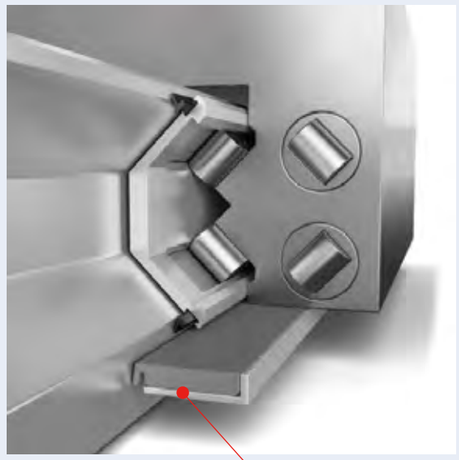

Photo 6 Highly dustproof V1 bottom seal

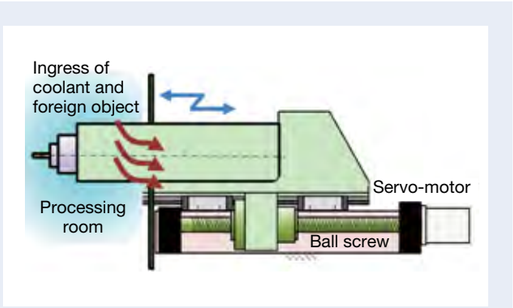

Fig. 15 Example of use in an upside-down arrangement for the roller guide

4. Postscript

In light of the trends expressed in the exhibition of machine tools, this article describes the technology trends of machine tools and the state-of-the-art technology of spindles, ball screws, and linear guides, all element parts of machine tools.

For IoT and next-generation manufacturing as advocated in Industry 4.0, further development of the machine tools supporting all the manufacturing will surely play a key role.

NSK will continue to develop high performance, high quality products capable of contributing to the progress of such machine tools.

References

1) "Ultra-high-speed Angular Contact Ball Bearings with New SURSAVE™ Cage for Machine Tools," Science of Machine, 69-12 (2017)
2) "Ultra-high-speed Spindles using Grease Lubrication for Grinding Process," Science of Machine, 70-7 (2018).

Mitsuho Aoki

Hidenori Saito

Technical Trends of Railway Products

Mineo Kameko
Railroad Group, Railroad & Aerospace Bearing Technology Department, Industrial Machinery Bearing Technology Center
Yoshihiko Shirosaki
Railroad Group, Railroad & Aerospace Bearing Technology Department, Industrial Machinery Bearing Technology Center
Shigeru Endo
New Field Products Development Center, Technology Development Department 2

Abstract

Trains have been and will remain one of the most important modes of transportation in the world, especially from the point of mass-transit and economical way. Safety always comes first in its operation and we have kept proposing the way to achieve that requirement through our history. This article focuses on the technical trend of railway bearings for axle, gear unit, and traction motor for how they can realize reliability and contribute to safety operation. This article also includes technical information of relevant products of the sensor, condition monitoring system, and actuator for active suspension, which are gaining their positions especially in the higher speed trains for more safety and comfortability. We are responsible for contributing to railway operations, from various points of view, with our technical solutions, now and in the future.

1. Introduction

Railroads are a very economical means of mass transportation that support people's daily lives. Railroads have a long history; vehicles were pulled over the track paved with hewn stones dating back to the Roman Empire at least 2 000 years ago. Steam locomotive railways were put to practical use at the beginning of the 18th century, first in Great Britain, and then usage expanded throughout Europe and the U.S. In Japan, the first railroad started its service in 1862 between Shinbashi and Yokohama, 50 years behind Great Britain. The Japanese railroad technology developed into the present Shinkansen, and the commercial operation of the linear Shinkansen is drawing near. Overseas, especially in developing countries, installing the infrastructure for subways and high speed railroads is in progress. This is an effective countermeasure against chronic traffic jams due to the pressing issues of population concentration in metropolitan areas and environmental problems. This article describes the technology trend of bearings supporting railroad transportation and related technology development in NSK.

2. Technology Trends

2.1 Railroad vehicles

Since the advent of the zero-series Shinkansen, railroad vehicles are becoming faster. In recent years, China has made rapid progress in high speed railroad networks and already operates railroad vehicles with a maximum speed of 380 km/h. Great Britain also plans to implement vehicles capable of reaching a speed of 400 km/h. On the other hand, in Europe and also in South Korea, where much of the terrain is mountainous, and in light of economical merits including maintenance, vehicle speed is being reduced to about 250km/h.

At the international railroad technology exhibition (InnoTrans) in recent years, these trends could be seen. To improve Life Cycle Cost (LCC) and also as a countermeasure against the diminution of the working-age population, the reduction of maintenance and improvement of maintainability are expected especially in the Japanese market. In addition, standardization of various specifications has been progressing overseas. Particularly in Europe, in view of mutual track sharing and the aim to expand the European specifications all over the world, the movement of further standardization is evident.

2.2 Bearings for railroad vehicles

Bearings being used around the axle are shown in Figure 1. Bearings are classified into three types: axle bearing, gear unit bearing, and traction motor bearing.

2.2.1 Bearings for axle

Bearings for axle are important because they directly support the vehicle. Damaged bearings could have a serious impact on the safe operation of the vehicle. Therefore, there is growing demand for higher bearing reliability. NSK is responding to this by optimizing internal specifications, adopting high cleanliness steel, and applying a non-destructive inspection of materials.

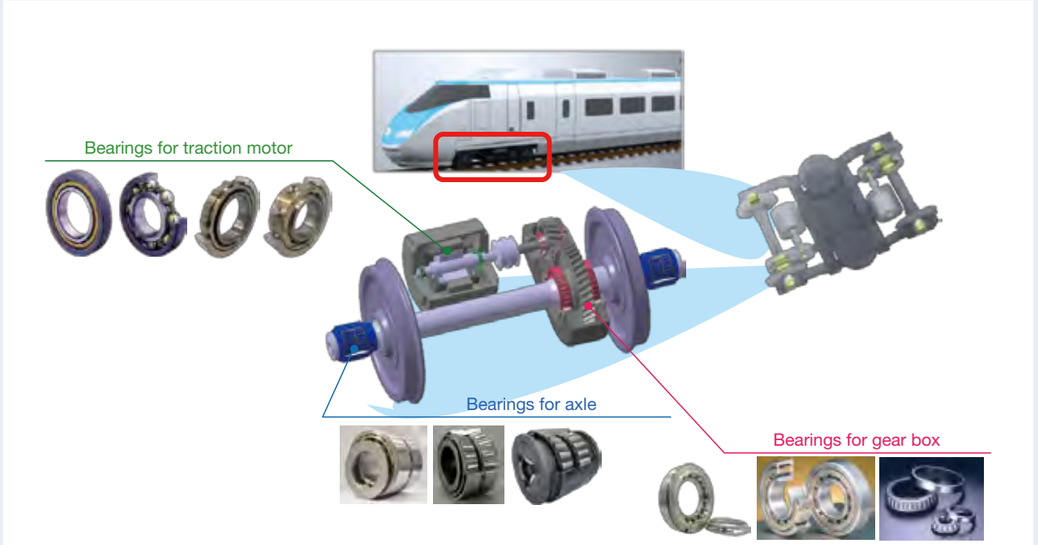

Fig. 1 Locations of NSK bearings for railways

Photo 1 Axle bearing with plastic cages

Table 1 EN standards for railway bearings

Standard	Content
EN12080 Roller bearing	Basic specifications of the axle bearing: Specifying the material purity, hardness, marking, and test level; also specifying the ultrasonic probing method, magnetic powder test method, eddy current flaw detection method, and strength test method of the plastic cage.
EN12081 Lubrication grease	Grease quality specifications: Grease types are categorized according to the speed up of a vehicle to a maximum speed of 200 km/h. Evaluation will be made by various tests on the grease itself as well as tests on the bogie and actual vehicle by EN12082.
EN12082 Endurance test	Specifications of the endurance test method of the grease-including bearing: Includes both tests on the bogie and on the actual vehicle. Specified are test conditions such as the simultaneous test evaluation of the two bearings in the test on the bogie. The judgment is evaluated by the bearing temperature during the test and the abnormalities of the bearing and grease after the test.

Almost all the axle bearings are lubricated by grease packed inside the bearing (Photo 1). For grease lubrication, it is important to know the grease behavior inside the bearing especially at high speed operation. In high speed rotation, grease is easily sputtered out to the seal case side by centrifugal force until it is finally settled at stable positions. So, it is important to control grease distribution inside the bearing by paying extreme care to the initial grease distribution and each grease amount.

In addition, from the viewpoint of grease leakage and foreign object ingress from outside, a grease-packed bearing must be sealed. Seals are classified typically into two types: contact type and labyrinth type. Both of these seal cases are fitted to the bearing outer ring. The seal rip contacts with rotating parts for contact type seal and keeps optimal clearance for the labyrinth type seal. The sealing method and material are selected in consideration of the sliding surface speed and environmental conditions. On the other hand, for oil lubrication adopted for the Shinkansen, while the countermeasures against oil leakage from the axle box are important, it is easy to monitor the bearing conditions by oil level, hue, and metallic debris, which is collected on the magnetic plug. Oil lubrication is considered to be a stable way to lubricate the bearing. Extension of the period between maintenances is in strong demand by the market from the LCC viewpoint. Especially to respond to the need of no disassembly of the bearing over a long period, suppression of grease degradation is the key. Adoption of plastic cages instead of the conventional steel press cages is one countermeasure. In addition, the bearing monitoring system, described later, is now expected to be a new method of extending the maintenance period, as shown at InnoTrans 2018.

In Europe, in accordance with the “Mandate on Mutual Operation of European High-Speed Rail Network,” the standard on the axle bearing for railroad vehicles was established as EN 12080, EN 12081, and EN 12082 (Table 1). These standards have standardized the bearing specifications, grease packed and evaluation methods of performance and durability. This enables the axle bearing to this specification to be used in the international trains, especially in Europe, keeping a certain level of quality performance. Moreover, the standard for RAMS (Reliability, Availability, Maintainability, and Safety) has also been established. To meet the requirements for globalization, NSK is also developing products based on the standards mentioned above.

2.2.2 Bearings for gear box

The gear box, which transmits the driving force from traction motor to axle, is equipped with bearings on a pinion shaft and large gear axis. These bearing types are mostly tapered roller bearings in Japan. The possible concerns about bearing failure could be fatigue failure and wear of the cage due to gear engaged vibration. In response to these issues, NSK has adopted a reinforced cage. The bearing on the pinion shaft is in a severe condition due to high speed rotation and vibration from coupling which is connected with traction motor. Because of this, NSK applied the surface treatment of soft nitriding to the cage if necessary.

On the other hand, for high speed vehicles overseas (especially in Europe), pinion shafts adopting cylindrical roller and ball bearings are typically used. It is necessary to adjust axial clearance in case of tapered roller bearings on installation of the bearings. However, ball bearings of that type can fix the clearance on their own, resulting in eliminating the need for this clearance adjustment.[1)] However, the increased number of bearing which leads to gain weight and total bearing width can be disadvantageous. Furthermore, in recent years, driving mechanisms are being developed in Japan with the use of double helical gears for Shinkansen trains. This type of gear reduces the axial load to the bearings, allowing for the adoption of cylindrical roller bearings. Nevertheless, it requires optimization of the specifications of the roller end and rib face on which possitive sliding contact can occur.

2.2.3 Bearings for traction motor

A number of trains apply AC motors, which are now controlled by VVVF (variable voltage variable frequency), with the aim of compactness and higher efficiency. Popularization of this brushless motor almost eliminated the sliding parts in the motor except for bearing. In this point the bearing life became a key to determining the maintenance interval because, in the motor, the bearing is the only part which has sliding elements. Since the long term sustainability of the lubrication performance of the bearing is important, the base oil of the grease changed (from mineral oil to synthetic oil) along with other improvements of the grease pocket[2], plastic cage, and ceramic rolling element, which have been proposed.

In addition, the weight load on the bearings of the railway traction motor is relatively low, except for those for locomotives. Therefore, in much higher speed conditions, due to insufficient rolling element driving force from the inner ring, consequent skidding damage could occur. Optimization of specifications inside the bearing as well as lubrication performance are important.

In railway traction motors, a part of the current (DC or AC) can penetrate through the bearing and make a spark through the oil film between the rolling surfaces in the bearing, damaging the raceway and rolling element surfaces. This is called electric erosion. Insulated bearings with insulation material on the outer ring of the bearing is now a common countermeasure against electric erosion (Photo 2). Also, insulation performance is better for higher impedances, and ceramics and resin are commonly used as insulation materials. Moreover, the hybrid type has become available, which adopts a ceramic rolling element to enhance the large impedance characteristics.

Photo 2 Cylindrical and ball bearing with electrically insulated outer ring for railway traction motors

3. Efforts for Related Technology

3.1 Sensing of bearings and bearing condition monitoring

To contribute to further safety and improvement of reliability for railroad vehicles and to transition from time-based to condition-based maintenance intervals, development of various sensors and a bearing damage prediction diagnosis system for early detection of bearing damage is underway.

The axle sensors (Photos 3 and 4) developed in 2004 were applied to the M250 series limited express container vehicle “Super Rail Cargo” (maximum speed 130 km/h). Japan Freight Railway Company started the operation of this series on March 13, 2004, and has been using it for more than 13 years. This sensor has a multi-sensor structure, with multiple sensing functions in a single sensor. A single sensor can contain internal sensors for temperature and vibration, or temperature and rotation velocity. There are several types of combinations. In addition, in 2012, axle boxes (Photo 5) containing a rotation speed sensor were developed and adopted in the 321 series and 521 series trains of West Japan Railway Company.

In recent years, progress has been made not only in regard to the development of the various sensors mentioned above but also for the development of a bearing damage prediction diagnosis system for the early detection of bearing damage with full utilization of information from the sensors. The feature of this diagnosis system is its ability to detect early symptoms of bearing damage. Information regarding bearing damage gained over a long time as a bearing manufacturer is indispensable for the construction of the diagnosis logic.

In the future and in accordance with the various activities utilizing IoT in the railroad industry, we will contribute to the improvement of safety and reliability for vehicle operations through the continued development of products with integrated sensing technology and diagnosis technology.

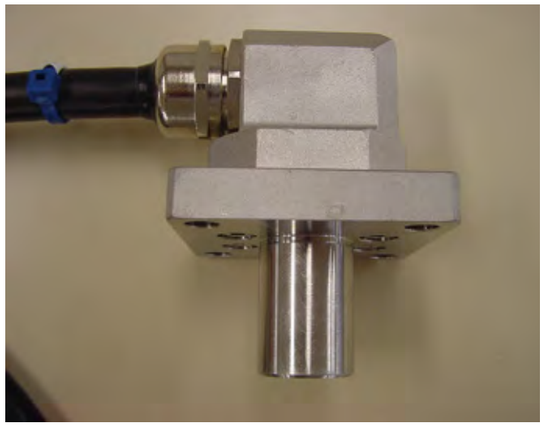

Photo 3 Multi-sensor for axle bearings

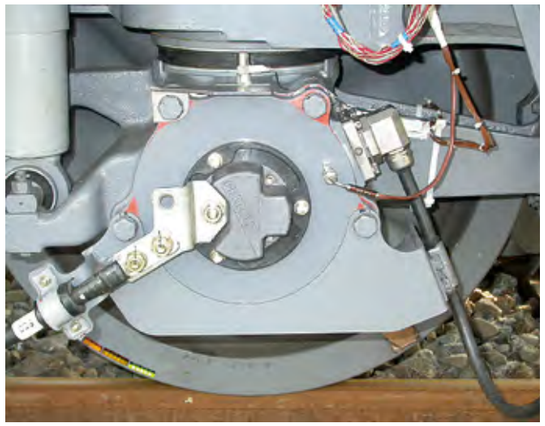

Photo 4 Multi-sensor mounted to an axle box

Photo 5 Axle bearing equipped with a sensor on the seal

3.2 Improvement of vehicle comfortability

3.2.1 Installation of active suspension

Railroad vehicles are expected to meet the technological demands for safety and reliability and, in the case of luxury trains, are expected to provide high comfort. In particular, suppression of vehicle vibration has gained prominent attention as an issue for assuring comfortability. Vehicle vibration stems from a variety of causes, including rail wobbling, gradient changes, and vehicle curves transmitted indirectly from the bogie to the vehicle body, and the surrounding air pressure directly shaking the vehicle body from side to side. To suppress these vehicle body vibrations, passive suspensions, as shown in Figure 2, such as axle springs, bolster springs, and lateral moving dampers, are installed on railroad vehicles.

To further improve comfortability, installation of active suspension is in progress, enabling active control of car body vibration.

Active suspensions are broadly classified into semi-active suspension and full active suspension. Semi-active suspension controls the damping force of dampers, and full active suspension actively eliminates the car body vibration through the use of pneumatic, hydraulic, and electric actuators through generating force in the opposite direction of the vibration force.

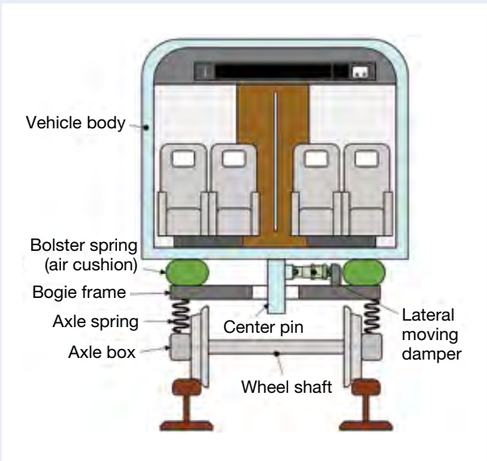

Fig. 2 Bogie and vehicle body model

3.2.2 Development of actuators for full active suspension

NSK has developed an electric actuator called the Vibration Control Actuator, using ball screws, for full active suspension to suppress the lateral vibration of railroad vehicles (Photo 6, Figure 3).

This actuator is installed between the bogie and the vehicle body in parallel with the lateral moving damper shown in Figure 2, generating driving force in the lateral direction in response to the command from the upper level control equipment. As a mechanism to convert the rotational movement of the electric motor to the linear movement of the output rod, a precision ball screw with high efficiency, low inertia, and high back drivability has been applied. High efficiency transmission of the driving force results in a lower torque demand on the electric motor. This allows for a more compact and power efficient actuator. In addition to the back drivability of the ball screw, the electric motor is compact and has low inertia. As a result, the response of this system can be improved and vibration can be suppressed.

Taking full active suspension control of this actuator, drastic reduction of lateral acceleration has been confirmed in the real vehicle running test (running through the tunnel section of the Chuo line at about 100 km/h) of a cruise train, the Train Suite Shikishima, of the East Japan Railway Company. In addition, the comfortability level derived from the effective value of the car body acceleration with adjustment at vibration frequencies, to which passengers are sensitive, has been confirmed to be improved by 11.1 dB[3].

Photo 6 NSK Vibration Control Actuator

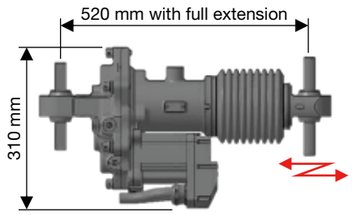

4. Future Technology Tasks

The products introduced here are important parts supporting the safety, reliability, and comfortability of railroad vehicles. Further improvement of their performance and reliability is our ongoing task. In addition, from the economical viewpoint, improvement of maintainability and reduction of maintenance (ultimately maintenance free) are in growing demand. For that task, development of material technology of each part including heat treatment, residual life diagnosis technology[4], and new technology on conditioning monitoring, introduced in this article, is of ever-growing importance. However, just fulfilling the demand for high-end technology will not satisfy the market needs, which are expected to be even more demanding in the future. Taking full advantage of the present technology supported by long-standing achievement, the development of more precise and accurate analysis/simulation technology and the continued provision of high cost performance with well-balanced performance and economic efficiency are our ongoing tasks as a supplier.

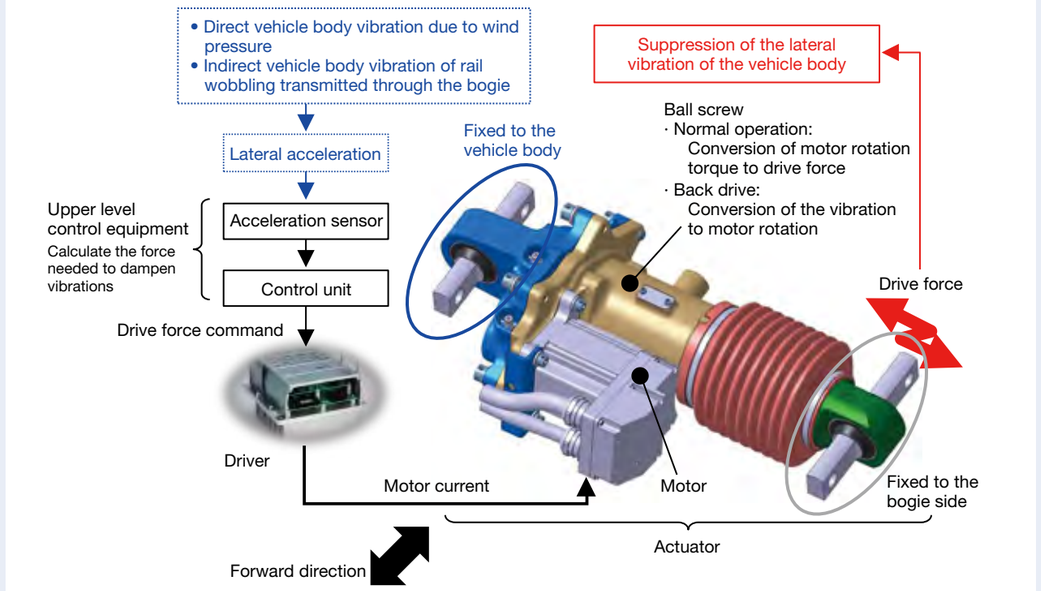

Fig. 3 NSK Vibration Control Actuator

5. Postscript

NSK products introduced in this article are installed on railroad vehicles used by many people as a means of transportation in everyday life, playing a significant role for many people. Even a minor malfunction could have a major impact on the lives of the general public. Being fully aware of our huge responsibility, we will continue contributing to the progress of railroads in the future.

References

1) T. Suzuki, "Bearings for Traction Gears," NSK Motion & Control, No. 7 (1999).
2) S. Hibino and M. Suzuki, "A Proposal of Grease Pocket Structure in Consideration of Base Oil Migration," Journal of Japanese Society of Tribologists, Vol. 50, No. 1, (2005) 39–46.
3) Rail and Tech. Publishing Co. Ltd., "Rolling Stock & Technology," Vol. 251 (Aug. 2017) 24–26.
4) K. Furumura, S. Shirota, and A. Fujii, "Fatigue Analysis of Rolling Bearings (Part 3)," NSK Technical Journal 646 (1986) 18–25.

Mineo Kameko

Yoshihiko Shirosaki

Shigeru Endo

ISO 13482 certificated and practical application of Guidance Robot LIGHBOT

Katsuyuki Sagayama, Mayuko Mori, and Ayako Tabuchi
New Field Products Development Center, Technology Development Department 1
Yosuke Fukushima
New Field Products Development Center, Technology Development Department 2

Abstract

We have developed a robot that guides visually impaired and elderly people to their destination at hospital. In this report, we introduce practical application and the approach of social implementation of this robot. Practical application is our ultimate goal. In order for robots to be accepted by society, we acquired the safety standard ISO 13482 for personal care robots. We also implemented a mechanism to disseminate sales forms, insurance, maintenance, subsidies, etc. The robot was introduced to Kanagawa Rehabilitation Center.

1. Introduction

In light of the low birthrate, aging population, and dwindling working population, a variety of approaches are ongoing in regard to personal care robots. Particularly, the number of visually-impaired people who require support by seeing-eye dogs and helpers is estimated to be 316 thousand[1] in Japan and 253 million[2] around the world.

Visually-impaired people state the following as the most serious problems they face when they are in public: crowds and traffic are scary and transportation is inconvenient. Other problems include public places are hard to use and building facilities are inadequate, highlighting complaints about facility inconvenience[3]. In addition, in wide spaces such as lobbies without any characteristic objects, it is especially difficult to find the way to a particular destination[4]. We have heard similar opinions in our independent interviews with those affected by vision loss. There is strong demand for assistance guiding visually-impaired people inside big facilities (hospitals, public places, administrative institutions, etc.). We have therefore set a target to realize transportation assistance robots that are mainly capable of guiding inside a building.

Within Japan, research on transportation assistance robots for visually-impaired people, including obstacle avoidance and point-to-point motion, is underway. Current research includes MELDOG[5] by the Tachi team and the walking guide robot[6] by the Mori team. In other countries, assistance equipment such as The GuideCane[7] of the Ulrich team, a walking stick with wheels using transportation robot technology, and the indoor navigation equipment[8] of the Kulkarni team are being developed. However, they are still at the research stage and have not yet been put to practical use in a facility.

On the other hand, there have been many practical applications and implementations of many autonomous mobile robots in recent years. These include Amazon Robotics and butler robots, for example, robots for delivery in the warehouse, robots for delivery outside the warehouse, and security robots. However, robots with a human interface and ability to move to a destination with a human have not been realized yet.

We have been working on the development of guidance robots capable of guiding visually-impaired people to destinations without them getting lost inside a hospital (even a big hospital), other public places, and administrative buildings. First, we have developed a robot with an emphasis on intuitive operation that moves smoothly in response to human input and avoids obstacles on the way[9]. Next, we installed map information along with self-localization and path generating functions on the robot. Then we developed a robot for guiding a user, carried out demonstration experiments and long-term monitoring tests, and made repetitive improvements in response to advice[10–12]. In addition, responding to demand from hospital operators, we have developed a robot with an intended user base expanded to include sighted people, specifically elderly people. Demonstration experiments have proven that there has been no reduction in its ability to be effectively used by visually-impaired people. Those affected by vision impairment have made passionate requests for its early realization[13–14].

In this manuscript, on the basis of experience developed through the development and demonstration experiments made so far, we discuss the results of our work on the condition of realization and social implementation, acquisition of safety certificate ISO 13482, and the framework for social implementation.

2. Approach for Realization and Social Implementation

Realization and social implementation of personal care robots will be beneficial for both users and managers as well as for the safety of third parties. For that purpose, we think that the following three conditions need to be satisfied.

(1) assurance of safety for social acceptance
(2) high cost efficiency
(3) scheme for popularization including sales methods, insurance, maintenance, and subsidies

This section describes the outline of (1) and (2). Section 3 explains the acquisition of safety certificate ISO 13482, and section 4 explains details of the scheme construction.

2.1. Safety standard

In response to a comment from a hospital operator requesting safety certification from a third party, we obtained the only international standard on the safety of personal care robots, ISO 13482, issued in February 2014. That marked the 11th acquisition in Japan[15], following Resyone of Panasonic and HAL of Cyberdyne. In addition, it is the first acquisition for a robot with an intuitive interface, moving together with the user.

2.2. Cost efficiency

Cost efficiency is, in other words, the operating ratio. From interviews with hospital operators, it was estimated that a guiding robot specialized for visually-impaired people will be needed about once or twice a month in a big hospital. It was pointed out that if a robot is specialized for visually-impaired people only, the cost efficiency would be low. On the other hand, it is common for even sighted people to get lost in a big hospital. In response to the comment that a robot guiding elderly people also would improve patient satisfaction, the target users have been expanded to sighted people who are unfamiliar with the layout in the hospital, in particular elderly people.

The numbers of new patients per day estimated on the basis of information made available on the Internet by hospitals are about 152 at Tokyo Metropolitan Tama General Medical Center (as of 2016)[16], about 202 at Juntendo University Medical Department Urayasu Hospital (as of 2012)[17], about 120 at Jichi Medical School Hospital (as of 2014)[18], about 182 at the Hospital of the University of Occupational and Environmental Health (as of 2014)[19], and about 111 at Yokohama Municipal Citizen's Hospital (as of 2016)[20]; there is an average range of about 100–200 new patients per day. With an assumption of a guiding time of 3 minutes per patient, it would take 5–10 hours to guide every new patient, indicating that a transportation assistance robot capable of guiding patients would alleviate the workload of receptionists, providing a big benefit to the hospital.

3. Acquisition of ISO 13482

3.1. Risk assessment

ISO 13482 was issued in February 2014 as the only international standard on the safety of personal care robots. It is a safety standard on the basis of risk assessment (RA) (Figure 1)[21]. Through RA, hazard sources and hazardous events are identified and then the risks are analyzed, and processes that minimize the risk to an acceptable level are evaluated. As there is no test method clearly defined or standard value such as conventional standards for industrial products, we have independently optimized evaluation standards on the basis of the design philosophy of the manufacturer and concepts of the equipment developed in addition to RA.

To obtain ISO 13482, it is recommended to cooperate with the certification organization from the design phase. We proceeded with authentication with confirmation of the Certification System Development Promotion Office, Japan Quality Assurance Organization (JQA).

Figure 2 shows the authentication process. In Phase 1, the development flow of a specification decision and design, as well as the design control system, are audited. In Phase 2, the systems of evaluation, validation, production, and production control are audited.

RA was carried out on the device[11] that had already been developed for demonstration experiments, and design changes were made where necessary. The sheet[22] developed by the National Institute of Occupational Safety and Health, in a project with the New Energy and Industrial Technology Development Organization (NEDO) Incorporated Administrative Agency, was adopted as the RA sheet. Visually impaired people, who do not have any difficulty in walking by themselves, and elderly people were preset as the users, and a handicapped accessible hospital was assumed as the usage environment.

Hazard sources were identified in accordance with ISO 13482 Appendix A. With additional hazard sources identified on the basis of hazardous events identified through our demonstration experiments in the past, we have identified and performed risk assessment on a total of 102 hazard sources. Table 1 shows an excerpt of the RA sheet.

For hazard sources with high scores as the result of the initial risk assessment, risk mitigation measures were carried out on each of them. Falling down on a step was the hazardous event with the highest risk score, which was reduced by careful operation and reinforcement of the safety device.

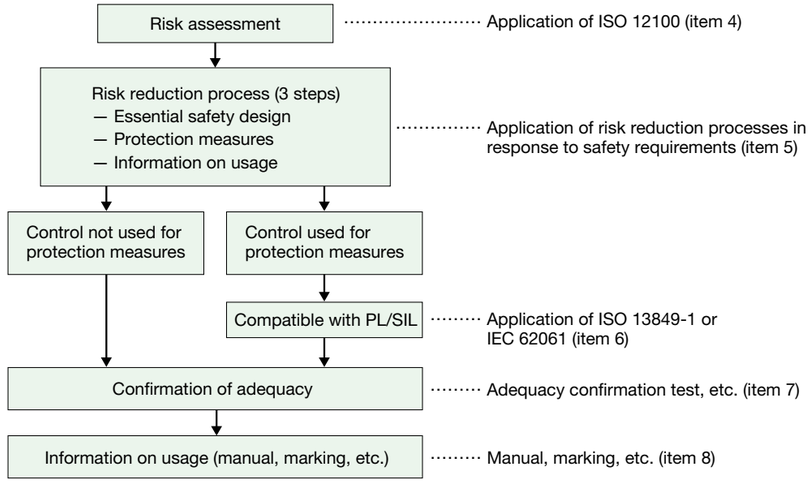

Fig. 1 Overview of the ISO 13482 safety requirements (source: JQA document)

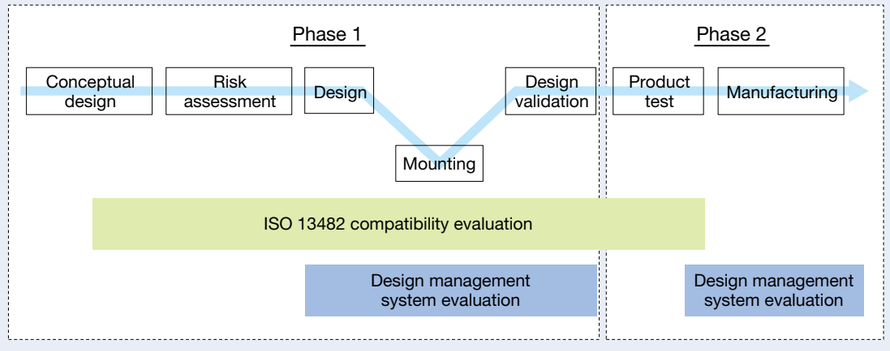

Fig. 2 Process of ISO 13482 certification (source: JQA document)

Table 1 EN standards for railway bearings

(a) Risk matrix

Severity of damage: S		Damage occurrence probability									Frequency of exposure/time: F		Hazardous event occurrence probability: P		Hazard avoidance/ mitigation probability: A	
		3	4	5	6	7	8	9	10	11						
Serious injury (long-term medical treatment)	4	12	16	20	24	28	32	36	40	44	Continuous/ steady	4	Very probable	4		
Medical treatment (short-term medical treatment)	3	9	12	15	18	21	24	27	30	33	Frequent/ long time	3	Highly possible	3	Impossible	3
Recovery by first aid treatment	2	6	8	10	12	14	16	18	20	22	Sometimes/ short time	2	Possible	2	Possible	2
No injury/temporary pain	1	3	4	5	6	7	8	9	10	11	Rare/ instantaneous	1	Rare	1	Easy	1

(b) Initial risk assessment

Hazard source identification							Risk assessment							
Hazard source category	Hazard source	Potential result	Phase	Victim (who)	Hazard area (location)/ frequency point of view	Hazardous event (hazardous situation)	Severity of damage	Damage occurrence probability Ph	Frequency F	Hazardous event occurrence probability P	Avoidance A	Risk mark	Reference for risk scenarios	· Response, measure (10) · Remarks
Hazard source associated with battery recharge	Overload of battery	Fire, hazardous smoke, or emission of hazardous material	Start-up (turning off)	Manager	Battery	Catching fire and receiving burns (1st degree)	2	7	3	1	3	14	ISO 13482 FTA (A34)	Risk reduction (reservations accepted) refer to the sheet
	Recharge of deeply discharged battery	Fire, hazardous smoke, or emission of hazardous material	Start-up (turning off)	Manager	Battery	Catching fire and receiving burns (1st degree)	2	7	3	1	3	14	ISO 13482 FTA (A35)	
	Contact with battery hot terminal	Electric shock	Start-up (turning off)	Manager	Battery	Contacting the hot terminal of battery and receiving electric shock (tingle)	2	7	3	1	3	14	ISO 13482 FTA (A31)	
	Short-circuiting of battery	Fire, hazardous smoke, or emission of hazardous material	Start-up (turning off)	Manager	Battery	Catching fire and receiving burns (1st degree)	2	7	3	1	3	14	ISO 13482 FTA (A36, A37)	
Hazard source associated with the energy storage and energy supply	Hazardous contact with a high electric energy source	Electric shock, burn	Battery and recharger as a set. Refer to a similar scenario No. 3.				—	—	—	—	—	—	—	Appropriate item number of the requirement summary sheet
	Electrical charging of electric/non-electric part in a malfunction condition	Electric shock	Start-up, navigation	User	Robot metallic surface part	Malfunction causes electrical leak. Without noticing it, one contacts the hazardous portion of the robot and receives an electric shock.	2	7	2	2	3	14	ISO 13482 FTA (A31, A32)	Risk reduction (reservations accepted) refer to the sheet

(c) Risk reduction

Initial risk analysis result					Risk reassessment							
Hazard source category	Hazard source	Hazardous event (hazardous situation)	Risk mark R	Engineering method by the manufacturer	S	Ph	F	P	A	Risk mark	When protection measures are combined R	· Response, measure (3) · remarks
Hazard source due to an error of the position confirmation or navigation	Position confirmation error that can cause ingress into hazardous area	Due to many navigation errors, the user is lost, intrudes into a hazardous area (descending stairs), and the user and the robot fall.	24	Avoid a route with descending stairs as much as possible. A marker on the ceiling around the descending stairs to minimize the navigation error and avoid going near stairs.	4	5	1	2	2	20	16 (4)	Appropriate item number of the requirement summary sheet
				Equip with a tumble prevention sensor and brakes (1). Detect areas susceptible to falling and perform a stop.	4	5	2	1	2	20		
Hazard source due to an error of the position confirmation or navigation	Tumbling robot	Robot falls down the descending stairs and collides with people around the bottom of the stairs.	18	Take measures 81-1	3	4	1	1	2	12	12 (4)	Appropriate item number of the requirement summary sheet
Hazard source category peculiar to this robot	Mistaken operation (with left hand)	Because the user is bigger than the robot, the paths of the robot and the user are different. The robot avoids colliding, but the user collides with an obstacle.	18	Make the grip shape difficult for a left hand grasp	2	6	2	1	3	12	12	Appropriate item number of the requirement summary sheet

3.2. Design

Detailed specifications were determined in consideration of the specification defined by required capabilities, feedback from RA, and design validation. Table 2 shows the representative specification.

As the intended user base is visually-impaired people and elderly people, the average height of Japanese elderly people[23], easy-to-read text size[24], and walking speed[25] were considered for elderly people, and operation was made possible by merely touching the remote controller for visually-impaired people. In addition, for use inside a hospital, it is necessary to satisfy Class B emission of CISPR 11 regarding EMC, which is more stringent than specifications for general industrial machinery.

Table 2 Main specifications

Outer size	D 500 × W 390 × H 960 mm
Weight	25 kg
Maximum speed	3 km/h (inside the restricted area: 1 km/h)
Climbable slope	5°
Loading capacity	5 kg
Driving source	Li-ion battery (22.2 V, 450 Wh)
Interface	Setting of destination: touch panel, remote controller Displacement: grip (force sensor)
EMC (emission)	CISPR11 Class B
Usage temperature/ humidity	8–30°C/40–70%

Design of each part continued to satisfy the users in terms of the detailed specifications that were selected. Figures 3, 4, and 5 show the system block diagram, assembly drawing, and overview of the robot, respectively.

Here the main safety equipment of the robot is shown. As a policy, the following safety equipment does not involve software.

• Items associated with prevention of falling down

To prevent falling down, the floor in front, right, and left (distance to the floors) shall be detected. Ranging sensors are selected; one sensor is installed on the right and left sides. The data on the distance to the floor detected as an analog signal, and if the signal is determined to be higher than a certain threshold by a comparator circuit, it is digitally displayed. The threshold can be adjusted with a variable resistor in accordance with the usage environment of the robot. The digital output from the sensor is fed into the motor driver. If no floor is judged to exist, the motor driver is stopped and simultaneously the brake is applied on the drive shaft.

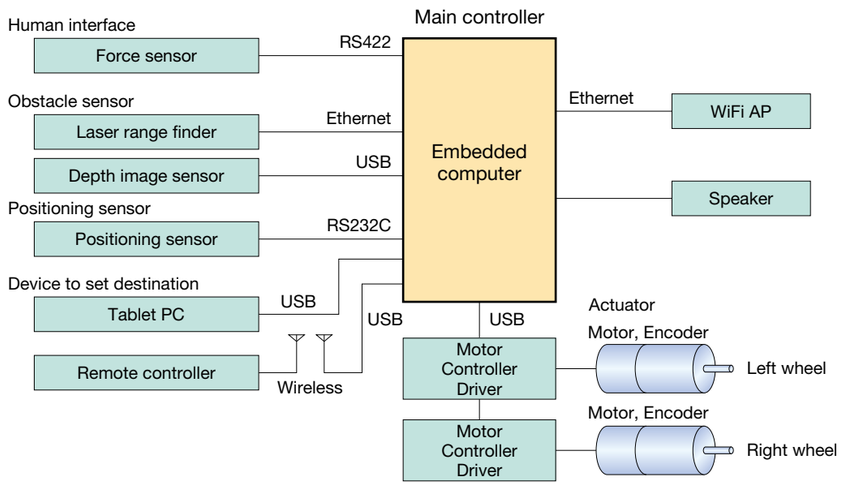

Fig. 3 System block diagram

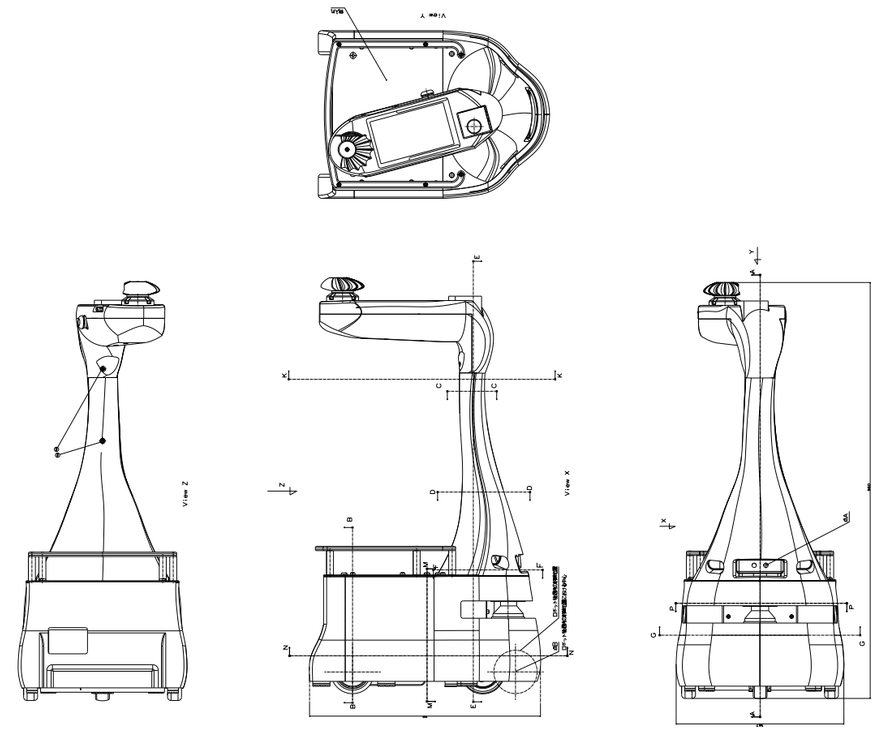

Fig. 4 Assembly drawing of a robot

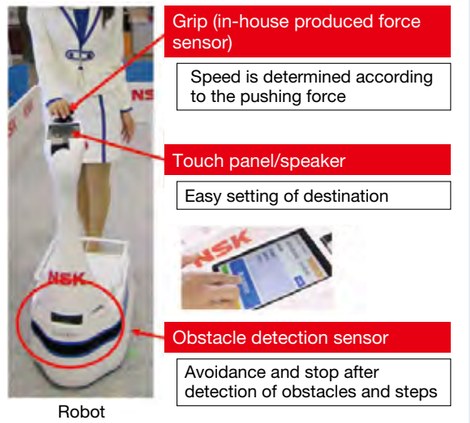

Fig. 5 Overview of a robot

• Items associated with obstacle detection

Human detection required by the ISO 13482 standard specification presupposes the use of electric sensor protection equipment (ESPE) in accordance with the corresponding instructions of IEC 61496. Figure 6 shows the obstacle detecting area. If an obstacle enters area ⑤, the speed limit is set at 1 km/h. In case of area ④, a motion maneuvering around the obstacle is set by the software. In case the motion maneuvering around the obstacle does not work properly, or an obstacle enters suddenly into area ② or ③, the motors driving the wheels on the opposite side of area ② or ③ are stopped and a maneuvering motion is carried out. In addition, area ① near the robot is set as the protective area. If an obstacle is detected in this area, the motor driver is stopped and the brake is applied, forcing an instantaneous stop. If the obstacle disappears, one can select either manual resetting or automatic resetting. Due to the policy of no software involvement in the safety-related system, the procedure of manual restart is adopted. The selected sensor satisfies PL = d as a single body.

3.3. Validation

To confirm that the design specifications are met, validation has been carried out. The content and validation results are shown for the representative validation test.

3.3.1 EMC

At the NVLAP certification test site, tests were carried out on each test item on emission and immunity, showing that the applied standards were satisfied, as shown in Table 3.

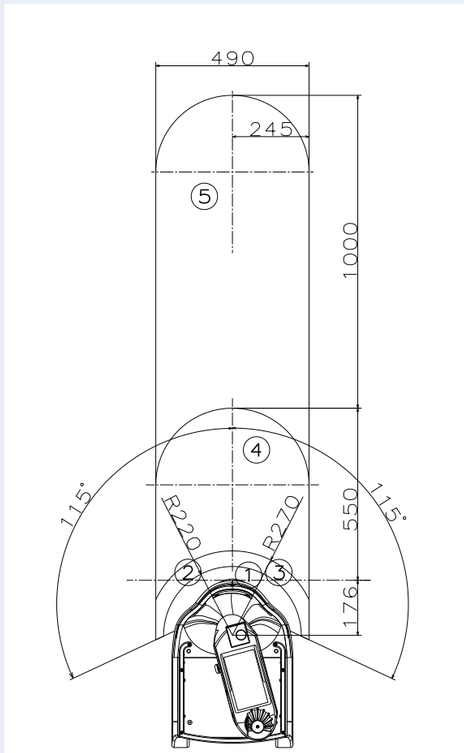

Fig. 6 Obstacle detecting area of a robot

Table 3 EMC results

Emission test	Applied standard	Standard value	Frequency (Hz)	Measured value	Margin	Result
Power source port conduction interference wave test	CISPR Pub.11 Gr.1 : 2015	50.0 dBμV	10.034 MHz	37.2 dBμV	12.8 dB	Applicable
Communication port conduction interference wave test	CISPR Pub.11 Gr.1 : 2015	Not applicable	Not applicable	Not applicable	Not applicable	Not applicable
Interference wave electric field test	CISPR Pub.11 Gr.1 : 2015	37.0 dBμV/m	450.000 MHz	35.4 dBμV/m	1.6 dB	Applicable

Immunity test	Margin	Result
Electrostatic discharge immunity test	IEC61000-4-2: 2008	Applicable
Radiative microwave frequency electromagnetic field immunity test	IEC61000-4-3: 2006 + A1: 2007 + A2: 2010	Applicable
Electric fast transient/burst immunity test	IEC61000-4-4: 2012	Applicable
Surge immunity test	IEC61000-4-5: 2014	Applicable
Immunity against conduction interference induced by a microwave frequency electromagnetic field	IEC61000-4-6: 2013	Applicable
Immunity test of the voltage dip, short time blackout, and voltage fluctuation	IEC61000-4-11: 2004	Applicable

3.3.2 Running the stability test

Referring to the robot safety validation method[27] and the standard of electric wheelchairs[26] of NEDO, we have set the conditions of running stability tests, as shown in Table 4. The inclination angle was negative for the downward slope and positive for the upward slope. Test 1 is a test stopping either wheel, assuming a downward slope and rapid avoidance of an obstacle. The right and left wheels were both tested. Test 2 was a test of a sudden stop on a downhill; Test 3 was a rapid start-up on an uphill; and Test 4 was a circulation test on flat ground with a minimum circulation radius of about 1.4 m during navigation and carried out on both wheels. In the experiments associated with maneuvering around an obstacle, the initial wheel rotation speed was set to 5.6 rad/s, corresponding to the robot speed of 1 km/h, due to the limitation of the real operation speed of 1 km/h. In each test, no fall of the load and no tumbling of the robot itself were the criteria for determination. Additionally, no problem in running uphill for Test 3 was a criterion for determination. The validation test was carried out in the Life-Supporting Robot Safety Validation Center in Tsukuba City, Ibaraki Prefecture (Figure 7), and no problems were found.

In all the tests, the running road surface was paved with P tiles, similar to the hospital floor of the assumed environment, and the forward running direction and a load of 5 kg were set.

In addition, as reference confirmation, Tests 1 and 2 were performed with a running speed of 3 km/h, or a wheel angular rotation speed of 16.7 rad/s, and Tests 1, 2, and 3 were performed with an inclination angle of 8°. Through these tests, it was confirmed that there was no tumbling of the robot, no fall of the load, and no problems in terms of running uphill.

3.3.3 Running endurance test of the drive unit

The durability of the whole robot has been validated in a separate vibration test. Running durability was examined with a focus on the driving mechanism including the motor, reducing gears, and wheel. Referring to the robot safety validation method of NEDO[27], we have fabricated a testing machine, as shown in Figure 8, and have planned and carried out the test.

A running road surface of unlimited length is simulated by a drum. Also, a power brake was installed on the drum to make a configuration to give a load.

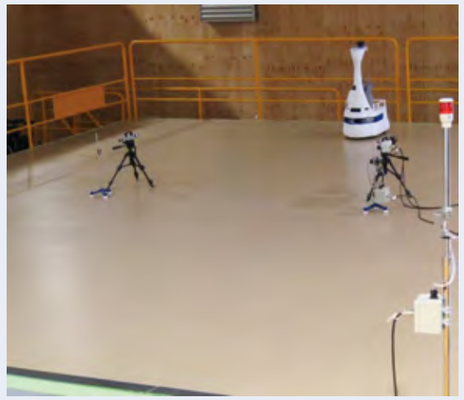

Fig. 7 Running stability test

Fig. 8 Endurance test of the driving unit

Table 4 Parameter of the running stability test

Test	Applied standard	Wheel initial angular velocity rad/s		Test angular velocity rad/s	
		ω_L	ω_R	ω_L	ω_R
1a	–5°	5.6	5.6	0	5.6
1b	–5°	5.6	5.6	5.6	0
2	–5°	5.6	5.6	0	0
3	5°	0	0	16.7	16.7
4a	0°	16.7	16.7	16.7	13.2
4b	0°	16.7	16.7	13.2	16.7

To simulate the operation situation of the robot, repeated tests were carried out with test cycles, command speeds, and wheel loads, shown in Table 5. The load torque provides the difference between the torque for the robot to run on the ground and the torque for the rotation on the drum. During the rental period of three years (assumed usage time of 1 014 hours), replacement of service parts should be needed only once; in other words, the judgment condition was the capability of running for more than 507 hours.

The result was a continuous running for about 588 hours, satisfying the judgment condition. The cause of the stop was erosion of the rubber of the driving wheel, the powder of which accumulated on all the parts of the driving unit, and many of them were attached to the bearings, and the running resistance increased. The validation experiments performed in hospitals so far have not shown any powder generation or attaching of powder, leading us to consider that the present test result was due to conditions harsher than those simulated, peculiar to endurance tests in a closed space with continuous operation with no displacement. The result has shown that maintenance is required at least once every 1.5 years, which is within the acceptable limit.

Table 5 Cycle of the running endurance test

	Command speed	Load torque	Time
Acceleration	3 (km/h)	0.49 (N·m)	1 s
Constant speed	3 (km/h)	0.049 (N·m)	5.58 min.
Deceleration	0 (km/h)	0.49 (N·m)	1 s
Stop	0 (km/h)	0.49 (N·m)	2 s

Table 6 Parameter of the detecting obstacle test

Test No.	Initial speed	Judging standard
1	3 ± 0.15 km/h	Deceleration at ⑤, avoidance at ④
2	1 ± 0.15 km/h	Avoidance at ③ (overriding ④)
3	1 ± 0.15 km/h	Avoidance at ② (overriding ④)
4	1 ± 0.15 km/h	① Stop (overriding ②③④)

3.3.4 Obstacle detection experiment

Referring to the robot safety validation method[27], and the standard[28] of NEDO for statically stable movable working robots without a manipulator, tests were carried out to confirm deceleration and avoidance in each obstacle detection area shown in Figure 6. The running surface was concrete, and a white cylinder with a diameter of 60 mm was used for a static obstacle. Table 6 shows the testing conditions. Figure 9 shows an example of the obstacle detection test. The robot was made to approach the static obstacle head on. The robot behavior was observed to confirm that no problem occurred.

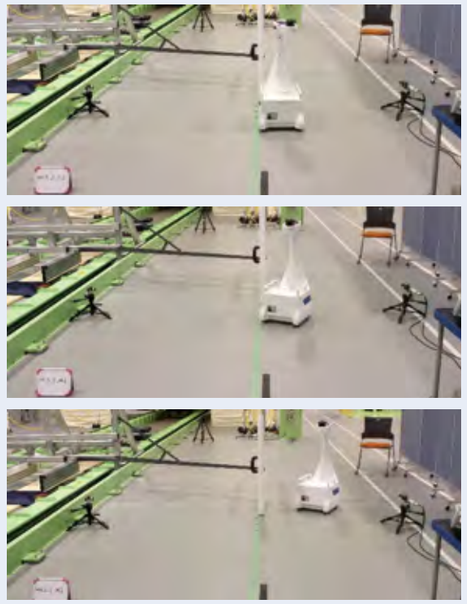

Fig. 9 Example of the obstacle detecting test

3.3.5 Compound environmental test

Referring to the standard[29] of the environmental test of industrial machinery, tests were carried out at the Personal Care Robot Safety Validation Center. On the basis of the usage temperature and usage humidity of robots, a robot was exposed to the testing conditions shown in Table 7. After the exposure, operation of safety functions (fall detection, etc.) and basic functions (robot control by grip, etc.) were confirmed without any problems. Figure 10 shows the compound environmental test.

3.4 Manuals and labels

ISO 13482 specifies that manuals are to be also examined. Since this robot will be used in facilities such as hospitals, robot management manuals for facilities, assembly manuals for robot manufacture, and maintenance manuals, etc., in consideration of future maintenance, were made and submitted for examination for certification. In addition, labels were also the object of examination. After risk suppression by RA, robots were labeled in reference to the items in the ALARP domain. Visually-impaired people are urged by hospital staff to pay attention.

3.5 Design management system, production management system

ISO 13482 is a standard for safety. Its certification presupposes the evaluation of the design management system and production management system.

On the basis of the system of the department in our company, which acquired ISO 9001, the management system has been completed.

For the design management system, general rules and procedures were documented on record management, purchasing process, requirements on competence, and more.

For the production management system, general rules and procedures were made similarly on record management and the management of defective products, and documentation was made on examination documents on the acceptance, assembly, and shipping examinations.

3.6 Acquisition of certification

On March 13, 2017, certification was given by the Japan Quality Assurance Organization (JQA) (Figure 11). It was the 11th ISO 13482 certification and marks the first certification of the world for a guiding a robot with human interface.

Table 7 Parameter of the compound environmental test

	Temperature	Humidity	Test duration
High temperature, high humidity (steady state) test	33°C ± 2°C	70% ± 3 %	16 h
Low temperature (low temperature resistance) test	5°C ± 2°C	No specification	16 h

Fig. 10 Compound environmental test

Fig. 11 ISO 13482 Certificated

4. Structure Forming

4.1 System for rental, lease, and insurance

Even after safety is certified, people have reservations about introducing robots with no or few past records of implementation. Examination of sales system shows that leasing and renting costs can be processed not as facility costs but as expenses and are more acceptable for hospitals. In addition, we have become strongly aware that whereas leasing, in which midterm cancellation is impossible in principle, makes implementation difficult, and renting, in which cancellation is allowed at any time in principle, these facilitate implementation.

Leasing after renting a leased product at the initial time of introduction and checking the reality of its maintenance is a matter of common practice, and we consider this as a suitable way our robots can proceed, as we have negotiated with a leasing company and established the system shown in Figure 12.

In addition, insurance for robots was discussed between insurance companies and manufacturers in a working group of the former Association to Promote Robot Businesses. Negotiation between the insurance companies and us has enabled manufacturers and leasing companies to join product liability insurance and movable insurance, and it has also enabled the facility manager to join facility owner liability insurance and personal liability insurance in addition to the conventional facility insurance.

4.2 Maintenance

The replacement timing is known beforehand for some parts after endurance tests, etc., but unexpected symptoms can arise in a real environment. Accordingly, we have made the following policy. For the time being, robots are introduced in a limited number of facilities so that we can quickly carry out maintenance work. After accumulating experience in performing maintenance on our own, we will outsource the work to maintenance companies.

4.3 Subsidy for introduction

Due to the need to use sensors with certification and parts with low failure rates, reduction of the production cost of the robot itself has a real limit. However, a high cost would prevent hospitals from implementing robots, despite being well aware of their usefulness. We have therefore examined and considered subsidies that facilities can receive. For nursing-care robots, a subsidy system is being established. The Japan Agency for Medical Research and Development (AMED) has applied such a system, but it targets only prescribed kinds of robots and does not cover the wide popularization of robot technology in the fields of nursing care and welfare. No applicable subsidy system of governmental agencies and foundations, satisfying the conditions, exists. We have petitioned for one but have not established any system applicable to all of Japan. Only Kanagawa Prefecture has granted a subsidy system applicable only inside the prefecture. For the popularization of new products such as robots and culture, we believe that support from the government is essential. We hope that this trend will spread across the whole country.

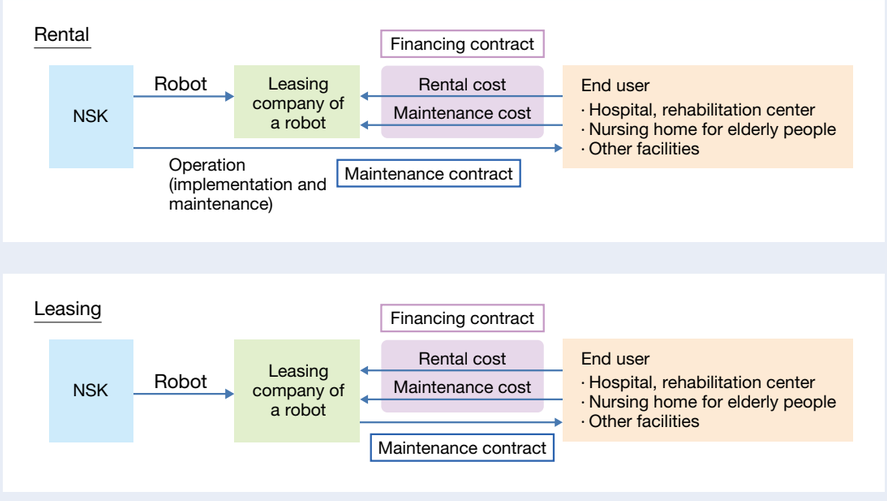

Fig. 12 Framework of the sales structure

5. Summary

We have reported our activities to acquire ISO 13482 Safety Certification and organize the system for the realization and social implementation of robots guiding visually-impaired people and elderly people inside a facility. So far, we do not have a sales record, but we have introduced a robot for which we have carried out the in-house development product delivery process based on ISO 13482 certification and shipped to the Kanagawa General Rehabilitation Center, our development partner, in March 2017. After the introduction, we have received comments such as inconvenience due to the need of rebooting every time after a forced stop occurs when an obstacle approaches and the need for autonomous return to the receptionist after guiding a patient from the receptionist to a clinical department. Autonomous running is not covered by safety certification; however, for the facility using a robot, autonomous running improves return on investment and is in our future agenda.

Acknowledgments

This development was supported by the Development Promotion Project of Self-Reliance Support Equipment for the Handicapped of Ministry of Health, Labor and Welfare for the fiscal years of 2015 and 2016. Support was also provided as a priority project of the Sagami Robot Industry Special Zone of the Kanagawa Prefecture Industry Promotion Department. In addition, we would like to express our deep appreciation for the cooperation from the Kanagawa Prefecture Rehabilitation Center through a series of demonstration experiments and advice, leading to the realization of robots. Finally, we would like to thank Professor Kazuteru Tobita, Associate Professor at Shizuoka Institute of Science and Technology, who has collaborated with us in the development of guidance robots for 14 years.

References

1) Ministry of Health, Labor and Welfare, “Survey on the difficulty of living in 2011 (Survey on the actual situation of home-based people with disabilities in the whole country),” (2013).
2) World Health Organization, “Visual impairment and blindness,” (October, 2017).
3) Ministry of Health, Labor and Welfare, “Survey on persons with physical disability in 2006,” (2006).
4) National Rehabilitation Center for Persons with Disabilities, “Rehabilitation Manual 13, Tactile Paving,” (2003).
5) S. Tachi, and K. Komoriya: “Guide Dog Robot” Robotics Research: The Second International Symposium 1984, The MIT Press, pp. 333–340 (1985).
6) Mori, Matsumoto, Kobayashi, and Mototsune, “R & D for Practical Use of Robotic Travel Aid for the Visually Impaired,” Journal of the Robotics Society of Japan, 19-8 (2001) 26–29.
7) Iwan Ulrich and Johann Borenstein, “The GuideCane – Applying Mobile Robot Technologies to Assist the Visually Impaired,” IEEE Transactions on Systems, Man, and Cybernetics, Part A: Systems and Humans, Vol. 31, No. 2, (2001).
8) Aditi Kulkarni, Allan Wang, Lynn Urbina, Aaron Steinfeld, and Bernardine Dias, “Robotic Assistance in Indoor Navigation for People Who are Blind,” 11th ACM/IEEE International Conference on Human-Robot Interaction (HRI), (2016).
9) Tobita, Ogawa, and Sagayama, “Development of a Robot Substitute for a Guide Dog,” NSK Technical Journal, 686 (2013).
10) Tobita and Sagayama, “Efforts of Guidance Robot for Visually-impaired People,” Journal of the Japan Robot Association, 217 (2014).
11) Tobita and Sagayama, “Examination of the Guidance Robot for Visually-impaired People,” Journal of the Robotics Society of Japan, 33-8 (2015) 596–599.
12) Kazuteru Tobita, Katsuyuki Sagayama, and Hironori Ogawa, “Examination of a guidance robot for visually impaired people,” Journal of Robotics and Mechatronics, Vol. 29, No. 4, pp. (2017).
13) Murata, Kato, Tobita, et. al, “Efforts toward practical application of guidance robots for the visually impaired in robot town sagami,” The 31st Conference on the Advancement of Assistive and Rehabilitation Technology in Kochi, (2016).
14) Kazuteru Tobita, Katsuyuki Sagayama, Mayuko Mori, and Ayako Tabuchi, “Structure and Examination of the Guidance Robot LIGHBOT for Visually Impaired and Elderly People,” Journal of Robotics and Mechatronics, Vol. 30, No. 1, (2018).
15) List of JQA certified people: https://www.jqa.jp/service_list/fs/action/clientele/
16) Tama Medical Center, patient statistics: http://www.fuchu-hp.fuchu.tokyo.jp/about/data/stats_patient/
17) Juntendo University Medical Urayasu Hospital, Clinical Indicators and Achievements: http://www.hosp-urayasu.juntendo.ac.jp/about_hospital/qi.html
18) Jichi Medical University Hospital, Annual report: http://www.jichi.ac.jp/hospital/top/outline/report.html

19) Hospital of University of Occupational and Environmental Health, Japan, Medical examination achievements: http://www.uoeh-.ac.jp/hospital/hpgaiyo/sinryojisseki.html
20) Yokohama Municipal Citizen's Hospital, Medical examination achievements: http://yokohama-shiminhosp.jp/introduction/data/jisseki.html
21) ISO 13482:2014 Robots and robotic devices—Safety requirements for personal care robots: https://www.iso.org/standard/53820.html
22) RT-SIC, Risk assessment: http://www.rtnet-biz.jp/rtsic/info/sdesign/riskass.html
23) Ministry of Education, Culture, Sports, Science and Technology, "Survey on Physical Strength and Athletic Performance," (2014).
24) JIS S 0032:2003, "Guidelines for the elderly and people with disabilities—Visual signs and displays—Estimation of minimum legible size for a Japanese single character."
25) Research Institute of Human Engineering for Quality Life, "Stride, steps, speed during normal walking," (1998): http://www.hql.jp/project/funcdb1993/
26) JIS T 9203:2010, Electric wheelchairs.
27) NEDO, Project for practical applications of service robots, Research and development of safety level verification technology, 4.4.2 the dynamic stability tests, (2014).
28) JIS B 8446-1, Safety requirements for personal care robots—Part 1: Static stable mobile servant robot with no manipulator.
29) IEC60950-1, Information technology equipment, Safety—2.9.2: Securing of electrical insulation.

Katsuyuki Sagayama

Mayuko Mori

Ayako Tabuchi

Yosuke Fukushima

Development of Omnidirectional Mobile Electric Wheels

Ko Fujioka and Yasunori Oishi
New Field Products Development Center, Technology Development Department 2

Abstract

Many automatic guided vehicles (AGVs) are being used in warehouses and factories these days. The vehicles must be able to move in every direction for various special uses, but currently only differential motion allows them to turn on their driving wheels. Also, in cases such as sharp turns and moving between buildings, pushing the AGVs manually is faster. To address these problems, omnidirectional mobile electric wheels for both driving wheels and driven wheels were developed and evaluated.

1. Introduction

Currently, many automatic guided vehicles (AGVs) have two parallel driving wheels on either side, and turning an AGV is controlled by the differential motion of these wheels. These AGVs generally run along a pre-programmed path. However, the vehicles must be capable of moving in every direction for a range of special uses. In addition, manual pushing of a truck could be more effective in cases such as the fine adjustment of position and movement to places that have not been pre-programmed. The wheels on commercialized omnidirectional mobiles trucks include Omniwheels and Mecanum wheels. These types of wheels have free rollers, so they are susceptible to vibration and incapable of handling bumpy roads. Also, since they are connected to the motor through a reducer, manual movement of the truck is difficult due to the high reversed operation torque.

Considering these problems, omnidirectional mobile electric wheels have been developed and evaluated. Omnidirectional movement is realized with an Active-caster[1)], which can move omnidirectionally by controlling both a driving wheel and a steering axle by motor. Since the Active-caster structure is similar to that of a swivel caster, its vibration is low, and it can handle bumpy roads well. For manual operation, a direct drive motor (DD motor) will be used in future, and the reducer will not be necessary on the caster due to the DD motor's high torque. These characteristics will allow for smooth manual operation of the truck.

In this article, the omnidirectional movement of an Active-caster is evaluated with a system that applies servomotors and reducers instead of a DD motor. The system has two clutches, one connecting the servomotor to the wheel and the other connecting the servomotor to the steering axle. By letting out the clutch, manual operation with a passive rotation caster is enabled. The prototype of this omnidirectional mobile electric wheel has also been evaluated.

2. Structure and Kinematics of Active-caster

2.1 Structure of a double-wheel Active-caster

The double-wheel Active-caster, shown in Figure 1, is designed to mitigate the steering force for smooth manual operation. Two servomotors are installed on the caster: one drives the wheel and the other the steering axle. The steering axle is driven by a motor and simple gear, but motors for the wheel are driven by differential gears and a belt. Differential gears have been installed to absorb the mismatch of the rotation between the two wheels. In addition, suspensions are installed on both wheels to ensure they are in contact with the ground so as to prevent traction loss. Electromagnetic clutches are installed between each motor and the wheel or the steering axle. If the motor is connected to the wheel and steering axle, then the Active-caster can move, but if the motor is disconnected, it can only passively be moved. The wheel diameter is 125 mm, the distance between the double wheels is 56 mm, and the distance between the steering axle and wheel axis is 40 mm.

2.2. Kinematics of double-wheel Active-caster

Figure 2 shows the kinematics model of the Active-caster[2)], where V_x and V_y are X and Y components of the Active-caster moving velocity, respectively, ω_L, and ω_R are the wheel angular velocity, ω_s is the steering wheel angular velocity, r is the wheel radius, s is the distance between the steering axle and wheel axis, W is the distance between the two wheels, and ϕ is the steering wheel angle. Then, the wheel average angular velocity and the steering angular velocity of the Active-caster ω_w and ω_s, Active-caster are expressed by eq. (1).

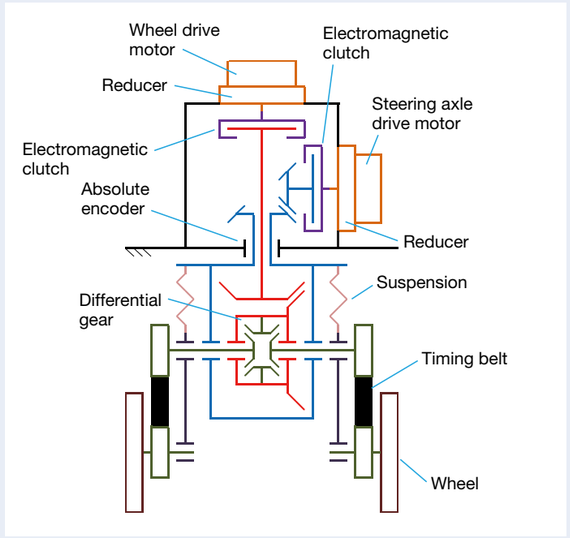

Fig. 1 Double wheel Active-caster

$$\omega_W = \frac{\omega_R + \omega_L}{2} \quad \cdots\cdots (1)$$

$$\omega_S = \frac{\omega_R - \omega_L}{W}$$

The relationship between the caster moving velocity and angular velocity of the wheel drive axis and steering axle is expressed by eq. (2)

$$\begin{bmatrix} \omega_W \\ \omega_S \end{bmatrix} = \begin{bmatrix} \frac{cos\,\phi}{r} & \frac{sin\,\phi}{r} \\ -\frac{sin\,\phi}{s} & \frac{cos\,\phi}{s} \end{bmatrix} \begin{bmatrix} V_x \\ V_y \end{bmatrix} \quad \cdots\cdots (2)$$

The controlling unit calculates the steering wheel angle ϕ and the speed command for each motor by eq. (2) with the absolute encoder value.

Figure 3 shows the kinematics model of the truck with two Active-casters. The truck's rear wheels are Active-casters and its front wheels are passive casters. W_c is the distance between the Active-casters, L_c is the longitudinal distance between the Active-caster and the center of the truck, V_x and V_y are the X and Y components of the moving truck's velocity, ω is the rotation angular velocity, and V_{xR}, V_{yR}, V_{xL}, and V_{yL} are the X and Y components of the moving velocities of the right and left Active-casters, respectively. In this case, the relationship of the truck's moving velocity, the rotation angular velocity, and the moving velocities of the right and left Active-casters is expressed by eq. (3).

$$\begin{bmatrix} V_{xR} \\ V_{xL} \\ V_{yR} \\ V_{yL} \end{bmatrix} = \begin{bmatrix} 1 & 0 & \frac{W_C}{2} \\ 0 & 1 & -L_C \\ 1 & 0 & -\frac{W_C}{2} \\ 0 & 1 & -L_C \end{bmatrix} \begin{bmatrix} V_x \\ V_y \\ \omega \end{bmatrix} \quad \cdots\cdots (3)$$

3. Installation of a Double-Wheel Active-caster on a Truck

3.1. Truck structure

Figures 4 and 5 show the developed truck with an Active-caster. Table 1 shows its specifications. The double-wheel type swivel casters are installed as the truck's front wheels. In addition, lithium ion batteries are installed in the battery box at the front of the truck. Motor drivers and controlling units, such as a controlling PC, are installed on the control rack at the rear of the truck.

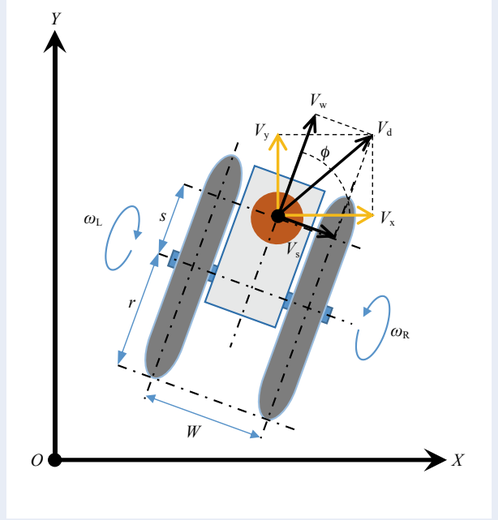

Fig. 2 Active-caster kinematics

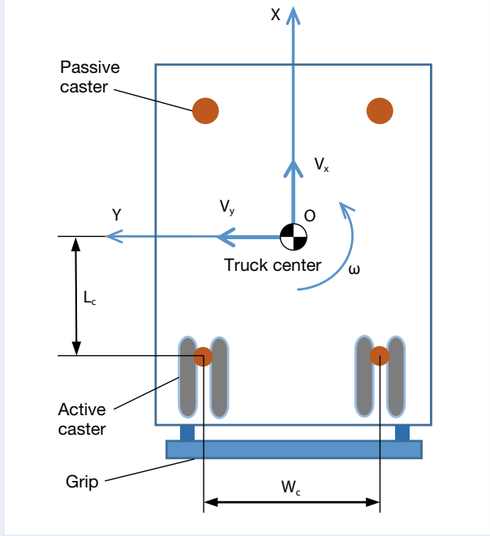

Fig. 3 Truck with two Active-casters

Figure 6 shows the controlling system configuration of the truck with two Active-casters. A tablet PC is used as the control unit. The truck can be controlled remotely and has an automatic running function with a path plan. The PC sends out the commands of each motor rotational speed in analog voltage through an AIO interface. The command values are calculated by eqs. (2) and (3). The relative angle (steering angle ϕ) of each wheel to the truck body is measured by the absolute encoder output installed on the Active-casters through a DIO interface. In addition, the clutch-control and mode change as well as automatic running mode and manual mode can be applied with the PC. There are also two automatic running modes: omnidirectional mobile mode and rigid mode. The omnidirectional mobile mode controls movement in every direction, while the rigid mode is used for the steering angle of the wheels, which can be adjusted with this procedure: first drive the truck to where the steering angle of the wheels can be fixed, and when the driving wheels are parallel to the electromagnetic brake, the truck can be steered by the differential rotation of the two driving wheels.

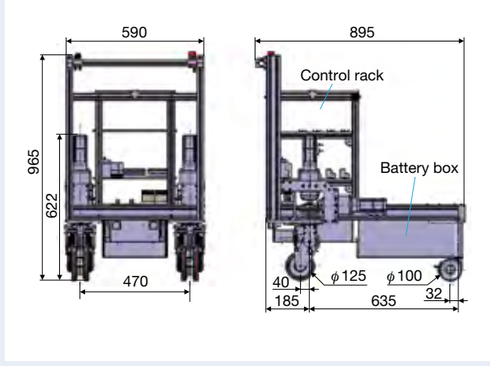

Fig. 4 Active-casters in a truck

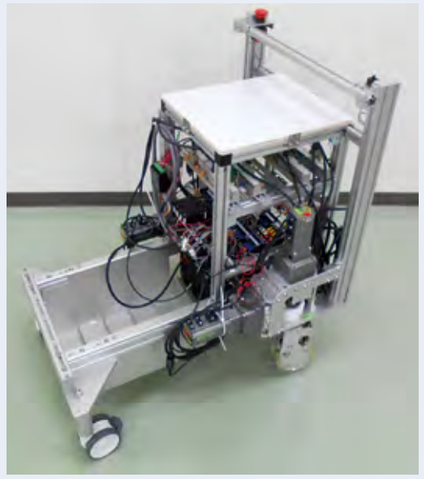

Fig. 5 Prototype of Active-caster truck

Table 1 Specifications

Total length	895 mm
Total width	590 mm
Total height	965 mm
Weight	82 kg
Control equipment	Windows PC
Motor	AC servo (with electromagnetic brake)
Motor control method	Speed
Motor control command	Analog voltage

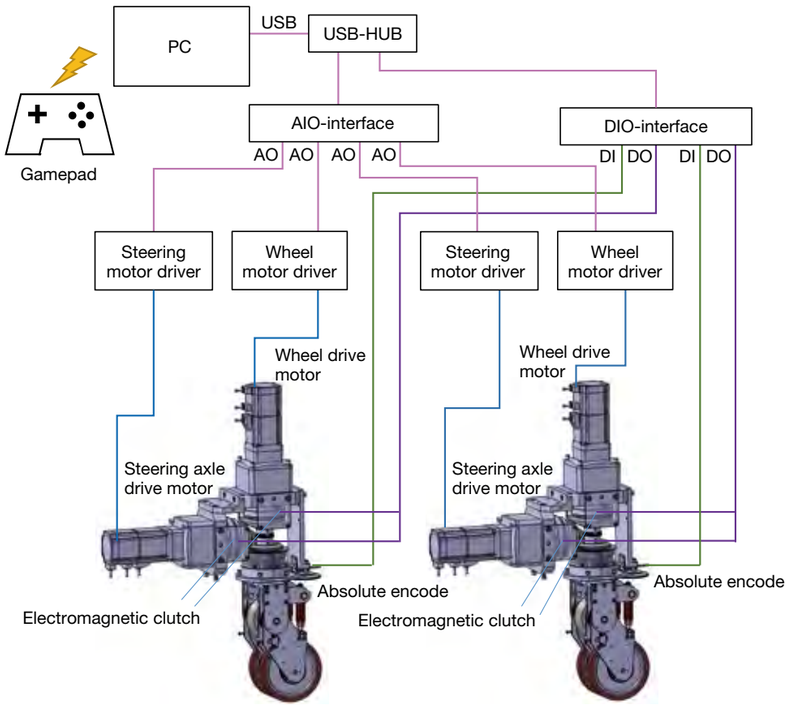

Fig.6 Controlling system

Table 2 Experimental parameters and results

	Initial angle (°)	Wheel configuration (shown from above)	Record waveform	Maximum displacement W_D (mm)
①	ϕ_L: 0 ϕ_R: 90			0.8
②	ϕ_L: 0 ϕ_R: 175			2.1
③	ϕ_L: 0 ϕ_R: 180			17.0

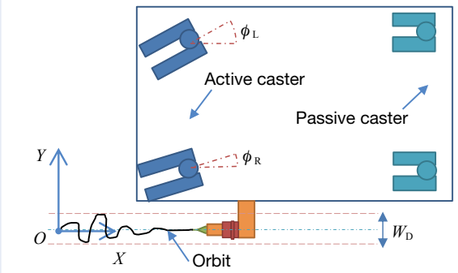

Fig. 7 Evaluation of rectilinearity

Table 3 Tensile experiment results

Unit: N

	Manual operation mode	Manually moving truck
Forward direction	14.6	13.5
Backward direction	12.9	15.6
Right direction	31.1	28.3

3.2. Evaluation of movement after changing modes

After movement in manual mode, the steering angles of two Active-casters are different and the angle becomes automatically fixed when the mode changes to rigid mode. In order to check if the truck is moving straight once the mode has changed, an experiment must be performed.

As shown in Figure 7, the steering angles of the right and left Active-casters ϕ_L and ϕ_R were set in the initial condition, then a forward movement command was given. After that, the truck traveled for about 500 mm in the X direction, the path was recorded, and the maximum deviation in the Y direction W_D was measured.

Table 2 shows the results of the three conditions as examples. In all the experimental conditions, the maximum deviation toward the Y direction W_D was 17 mm, a deviation ratio of 3.4% relative to a straight moving distance of 500 mm. As this experiment was undertaken without any truck position control by an internal or external sensor, the deviation could be decreased with the optional position control. Considering that a typical AGV's deviation is about ±50 mm, the Active-caster can be installed on the AGV.

3.3. Evaluation of smoothness under manual operation

As shown in Figure 1, the electromagnetic clutch of the Active-caster is placed next to the reducer. Because this Active-caster has timing belts, differential gears, and crown gears between the clutch and wheel, how smoothly the truck moves can be affected for the worse in line with the load of its mechanical structure. Therefore, a truck towing experiment has been carried out to evaluate the truck's smoothness in movement with an Active-caster used in manual mode. In addition, a similar experiment was carried out in order to compare the smoothness of movement of a truck with four passive casters. The manually-moving truck had the same weight, same caster specifications, and same caster position as the Active-caster truck. In the experiment, the trucks were towed at the same velocity from the forward, backward, and right directions, and the maximum towing force required was measured. Table 3 shows the results.

In the table, the required towing forces are almost the same both for the Active-caster truck and the manually-moving truck. The Active-caster truck in manual mode is thus just as smooth as the one that moves manually.

4. Conclusion

We examined the Active-caster and determined it is feasible to use it with omnidirectional mobile electric wheels, which can be driven both electrically and manually. In addition to omnidirectional movement, the wheels allow for passive manual operation and therefore trucks and AGVs can be more flexible. The system using an electrical clutch and described in this article ensures smooth movement in manual mode. To simplify the system's structure while also ensuring smooth movement, a prototype with a DD motor is planned, as shown in Figure 8.

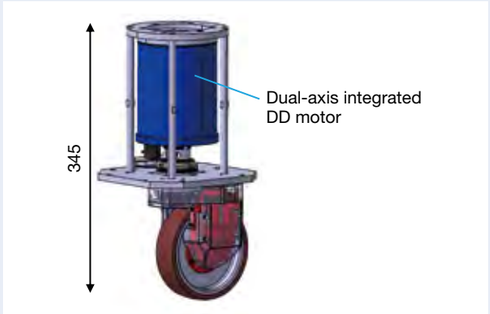

Fig. 8 Drive wheel of the DD motor type

Acknowledgments

Development of the omnidirectional mobile electric wheels was carried out in cooperation with Dr. Masayoshi Wada, associate professor of the Department of Mechanical Systems Engineering, Institute of Engineering, Tokyo University of Agriculture and Technology. We would like to express our appreciation to Dr. Wada for his fruitful cooperation in developing the body design and driving control of the Active-caster.

References

1) Masayoshi Wada, "Modeling and Control of Omnidirectional Mobile Robots with– Active Casters, Journal of the Robotics Society of Japan, Vol. 25, No. 7, pp. 1,100–1,107, 2007.
2) Masayoshi Wada, "Development of an Omnidirectional Cart with Dual-wheel Active-casters," The Robotics and Mechatronics Conference 2018, 2A1-H04, 2018.

Ko Fujioka

Yasunori Oishi

Analysis Prediction Technique of Flaking Expansion in Roller Bearings for Wind turbines.

Taketoshi Chifu and Kang Zhou
Core Technology R&D Center
Hiroki Mizokuchi
Industrial Machinery Technology Center, CMS Development Department

Abstract

Wind power has been rapidly spread as clean energy. In recent years however, profitability has been emphasized. Therefore, bearings for wind turbines are required to have a lifetime longer than a general flaking lifetime. In order to realize it, NSK is conducting research on prediction analysis technology of flaking expansion. This report describes the prediction analysis method well in agreement with the reproduction test.

1. Introduction

Wind power generation, like solar power generation, does not emit the greenhouse gases that cause global warming. Accordingly, wind power generation is being implemented globally as a symbol of environmentally friendly renewable energy, and it is expected to expand in the future (Figure 1). As more wind power generators (wind turbines) are implemented, effective O&M (Operation and Maintenance) is required, and CBM (Condition Based Maintenance), with the use of CMS (Condition Monitoring System) has become common. At present, it has been proven to be effective in preventing sudden accidents, etc. On top of this, the prediction of RUL (Remaining Useful Life) is considered to be one of the market needs.

The following three effects are expected from RUL prediction:

(1) cost reduction by the use of parts up to their usage limit
(2) downtime reduction by assuring the procurement period of the parts
(3) crane cost reduction by simultaneous exchange of large parts of multiple wind turbines

However, RUL prediction methodology based on the technological knowledge that does not rely on rules of thumb or RUL prediction methodology based on theory has not yet been put to practical use.

Accordingly, NSK is aiming for the provision of RUL that enables the safe use of bearings for wind turbines and is developing analysis technology for the prediction of the deterioration state. Such technology is considered indispensable for that goal, and the status of this development is described as follows.

Fig. 1 Wind turbines

2. Bearings for Speed-Up Gears for Wind Turbines

The drive train of a wind turbine is composed of the main axis, the speed-up gears, and the generator (Figure 2). Among them, the speed-up gears are the equipment for which the most bearings are used; it is common for speed-up gears to use more than 10 bearings. This is because a large speed multiplication factor requires many gears, whose axes require many bearings to support[1]. The cylindrical roller bearing, which can withstand a large radial load, is the most commonly used bearing. Therefore, this report explains the development status of analytical technology for predicting the deterioration state, with the cylindrical roller bearing as the analysis target.

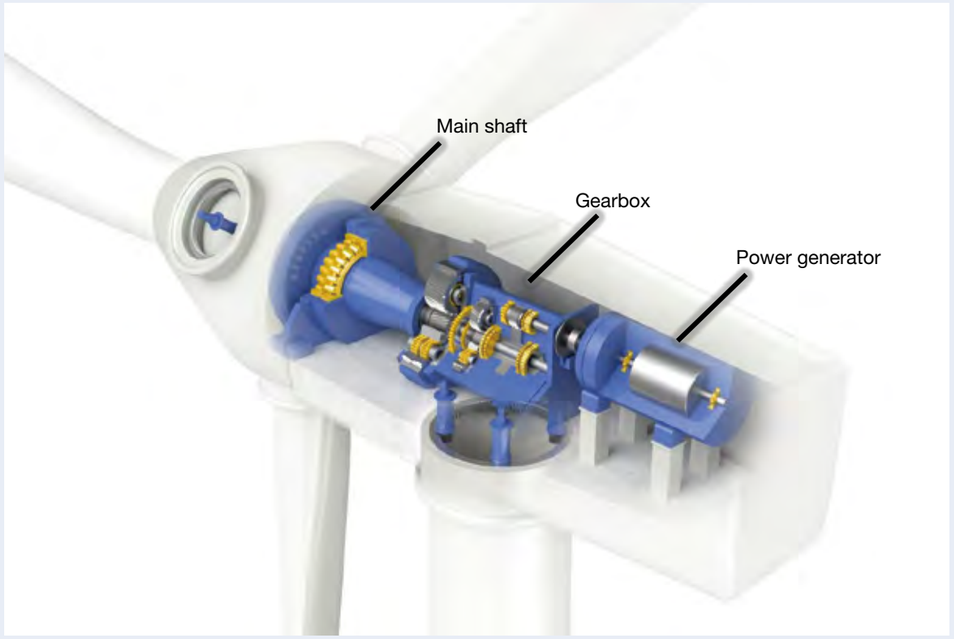

Fig. 2 Drive-train of wind turbines

3. Example of Bearing Damage

Figure 3 shows an example of damage of a cylindrical roller bearing for a wind turbine. Flaking, occurring on all inner ring raceway surfaces, expands to a large extent and leads to replacement. For many cases of bearings used in general machines, the operator takes notice of abnormal noise or large vibration and replaces the bearing at a flaking size much smaller than that shown in Figure 3.

A wind turbine is a large device. Preparation of the repair work and procurement of parts take a long time. Therefore, even after an abnormality is found, operation could be continued until the replacement parts are procured, by taking measures such as limiting the output. For that reason, a large flaking, as shown in Figure 3, can be found. If the replacement is delayed and the flaking progresses further, huge amounts of flaking debris could get stuck in the gears or the inner ring could crack. In the worst case, this could lead to complete failure, such as a shutdown of the machine.

To avoid that, NSK is developing analytical technology for the prediction of the deterioration status to enable reliable use of wind turbine bearings for a little longer after minor flaking.

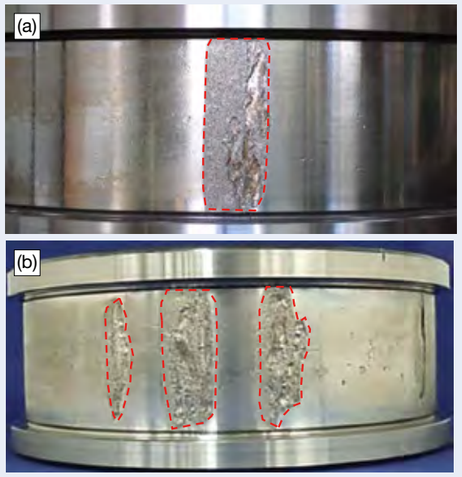

Fig. 3 Examples of flaking in roller bearings for wind turbines
(a) Large flaking on the bearing inner ring raceway
(b) Large flaking on the bearing inner ring raceway

4. Reproduction Test

To investigate the mechanism of flaking progress and to realize the prediction of the deteriorated state, reproduction tests were carried out. To shorten the test period, an artificial defect was made on the inner ring, as shown in Figure 4, before the experiment. Next, in a preliminary test, initial flaking was made with an in-house endurance test machine (Figure 5 (b)). An endurance test was started from this initial flaking condition. The flaking reached the status shown in Figure 5 (c) at a similar size and shape closely resembling the replaced part shown in Figure 3, and this indicates that the flaking was successfully reproduced. In the continued endurance test, the flaking expanded in proportion to time up to Figure 5 (d). However, shortly after that, the flaking expanded rapidly (Figure 5 (e)), terminating the experiment.

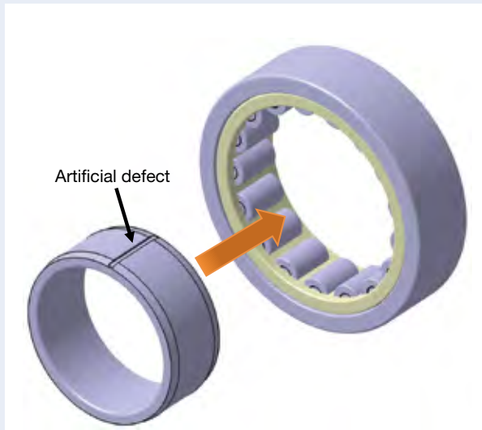

Fig. 4 Test bearing with an artificial defect

Fig. 5 Reproduction test results for flaking expansion

5. Development of an Analytical Method to Predict the Deteriorated State

5.1 Comprehensive flow of the deteriorated state prediction calculation

Figure 6 shows the calculation flow for deteriorated state prediction. After flaking, the roller weight load is calculated with the flaking shape as input. The cracking progress analysis by FEM predicts the flaking shape in the next stage. This calculation process is repeated until the unsafe use criteria are met. The time until the criteria are reached is displayed as the time up to the maintenance period.

The details of the calculation are described as follows.

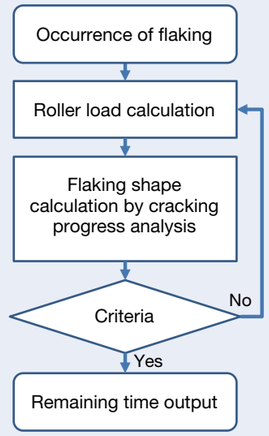

Fig. 6 Calculation flow of the roller bearing deteriorated state

5.2 Roller load calculation

In general, bearing life is assumed to be the time up to the occurrence of minor flaking. Therefore, the load on each roller is calculated from the axis load shown in Figure 7 (a).

However, this consideration is inadequate after the flaking occurrence because when a roller passes by the flaking, due to the clearance made by the flaking between the roller and inner and outer ring, the load is not applied to the roller. Figure 7 (b) shows the roller load calculation result after the flaking occurrence. It is confirmed that the roller passing the flaking does not receive the load. In addition, due to the lower number of rollers sharing the axis load, the maximum load increases compared to the condition without the flaking. Furthermore, the rotation changes the relative position of the flaking and the rollers. As a consequence, the roller load changed gradually as the flaking expanded.

To summarize, the load calculation of each roller with consideration of these phenomena is important for the prediction of deteriorated state.

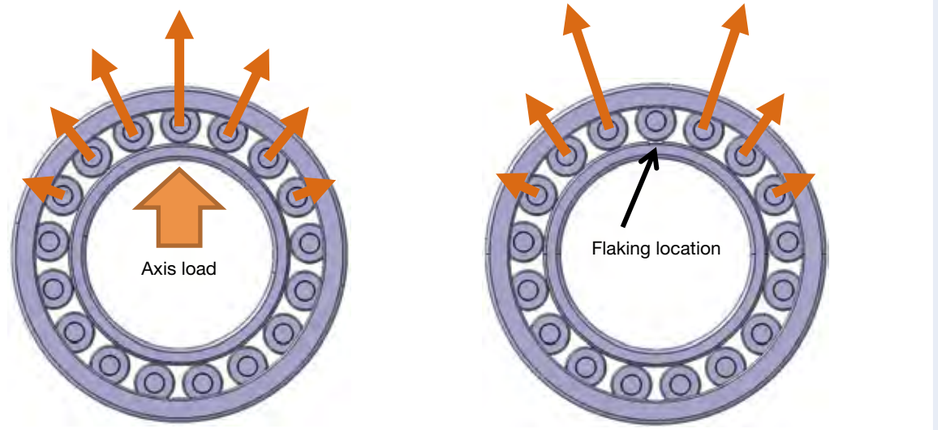

Fig. 7 Examples of a bearing roller load calculation

5.3 Cracking progress analysis by FEM

The initial flaking expansion from the minor flaking is caused by the cracking progress due to cyclic fatigue. Accordingly, we have decided to predict the slowly growing flaking size by cracking progress analysis based on fracture mechanics by FEM, as shown in Figure 8. The flaking depth was assumed to be constant. The shape model was as simple as possible. The gradually changing load calculated in detail in section 5.2 was used for the input load on the roller for the analysis.

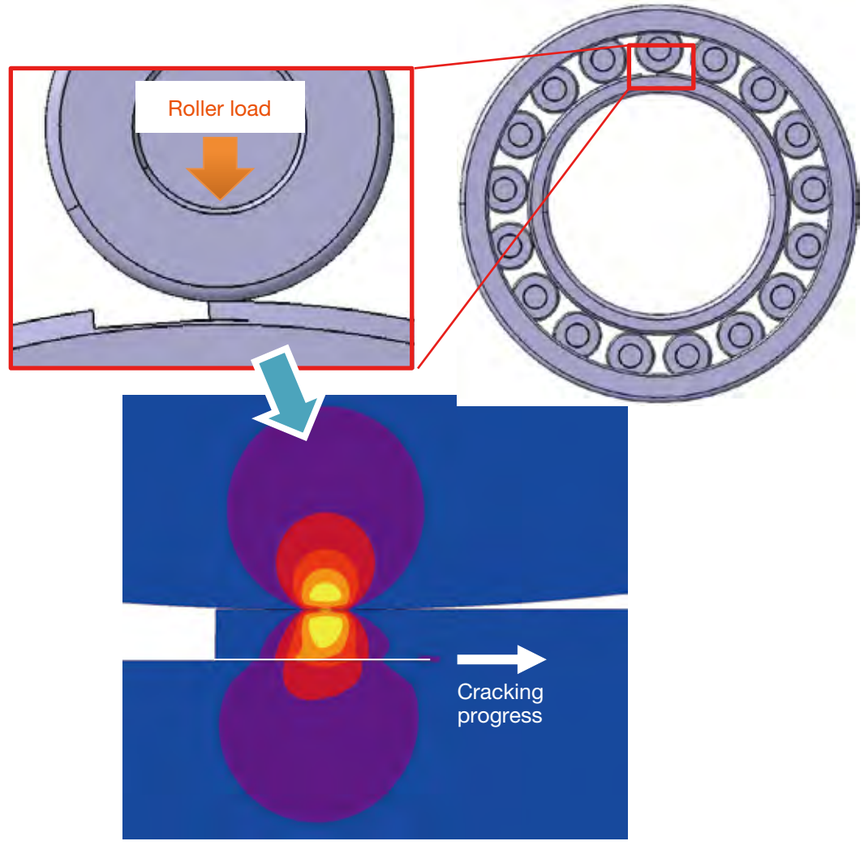

Fig. 8 Example of crack propagation during finite element analysis

6. Prediction Results

Figure 9 shows the test results and prediction results of flaking. The vertical axis shows the flaking size (flaking length in the circumferential direction). The horizontal axis shows the elapsed time. Although the predicted result by calculation is a little faster, the prediction was accurate. In addition, the rapid expansion of flaking observed in the reproduction test was reproduced by the calculation.

To investigate the mechanism of this rapid flaking expansion, the roller load at the rapid flaking expansion was confirmed (Figure 10). As shown in Figure 10, the flaking is expanded in such a way that two rollers cannot receive the load simultaneously. As a result, the number of rollers sharing the load decreased even more so than depicted in Figure 7 (b), and the load for each roller increased enormously. The large change in the load is considered to be the main cause of the rapid flaking expansion.

In addition, at present, the flaking size of two rollers, which is the start point of this rapid flaking expansion, is one of the criteria for safe operation. On the other hand, the amount of flaking debris, vibration, noise, etc., are also effective parameters to stop the wind turbines safely and preemptively. For that reason, we consider that criteria should be decided for multiple causes, as more experience will be accumulated in the future.

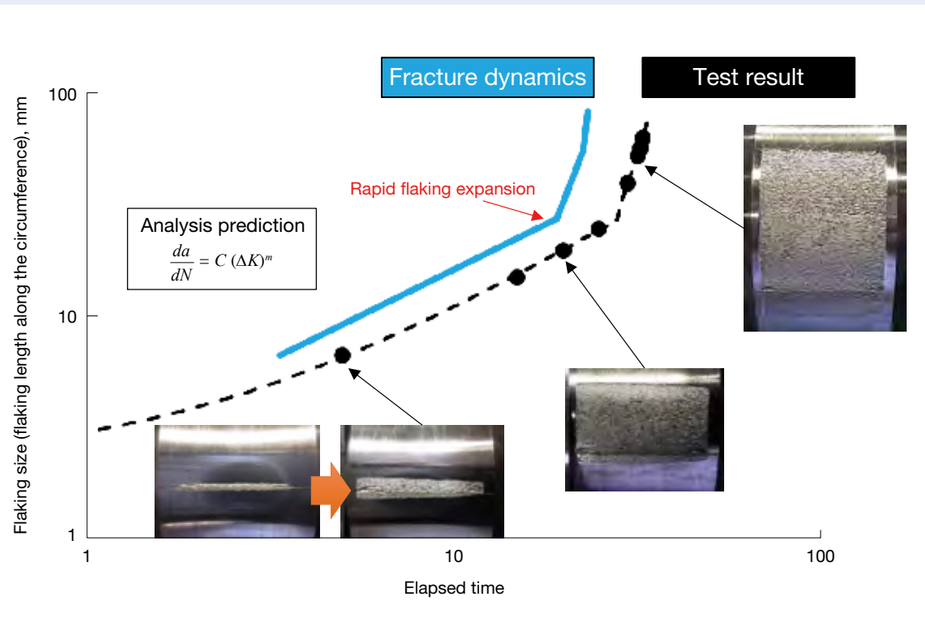

Fig. 9 Relationship between the experiment results and calculation results

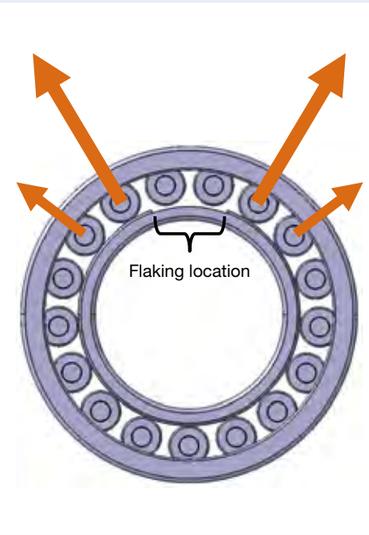

Fig. 10 Example of bearing roller load calculation when flaking is rapidly expanded

7. Postscript

NSK would like to make a contribution by providing long and safe bearing use periods toward the popularization and development of wind turbines. For that purpose, continued development and progress are essential as is the accumulation of experience on the prediction analysis of the deteriorated state we introduced in this article.

References

1) T. Suzuki and M. Fukunaga, "Technical Trends of Bearings and Enlarging the Size of Wind-Power Generators," NSK Technical Journal, No. 687, (2015) 23–27.

Taketoshi Chifu

Kang Zhou

Hiroki Mizokuchi

Simultaneous Measurement of Oil Film Thickness and Breakdown Ratio in EHD Contacts—Verification of Electrical Impedance Method

Masayuki Maeda and Taisuke Maruyama
Core technology R&D center, Lubricant research laboratory
Ken Nakano
Yokohama National University

Abstract

An electrical method using the complex impedance analysis has been developed for simultaneously quantifications of the thickness (h) and breakdown ratio (α) of oil films in elastohydrodynamic contacts. To verify the proposed measurement principle, oil film thickness measurements were conducted by using the electrical method together with the optical interferometry method in a ball-on-disc-type apparatus. As a result, it was confirmed that the measured h-values obtained by the electrical method agreed well with those obtained by the optical method, under test condition with changing the entrainment speed. Besides, it was also confirmed that the measured α-values obtained by the electrical method showed consistent correlations with the friction coefficient.

1. Introduction

Rolling bearings in various machines are mainly used for smoothly supporting rotating shafts for a long period of time. The oil film thickness in the elastohydrodynamic (EHD) contact of a bearing has a significant influence on the bearing torque and life. Accordingly, the measurement technology of oil film thickness in practical bearings is extremely effective to achieve the lower torque and longer life of bearings. Conventionally in the basic research field, optical interferometry has been used as accurate methods for measuring the oil film thickness in EHD contacts. However, to apply the optical method, it is necessary to use a transparent material that transmits light. Due to this limitation, it is impossible to monitor the lubricating conditions in practical bearings using the optical method.

In this viewpoint, electrical methods have an advantage because most practical bearings are made of steel, which is an electrically conductive material. Usually, the electrical resistance method and the electrical impedance method are mainly used as monitoring techniques for steel/steel contacts. The electrical resistance method can evaluate the breakdown of oil films by measuring the electrical resistance of EHD contacts. However, it is impossible to measure the oil film thickness quantitatively. In addition, the electrical impedance method can evaluate the oil film thickness by measuring the electrical capacitance in EHD contacts, but its measurement accuracy is insufficient.

This research has improved the conventional electrical impedance method[1)], which can measure the oil film thickness with high accuracy comparable to the optical interferometry. To verify the accuracy of the developed method, oil film thickness measurements were conducted by using the electrical method together with the optical interferometry method. Besides, this method can measure not only oil film thickness but also the breakdown ratio of oil film simultaneously. We have qualitatively evaluated the measured breakdown ratio of oil films by comparison with the friction coefficient occurring in EHD contacts.

2. Measurement Principle

Figure 1 shows a physical model of a ball specimen in contact with a disc specimen under the mixed lubrication. Here, r is ball specimen radius, a is Hertzian contact radius, S is Hertzian contact area, $f(x)$ is function describing the clearance between the ball and disc specimen, h_1 is oil film thickness in the area where the oil film is formed in EHD contacts, and α is breakdown ratio of oil films. Figure 2 shows an equivalent electrical circuit, which is based on the physical model shown in Fig. 1. Here, R_1 is resistance of the breakdown area in the EHD contact, C_1 is capacitor of the lubricated area in the EHD contact, and C_2 is capacitor of surround area where the clearance between the two surfaces are filled with the oil. In short, the oil film thickness and breakdown ratio were obtained by measuring the complex impedance Z, as shown in Figure 2.

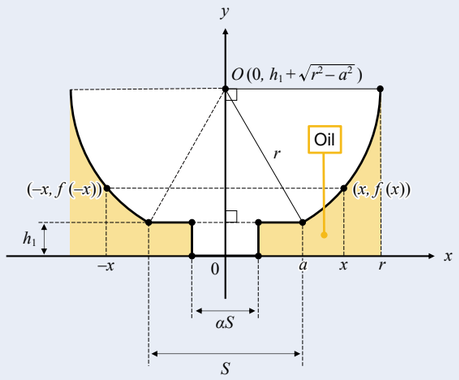

Fig. 1 Physical model

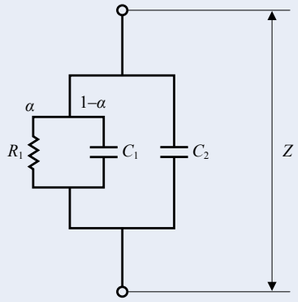

Fig. 2 Equivalent electrical circuit

3. Experimental Method

Figure 3 is a schematic diagram of the experimental apparatus used in this study. This apparatus uses a pure sliding contact between a steel ball (diameter: 25.4 mm and material: AISI 52100 steel) and a glass disc (diameter: 100 mm, thickness: 10 mm and BK7). The disc surface in contact with the ball is coated with a semi reflecting layer of 5-nm-thick chromium and a spacer layer of 1-μm-thick indium tin oxide (ITO). In this study, the ITO film is used, not only as a "transparent film" in optical measurements but also as a "conductive film" in electrical measurements. For electrical measurements, AC voltage is applied between the contacts, AC current passing through the contact is measured, and the complex impedance Z (i.e., $|Z|$ and θ) is obtained, which is automatically performed with a commercially available impedance meter. From the electrical measurements based on the measurement principle described in the previous section, we can quantify the oil film thickness h and the breakdown ratio a simultaneously. The test conditions are shown in Table 1. For friction measurements, a torque meter is installed to the vertical shaft, which measures the torque needed to rotate the disc at EHD contact conditions and determines the friction coefficient μ. As the oil, two types of polyalphaolefin (PAO) with different viscosities were used, as shown in Table 2.

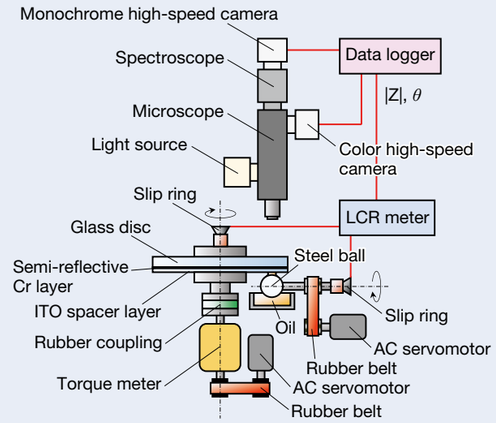

Fig. 3 Schematic diagram of an EHL test rig

Table 1 Test conditions

Temperature, °C	25
Entrainment speed, m/s	0.005 to 0.5
Slide-to-roll ratio, %	200
Maximum contact pressure, GPa	0.34
Hertzian contact radius, mm	0.12
RMS amplitude, V	1.0
AC frequency, MHz	1.0

Table 2 Oil properties

	PAO_A	PAO_B
Kinematic viscosity, mm²/s at 40°C	30	396
Pressure-viscosity coefficient, GPa⁻¹ at 25°C	12.5	16.3
Relative permittivity	2.1	2.1

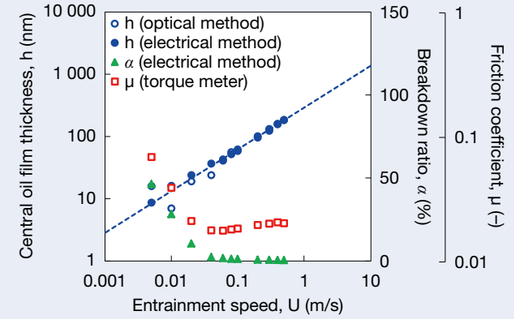

Fig. 4 Influence of entrainment speed (PAO_A)

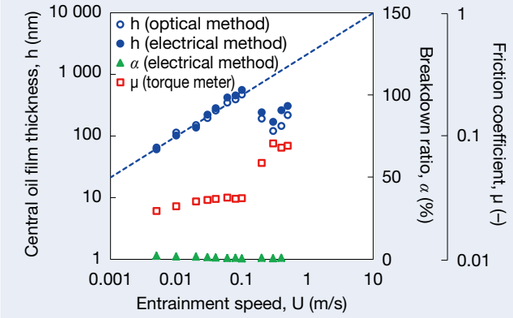

Fig. 5 Influence of entrainment speed (PAO_B)

4. Results and Discussion

Figure 4 shows the measurement results of oil film thickness, breakdown ratio, and friction coefficient when the entrainment speed U was changed for the lower-viscosity PAO, as shown in Table 2. The dashed line in the graph shows the theoretical values according to the Hamrock-Dowson equation. We have confirmed that the measured h-values obtained by the electrical method agree well with those obtained by the optical method. Therefore, we can naturally conclude that the electrical method measures the oil film thickness in EHD contacts with a high accuracy comparable to that of the optical method. Besides, Fig. 5 shows the experimental results when U was varied for the higher-viscosity PAO. When $U \geqq 0.2$ m/s, the measured h-values are located below the dashed line with considerable deviations. In addition, we find that the measured μ-values are higher than those extrapolated from the lower-U conditions (i.e., $U \leqq 0.1$ m/s). From these results, we suggest that the lubricant is starved at the higher-U conditions (i.e., $U \geqq 0.2$ m/s). However, even when under the starved lubrication, the measurement error does not seem to be fatal.

5. Summary

Simultaneous measurements of optical interferometry and the electrical impedance method with the use of the ball-on-disc-type apparatus has demonstrated that the developed method can measure the oil film thickness with high accuracy comparable to the optical interferometry. In addition, this method has confirmed that the breakdown ratio of oil films can also be measured simultaneously, and be qualitatively evaluated by comparison with the friction coefficient.

References

1) K. Nakano, Y. Akiyama, "Simultaneous measurement of film thickness and coverage of loaded boundary films with complex impedance analysis," Tribology Letters, Vol. 22, No. 1 (2006) 127.

Masayuki Maeda

Taisuke Maruyama

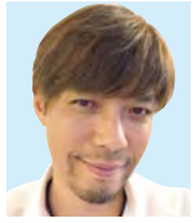

Ken Nakano

Low-Torque Ball Bearings for High-Efficiency Motors

With a growing awareness of the need for global environment protection, the world is moving toward reducing carbon dioxide and power consumption. It is said that electric power consumption of motors constitutes over 40% of the electric power consumption of the entire world. As reduction of electric power consumption by motors will have a big impact on energy saving, relevant activities are attracting a lot of attention. Consequently, many countries have established new regulations on the efficiency of energy-saving motors. Many motor manufacturers are taking various measures to reduce the loss in order to improve the efficiency by several percent. Although the loss by bearings (motor mechanical loss), converted to the efficiency, is as low as less than 1%, its improvement is expected as an element for a motor efficiency improvement of several percent.

Optimizing the bearing specifications, NSK has developed a bearing that realizes loss reduction associated with motor efficiency improvement (Photo 1).

In response to the expansion of the implementation of high efficiency motors for energy saving, the product has optimal performance for general industrial machine motors used in pumps, compressors, etc.

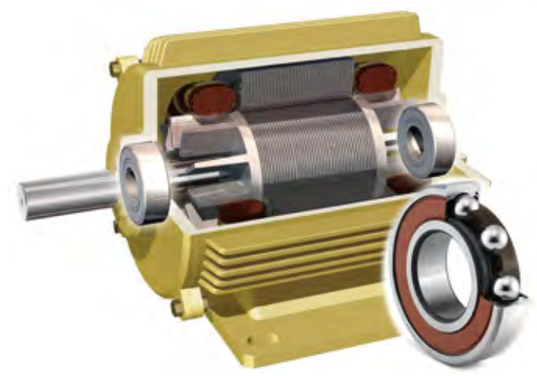

Photo 1 Low-Torque Ball Bearings for High-Efficiency Motors

1. Composition, Structure, and Specifications

Optimization of the kind and amount of grease has reduced shearing resistance and stirring resistance of the bearing grease (lubricant). In addition, low torque and long bearing life have been realized. Also, adopting a plastic cage would allow for further torque reduction and longer life.

2. Advantages

(1) Reduction of Motor Mechanical Loss and Endurance Improvement

Compared with bearings having conventional specifications, the motor mechanical loss has been reduced by a maximum of 60% (maximum reduction of 80% with plastic cages), and at the same time, the bearing life has been extended by a factor of 2.7 (Figures 1 and 2).

(2) Mechanical Loss Dependent on Motor Size

The optimized bearing specifications have a significant impact, especially on large motors (Figure 3).

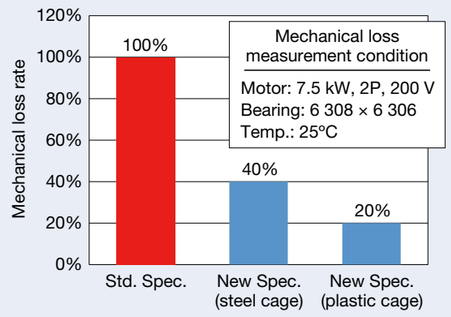

Fig. 1 Motor Mechanical Loss Rate

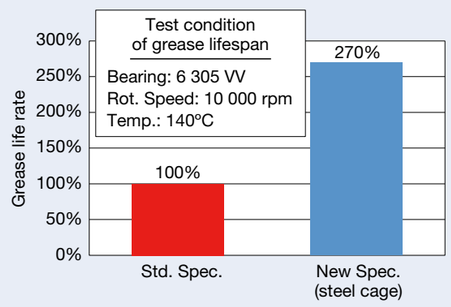

Fig. 2 Grease life

3. Fields for Application

This product is suitable for high efficiency motors for relatively light loads and general industrial motors.

4. Summary

Table 1 shows a lineup of bearings corresponding to a variety of motor sizes (5.5 kW–132 kW). These bearings are contributing to lowering the amount of energy consumed by motors.

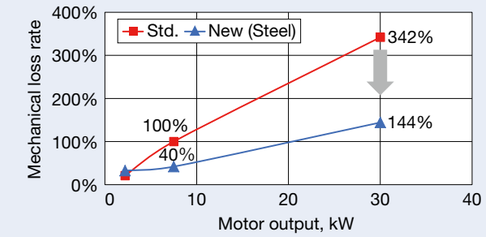

Fig. 3 Mechanical loss rate and motor size

Table 1 Series deployment of low-torque ball bearings

Note: These bearings correspond to motor sizes of 5.5 kW–132 kW

	Main size (mm)				Main size (mm)		
	Inner diameter	Outer diameter	Width		Inner diameter	Outer diameter	Width
6 200	10	26	8	6 300	10	35	11
6 201	12	32	10	6 301	12	37	12
6 202	15	35	11	6 302	15	42	13
6 203	17	40	12	6 303	17	47	14
6 204	20	47	14	6 304	20	52	15
6 205	25	52	15	6 305	25	62	17
6 206	30	62	16	6 306	30	72	19
6 207	35	72	17	6 307	35	80	21
6 208	40	80	18	6 308	40	90	23
6 209	45	85	19	6 309	45	100	25
6 210	50	90	20	6 310	50	110	27
6 211	55	100	21	6 311	55	120	29
6 212	60	110	22	6 312	60	130	31
6 213	65	120	23	6 313	65	140	33
6 214	70	125	24	6 314	70	150	35
6 215	75	130	25	6 315	75	160	37
6 216	80	140	26	6 316	80	170	39

Optimized Long-Life Cylindrical Roller Bearings for Continuous Casting Machines

Recently, higher productivity in metalwork has been achieved by operating stable facilities and reducing costs by extending maintenance intervals. Continuous casting machines continuously produce semi-finished pieces from melted metal. The types of pieces produced include slab (for plates), bloom (for shapes), and billet (for wire). Figure 1 shows an example structure of a slab continuous casting machine. One machine is composed of 10–15 roll segments, each having multiple rollers.

This type of continuous casting machine often has a segmented roll structure to improve product precision. Guide roll bearings used are generally self-aligning roller bearings capable of absorbing roll deflection on both the fixed and free sides. In addition, they are non-separable and easy to handle.

Toroidal roller bearings are often used, especially overseas, because they feature high load capacity and are capable of absorbing elongation by relative displacement of the inner and outer rings. These bearings are used in heavy load conditions over 30% of the basic dynamic load rating at extremely slow speeds (one or two cycles per minute) while exposed to coolant, vapor, scale, and high temperatures. These harsh conditions deteriorate lubrication and cause premature damage such as wear on the raceway surface and flaking. Consequently, there is a need for highly reliable, long-life bearings.

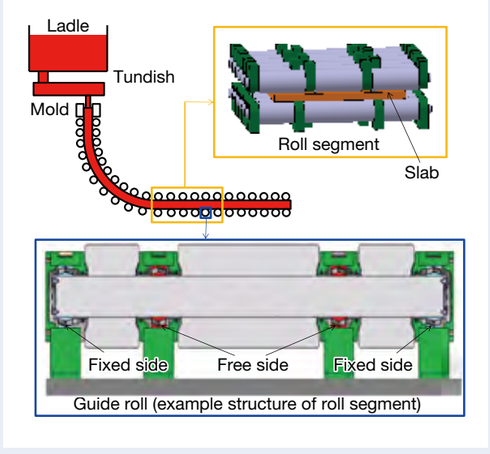

Fig. 1 Continuous casting machines and the guide roll structure

In response, NSK has developed optimized long-life, cylindrical roller bearings for the free side of continuous casting machines (Photo 1).

Photo 1 Optimized long-life cylindrical roller bearings for continuous casting machines (free side)

1. Structure and Specifications

These full complement cylindrical roller bearings are composed of an outer ring, inner ring, rolling elements (rollers), and a snap ring.

Figure 2 shows the structure of the developed bearing, while Table 2 lists designations and specifications. Cylindrical rollers suppress internal sliding and optimal roller and raceway crowning creates a shape that greatly improves capacity for inclination.

Table 1 Specifications

Boundary Dimensions (mm)			Bearing Designation	Basic Load Ratings (kN)	
Inner Diameter	Outer Diameter	Width		Dynamic Load Rating C_r	Static Load Rating C_{or}
120	180	60	120NUB40V	450	740
130	200	69	130NUB40V	570	950
140	210	69	140NUB40V	560	960
150	225	75	150NUB40V	665	1 160
160	240	80	160NUB40V	765	1 360

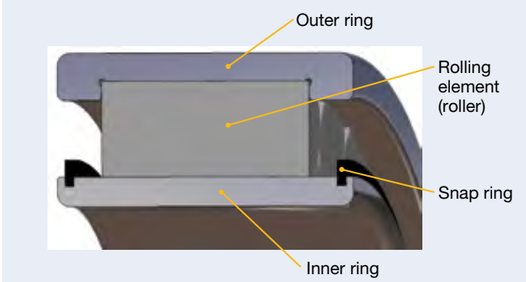

Fig. 2 Bearing structure

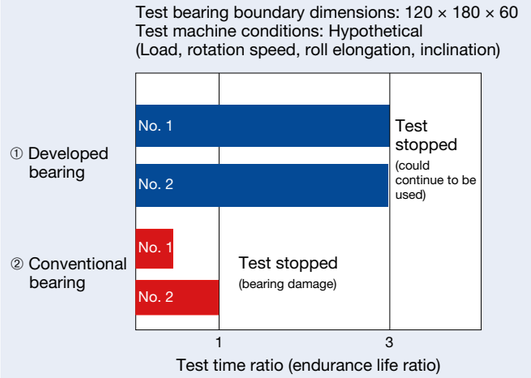

Fig. 3 Durability testing results

2. Advantages

• Long life and high load capacity

A refined full complement design maximizes load capacity. Endurance tests confirmed life triple that of conventional bearings (Fig. 3).

• Self-aligning

Absorbs deflection generated on the rolls of continuous casting machines. Uniformly distributes contact surface pressure between the roller and raceway in response to inclination (Fig. 4).

• Absorbs roll elongation

Relative displacement of the inner and outer rings easily handles roll elongation caused by heat.

• Ease of handling

Since the bearings are non-separable, there is no need for special tools, and assembly is easy (Fig. 5).

3. Applications

Suitable for the guide roll (free side) of a continuous casting machine for slab, bloom, or billet.

4. Summary

We confirmed the positive impact of these optimized long-life cylindrical roller bearings in actual slab continuous casting machines. We will continue our efforts to improve productivity through the stable operation of continuous casting machines.

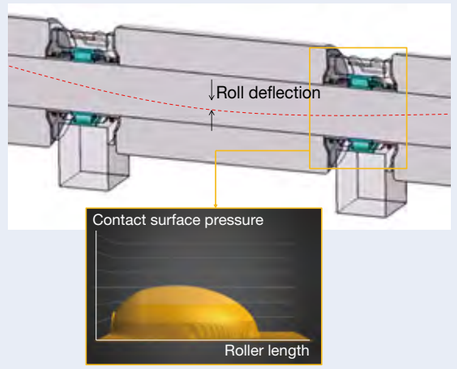

Contact surface pressure distribution between the roller and raceway

Fig. 4 Roll deflection and contact surface pressure between the roller and raceway

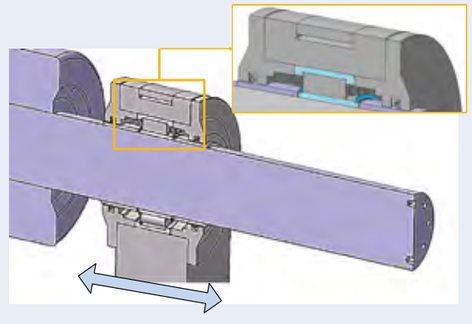

Fig. 5 Handling

Large (TL) Spherical Roller Bearings Resistant to Inner Ring Fracture for Paper Machines

Recently, while growth in printing paper and newsprint remains sluggish, paper makers are expecting increased demand for paperboard and sanitary paper. To prepare, manufacturers have been improving productivity by enhancing production facilities (paper machines) and operating them reliably at high speeds. As a result, the number of Yankee dryer rolls (Yankee rolls) are increasing in paper machines.

Figure 1 shows an example structure of a paper machine Yankee roll with a bearing attached. In the structure, a self-aligning roller bearing is set on the bearing bore with a sleeve between the bearing and bore. Remaining clearance in the bearing can be adjusted by pushing and creating tensile stress (hoop stress) on the inner ring. However, since a high-temperature medium (vapor) goes through the hollow axis of the dryer roll, the axis expands during operation and hoop stress increases, possibly causing the inner ring to fracture (Photo 1). Furthermore, creep damage can occur between the inner ring and axis since bearings are used for a long time in high-temperature conditions. Because inner ring fracture could cause a sudden stop of production, there is a need for bearings with measures to prevent such damage.

NSK developed TL (Tough & Long life) bearings in 1994 to respond to this problem. TL bearings are confirmed to have enhanced inner ring fracture strength and improved dimensional stability due to a uniquely developed steel for self-aligning roller bearings and a special carburizing process. So far, the corresponding size of TL bearings has been limited to the outer diameter of the bearing, or less than ϕ650 mm (231 Series). But now, to accommodate bearings for Yankee rolls, we have developed inner ring fracture-resistant large TL self-aligning roller bearings (Photo 2) with a maximum diameter of ϕ1 360 mm. For details, please see the next page.

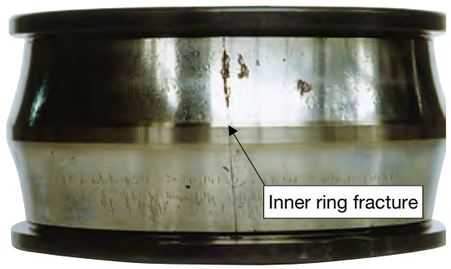

Photo 1 Inner ring fracture (spherical roller bearings)

Photo 2 Large anti inner ring fracture spherical roller bearings for paper machines

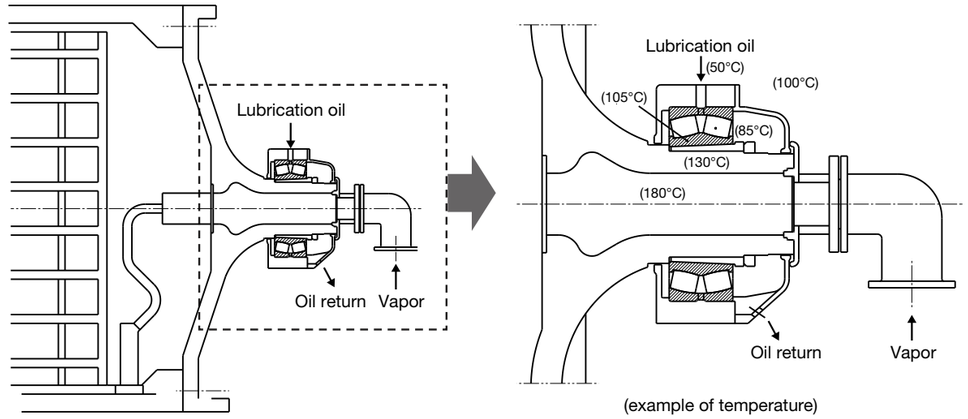

Fig. 1 Structure of Yankee dryer rolls (example)

1. Specifications

The new product features enhanced inner ring fracture strength and improved dimensional stability thanks to a uniquely developed steel for large self-aligning roller bearings and a special carburizing process.

2. Advantages

- Inner ring fracture strength
  Improvement of the material strength of the inner ring prevents inner ring fracture.

- Creep strength
  Heat treatment for size stability at high temperatures prevents inner ring creep.

3. Applications

The main applications in paper machines and representative part number ranges for the new bearings are listed in Table 1. These products are large self-aligning roller bearings with tapered bores on the inner ring bearing bore. They are particularly suitable for supporting dryer rolls and calendar rolls with hollow axes through which a high-temperature medium (vapor, oil) passes.

4. Summary

We believe our new product will help improve productivity by making the operation of paper machines more stable. We will continue to develop new products that meet user needs while also contributing to progress in the paper manufacturing industry.

Table 1 Main applications and bearing part number ranges

Bearing Part Number Range	Bearing Outer Diameter	Main Application(s)
TL239/600–TL239/1000	ϕ800–ϕ1 320	Press roll
TL230/560–TL230/950	ϕ820–ϕ1 360	Press roll, Yankee dryer roll
TL23180–TL231/710	ϕ650–ϕ1 150	Yankee dryer roll
TL23280–TL232/600	ϕ720–ϕ1 090	Calendar roll, press roll
TL240/530–TL240/750	ϕ780–ϕ1 090	Calendar roll
TL24164–TL241/710	ϕ540–ϕ1 150	Calendar roll

Vibration Control Actuator for Train Cars

Full active suspension systems, systems that actively control horizontal body vibration in railroad vehicles using pneumatic, hydraulic, and electric actuators, have recently been installed on high speed trains like the Shinkansen and limited express trains running on regular tracks, as well as tour-type luxurious sleeper trains.

NSK has developed the Vibration Control Actuator, an electric vibration prevention actuator with ball screws, for full active suspension of railroad vehicles, and it is introduced here.

1. Composition and Structure

NSK's Vibration Control Actuator is composed of: an electric motor, a reducing mechanism, a ball screw, and a slide rod (Photo 1). The upper-level control equipment (not shown) calculates and sends the drive commands to the actuator's motor driver.

Figure 1 and Photo 2 show the installation location of the actuator's main body. It is installed between the bogie and the vehicle body, and it drives laterally with respect to the moving direction.

Photo 1 NSK Vibration Control Actuator (left: actuator, right: driver)

Photo 2 Location of NSK's Vibration Control Actuator (photo: Kawasaki Heavy Industries Ltd.)

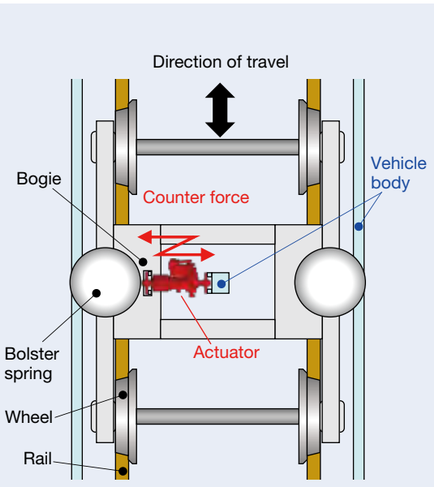

Fig. 1 Location of NSK's Vibration Control Actuator

2. Advantages

This actuator addresses technological issues with making products lighter, thinner, shorter, and smaller with the effect of making it more compact, lightweight, efficient, and responsive. On the other hand, technological and contradicting issues that favor heavier, larger products, such as endurance and anti-vibration strength, needed to be resolved. As a mechanism for converting the rotational, movement of electric motors to linear movement of the output rods, precision ball screws, although they are installed on railroad vehicles that require high drive power, have been applied due to their high efficiency, low inertia, and high reverse mobility.

Highly efficient in normal operation when converting rotational movement to linear movement, and capable of reducing the torque requirement on the electric motor, ball screws can make electric motors more compact while lowering inertia. Therefore, with the advantage of excellent response to the commands from the upper level control equipment, they can constitute a compact and energy-saving actuator. In addition, ball screws are excellent in reverse operation when converting from linear to rotational movement. This is very useful for efficiently absorbing the vibrations between the bogie and the vehicle body.

A dust-proof and water-proof design for environmental resistance includes measures such as the use of packing and a seal to prevent the ingress of water and dust. For vibration resistance, structural analysis of the design was performed to ensure it satisfied the requirements for railroad vehicles. Tests equivalent to a real vehicle also confirmed that the requirements had been satisfied.

The driver design incorporates the design philosophy of the Mega Torque Motor™, the culmination of mechatronics research and development, one of NSK's core technologies.

3. Fields for Application

This product is installed on the Chuo Line new model limited express vehicle E353 series of the East Japan Railway Company (JR East) and started operating on December 23, 2017 as a new vehicle called Super Azusa (Photo 3). In addition, it is also installed on the Train Suite Shikishima, a JR East cruise train that started operating on May 1, 2017 (Photo 4).

4. Summary

Taking full advantage of the ball screw's high efficiency conversion from rotational to linear movement, the Vibration Control Actuator is an electric actuator that suppresses the lateral vibration of railroad vehicles with high response performance.

NSK will continue to contribute to the improvement of safety, comfortability, and environmental performance for the railroad industry.

Photo 3 JR East Chuo Line Super Azusa service E353 series high speed train (photo: JR East)

Photo 4 JR East's Train Suite Shiki-shima, a luxury sleeper train (photo: JR East)

Worldwide Sales Offices

P: Phone F: Fax ☆: Head Office

NSK LTD.-HEADQUARTERS, TOKYO, JAPAN

Nissei Bldg., 1-6-3 Ohsaki, Shinagawa-ku, Tokyo 141-8560, Japan

INDUSTRIAL MACHINERY BUSINESS DIVISION-HEADQUARTERS
P: +81-3-3779-7227 F: +81-3-3779-7644

AUTOMOTIVE BUSINESS DIVISION-HEADQUARTERS
P: +81-3-3779-7189 F: +81-3-3779-7917

●Africa

South Africa:

NSK SOUTH AFRICA (PTY) LTD.

SANDTON 25 Galaxy Avenue, Linbro Business Park, Sandton 2146, South Africa
P: +27-11-458-3600 F: +27-11-458-3608

●Asia and Oceania

Australia:

NSK AUSTRALIA PTY. LTD.

MELBOURNE ☆ 100 Logis Boulevard, Dandenong South, Victoria, 3175, Australia
P: +61-3-9765-4400 F: +61-3-9765-4466

SYDNEY Suite A315, 20 Lexington Drive, Bella Vista, New South Wales, 2153, Australia
P: +61-2-9839-2300 F: +61-2-8824-5794

BRISBANE 1/69 Selhurst Street, Coopers Plains, Queensland 4108, Australia
P: +61-7-3347-2600 F: +61-7-3345-5376

PERTH Unit 1, 71 Tacoma Circuit, Canning Vale, Western Australia 6155, Australia
P: +61-8-9256-5000 F: +61-8-9256-1044

New Zealand:

NSK NEW ZEALAND LTD.

AUCKLAND 3 Te Apunga Place, Mt. Wellington, Auckland 1060, New Zealand
P: +64-9-276-4992 F: +64-9-276-4082

China:

NSK (SHANGHAI) TRADING CO., LTD.

JIANGSU No.8 NSK Rd., Huaqiao Economic Development Zone, Kunshan, Jiangsu, China (215332)
P: +86-512-5796-3000 F: +86-512-5796-3300

NSK (CHINA) INVESTMENT CO., LTD.

JIANGSU ☆ No.8 NSK Rd., Huaqiao Economic Development Zone, Kunshan, Jiangsu, China (215332)
P: +86-512-5796-3000 F: +86-512-5796-3300

BEIJING Room 1906, Beijing Fortune Bldg., No.5 Dong San Huan Bei Lu, Chao Yang District, Beijing, China (100004)
P: +86-10-6590-8161 F: +86-10-6590-8166

TIAN JIN Unit 4604, 46/F., Metropolitan Tower, 183 Nanjing Road, Heping District, Tianjin, China (300051)
P: +86-22-8319-5030 F: +86-22-8319-5033

CHANGCHUN Room 902-03, Changchun Hongwell International Plaza, No.3299 Renmin Street, Changchun, Jilin, China (130061)
P: +86-431-8898-8682 F: +86-431-8898-8670

SHENYANG Room 1101, China Resources Building, No. 286 Qingnian Street, Heping District, Shenyang Liaoning, China (110004)
P: +86-24-2334-2868 F: +86-24-2334-2058

DALIAN Room 1805 Xiwang Tower, No.136 Zhongshan Road, Zhongshan District, Dalian, Liaoning, China (116001)
P: +86-411-8800-8168 F: +86-411-8800-8160

NANJING Room A1 22F, Golden Eagle International Plaza, No.89 Hanzhong Road, Nanjing, Jiangsu, China (210029)
P: +86-25-8472-6671 F: +86-25-8472-6687

FUZHOU Room 1801-1811, B1#1A Class Office Building, Wanda Plaza, No.8 Aojiang Road, Fuzhou, China (350009)
P: +86-591-8380-1030 F: +86-591-8380-1225

WUHAN Room 1512, No.198Yuncai Road, Office Building, Oceanwide City Square, JiangHan, District, WuHan, China (400039)
P: +86-27-8556-9630 F: +86-27-8556-9615

QINGDAO Room 802, Farglory International Plaza, No.26 Xianggang Zhong Road, Shinan District, Qingdao, Shandong, China (266071)
P: +86-532-5568-3877 F: +86-532-5568-3876

GUANGZHOU Room 1011-16, Yuexiu Financial Tower, No.28 Zhujiang Road East, Zhujiang New Town, Guangzhou, Guangdong, China (510627)
P: +86-20-3817-7800 F: +86-20-3786-4501

CHANGSHA Room 1048, 10/F, Zhongtian Plaza, No.766 WuyiRoad, Changsha, Hunan, China (410005)
P: +86-731-8571-3100 F: +86-731-8571-3255

LUOYANG Room 1108, Fangda Hotel, 6 XiYuan Road, LuoYang HeNan, China (471003)
P: +86-379-6069-6188 F: +86-379-6069-6180

XI'AN Room 1007, B Changan Metropolls Center88 Nanguanzheng Steet, Xi'an, Shanxi, China (710068)
P: +86-29-8765-1896 F: +86-29-8765-1895

CHONGQING Room 612, Commercial Apartment, Sofitel Hotel, No.288, Keyuan Rd.4, Jiulongpo District, Chongqing, China (400039)
P: +86-23-6806-5310 F: +86-23-6806-5292

CHENGDU Room1117, Lippo Tower, No.62 North Kehua Road, Chengdu, Sichuan, China (610041)
P: +86-28-8528-3680 F: +86-28-8528-3690

NSK CHINA SALES CO., LTD.

JIANGSU No.8 NSK Rd., Huaqiao Economic Development Zone, Kunshan, Jiangsu, China (215332)
P: +86-512-5796-3000 F: +86-512-5796-3300

NSK HONG KONG LTD.

HONG KONG ☆ Suite 705, 7th Floor, South Tower, World Finance Centre, Harbour City, T.S.T, Kowloon, Hong Kong, China
P: +852-2739-9933 F: +852-2739-9323

SHENZHEN Room 624-626, 6/F, Kerry Center, Renminnan Road, Shenzhen, Guangdong, China
P: +86-755-25904886 F: +86-755-25904883

Taiwan:

TAIWAN NSK PRECISION CO., LTD.

TAIPEI ☆ 10F-A6, No.168, Sec.3, Nanjing East Rd., Zhongshan Dist., Taipei City 104, Taiwan
P: +886-2-2772-3355 F: +886-2-2772-3300

TAICHUNG 3F. -2, No. 540, Sec. 3, Taiwan Blvd., Xitun Dist., Taichung City 407, Taiwan
P: +886-4-2708-3393 F: +886-4-2708-3395

TAINAN Rm. A1, 9F., No.189, Sec. 1, Yongfu Rd., West Central Dist., Tainan City 700, Taiwan
P: +886-6-215-6058 F: +886-6-215-5518

India:

NSK BEARINGS INDIA PRIVATE LTD.

CHENNAI ☆ TVH Beliciaa Towers, 2nd Floor, Block I, No.71/1, MRC Nagar Main Road, MRC Nagar, Chennai, India - 600 028
P: +91-44-2847-9600 F: +91-44-2847-9601

DELHI Unit No-202, 2nd Floor, Block-A, Iris Tech Park, Sector-48, Sohna Road, Gurgaon-122018, Haryana, India
P: +91-124-4838000 F: +91-124-4104-532

MUMBAI 321, 'A' Wing, Ahura Centre, 82, Mahakali Caves Road, Andheri (East), Mumbai -400 093, India
P: +91-22-2838-7787 F: +91-22-2838-5191

Indonesia:

PT. NSK INDONESIA

JAKARTA Summitmas II, 6th Floor, Jl. Jend Sudirman Kav. 61-62, Jakarta 12190, Indonesia
P: +62-21-252-3458 F: +62-21-252-3223

Korea:

NSK KOREA CO., LTD.

SEOUL Posco Center (West Wing) 9F, Western-wing, 440, Teheran-ro, Gangnam-gu, Seoul, 135-777, Korea
P: +82-2-3287-0300 F: +82-2-3287-0345

Malaysia:

NSK BEARINGS (MALAYSIA) SDN. BHD.

SHAH ALAM ☆ No. 2, Jalan Pemaju, U1/15, Seksyen U1, Hicom Glenmarie Industrial Park, 40150 Shah Alam, Selangor, Malaysia
P: +60-3-7803-8859 F: +60-3-7806-5982

PRAI No.24, Jalan kikik, Taman Inderawasih, 13600 Prai, Penang, Malaysia
P: +60-4-3902275 F: +60-4-3991830

JOHOR BAHRU 88 Jalan Ros Merah 2/17, Taman Johor Jaya, 81100 Johor Bahru, Johor, Malaysia
P: +60-7-3546290 F: +60-7-3546291

IPOH No.10&10A, Jalan Industri Paloh, Kawasan Perindustrian Ringan Paloh, 30200 Ipoh, Perak Darul Ridzuan, Malaysia.
P: +60-5-2555000 F: +60-5-2553373

Philippines:

NSK REPRESENTATIVE OFFICE

MANILA 8th Floor The Salcedo Towers 169 H.V. dela Costa St., Salcedo Village Makati City, Philippines 1227
P: +63-2-893-9543 F: +63-2-893-9173

Singapore:

NSK INTERNATIONAL (SINGAPORE) PTE LTD.

SINGAPORE 238A, Thomson Road, #24-01/05, Novena Square Tower A, Singapore 307684
P: +65-6496-8000 F: +65-6250-5845

NSK SINGAPORE (PRIVATE) LTD.

SINGAPORE 238A, Thomson Road, #24-01/05, Novena Square Tower A, Singapore 307684
P: +65-6496-8000 F: +65-6250-5845

Thailand:

NSK BEARINGS (THAILAND) CO.,LTD.

BANGKOK 26 Soi Onnuch 55/1 Pravet Subdistrict, Pravet District, Bangkok 10250, Thailand
P: +66-2320-2555 F: +66-2320-2826

Vietnam:

NSK VIETNAM CO., LTD.

HANOI Techno Center, Room 204-205, Thang Long Industrial Park, Dong Anh District, Hanoi, Vietnam
P: +84-24-3955-0159 F: +84-24-3955-0158

NSK REPRESENTATIVE OFFICE

HO CHI MINH CITY Suite 307, Metropolitan Building, 235 Dong Khoi Street, District 1,HCMC, Vietnam
P: +84-28-3822-7907 F: +84-28-3822-7910

Worldwide Sales Offices

P: Phone F: Fax ☆: Head Office

●Europe

United Kingdom:

NSK EUROPE LTD. (EUROPEAN HEADQUARTERS)

MAIDENHEAD Belmont Place, Belmont Road, Maidenhead, Berkshire SL6 6TB, U.K.
P: +44-1628-509-800 F: +44-1628-509-808

NSK UK LTD.

NEWARK Northern Road, Newark, Nottinghamshire NG24 2JF, U.K.
P: +44-1636-605-123 F: +44-1636-605-000

France:

NSK FRANCE S.A.S.

PARIS Quartier de l'Europe, 2 Rue Georges Guynemer, 78283 Guyancourt, France
P: +33-1-30-57-39-39 F: +33-1-30-57-00-01

Germany:

NSK DEUTSCHLAND GMBH

DUSSELDORF ☆ Harkortstrasse 15, D-40880 Ratingen, Germany
P: +49-2102-4810 F: +49-2102-4812-290

STUTTGART Liebknechtstrasse 33, D-70565 Stuttgart-Vaihingen, Germany
P: +49-711-79082-0 F: +49-711-79082-289

WOLFSBURG Tischlerstrasse 3, D-38440 Wolfsburg, Germany
P: +49-5361-27647-10 F: +49-5361-27647-70

Italy:

NSK ITALIA S.P.A.

MILANO Via Garibaldi 215, Garbagnate Milanese (Milano) 20024, Italy
P: +39-299-5191 F: +39-299-025778

Netherlands:

NSK EUROPEAN DISTRIBUTION CENTRE B.V.

TILBURG De Kroonstraat 38, 5048 AP Tilburg, Netherlands
P: +31-13-4647647 F: +31-13-4647648

Poland:

NSK REPRESENTATIVE OFFICE

WARSAW Ul. Migdalowa 4/73, 02-796, Warsaw, Poland
P: +48-22-645-1525 F: +48-22-645-1529

Russia:

NSK POLSKA SP. Z O.O.

SAINT-PETERSBURG Office I 703, Bldg 29, 18th Line of Vasilievskiy Ostrov, Saint-Petersburg, Russia, 199178
P: +7-812-332-5071 F: +7-812-332-5072

Spain:

NSK SPAIN S.A.

BARCELONA C/Tarragona, 161 Cuerpo Bajo, 2a Planta, 08014, Barcelona, Spain
P: +34-93-289-2763 F: +34-93-433-5776

Turkey:

NSK RULMANLARI ORTA DOGU TIC. LTD. STI.

ISTANBUL 19 Mayis Mah. Ataturk Cad., Ulya Engin Is Merkezi No: 68 Kat. 6, P.K. : 34736, Kozyatagi-Istanbul, Turkey
P: +90-216-477-7111 F: +90-216-477-7174

United Arab Emirates:

NSK BEARINGS GULF TRADING CO.

DUBAI JAFZA View 19, Floor 24 Office LB192402/3, PO Box 262163, DownTown Jebel Ali, Dubai, UAE
P: +971-4-804-8207 F: +971-4-884-7227

●North and South America

United States of America:

NSK AMERICAS, INC. (AMERICAN HEADQUARTERS)

ANN ARBOR 4200 Goss Road, Ann Arbor, Michigan 48105, U.S.A.
P: +1-734-913-7500 F: +1-734-913-7511

NSK CORPORATION

ANN ARBOR 4200 Goss Road, Ann Arbor, Michigan 48105, U.S.A.
P: +1-734-913-7500 F: +1-734-913-7511

NSK PRECISION AMERICA, INC.

FRANKLIN ☆ 3450 Bearing Drive, Franklin, Indiana 46131, U.S.A.
P: +1-317-738-5000 F: +1-317-738-5050

SAN JOSE 780 Montague Expressway, Suite 505, San Jose, California, 95131, U.S.A.
P: +1-408-944-9400 F: +1-408-944-9405

NSK LATIN AMERICA, INC.

MIAMI 3470 NW 82nd Avenue Suite 625, Miami FL 33122, U.S.A.
P: +1-305-477-0605 F: +1-305-477-0377

Canada:

NSK CANADA INC.

TORONTO ☆ 5585 McAdam Road, Mississauga, Ontario, Canada L4Z 1N4
P: +1-905-890-0740 F: +1-800-800-2788

MONTREAL 2150-32E Avenue Lachine, Quebec, Canada H8T 3H7
P: +1-514-633-1220 F: +1-800-800-2788

VANCOUVER 3353 Wayburne Drive, Burnaby, British Columbia, Canada V5G 4L4
P: +1-877-994-6675 F: +1-800-800-2788

Argentina:

NSK ARGENTINA SRL

BUENOS AIRES Garcia del Rio 2477 Piso 7 Oficina "A" (1429) Buenos Aires-Argentina
P: +54-11-4704-5100 F: +54-11-4704-0033

Brazil:

NSK BRASIL LTDA.

SUZANO ☆ Av. Vereador Joao Batista Fitipaldi, 66, CEP 08685-000, Vila Maluf, Suzano, SP, Brazil
P: +55-11-4744-2500

BELO HORIZONTE Rua Ceara 1431-4th andar-sala 405-Funcionarios Belo Horizonte-MG, Brazil 30150-311
P: +55-31-3274-2591 F: +55-31-3273-4408

JOINVILLE Rua Blumenau, 178-sala 910-Centro Joinville-SC, Brazil 89204-250
P: +55-47-3422-2239 F: +55-47-3422-2817

PORTO ALEGRE Av. Cristovão Colombo, 1694-sala 202-Floresta Porto Alegre-RS, Brazil 90560 001
P: +55-51-3346-7851 F: +55-51-3222-2599

RECIFE Av. Conselheiro Aguiar, 2738-6th andar-conj. 604-Boa Viagem Recife-PE, Brazil 51020-020
P: +55-81-3326-3781 F: +55-81-3326-5047

Peru:

NSK PERU S.A.C.

LIMA Calle Teniente Enrique Palacios 360 Oficina 311 Miraflores, Lima, Peru
P: +51-1-493-4385

Mexico:

NSK RODAMIENTOS MEXICANA, S.A. DE C.V.

MEXICO CITY ☆ Av. Presidente Juarez No.2007 Lote 5, Col. San Jeronimo Tepetlacalco, Tlalnepantla, Estado de Mexico, Mexico, C.P.54090
P: +52-55-3682-2900 F: +52-55-3682-2937

MONTERREY Av. Ricardo Margain 575, IOS Torre C, Suite 516, Parque Corporativo Santa Engracia, San Pedro Garza Garcia, N.L. Mexico, C.P.66267
P: +52-81-8000-7300 F: +52-81-8000-7095

<As of October 2018>

For the latest information, please refer to the NSK website.

www.nsk.com

Motion & Control

No. 30 June 2019

Published by NSK Ltd.

Eco-awareness and reliability in motion

NSK

NSK used environmentally friendly printing methods for this publication.

CAT. No. ETJ-0030 2019 C-6 Printed in Japan